CHAPTER 5

RESULTS AND DISCUSSION

The **chapter 5** mainly comprises of two parts where **Part I** and **Part II** are focused on synthesized electrocatalysts Pd-Ni/C and Pd-Pt/C, respectively. At the beginning of **Part I**, the results of physical characterization of synthesized anode electrocatalyst Pd-Ni/C using X-ray Diffraction (XRD), scanning electron microscopy (SEM), energy dispersive X-ray (EDX) and transmission electron microscopy (TEM) are discussed. The electrochemical characterization using cyclic voltammetry (CV) and electrochemical impedance spectroscopy (EIS) analyses are also discussed. Further, the performance of synthesized Pd-Ni/C anode electrocatalysts in both Y-shaped and T-shaped air breathing microfluidic fuel cell are reported at the end of **Part I**. Similar to **Part I**, at the beginning of **Part II**, the results of physical characterization of synthesized anode electrocatalyst Pd-Pt/C using X- ray Diffraction (XRD), scanning electron microscopy (SEM), energy dispersive X- ray (EDX), transmission electron microscopy (TEM) are discussed. The electrochemical characterization using cyclic voltammetry (CV) and electrochemical impedance spectroscopy (EIS) analyses are also discussed just after physical characterization. Further, the performances using synthesized Pd-Pt/C anode electrocatalysts in both Y-shaped and T-shaped air breathing microfluidic fuel cell are presented. The results of optimization of process parameters using response surface methodology (RSM) are discussed in **Part II**. Finally, the dimensionless numbers, the efficiency of the fuel cell and stability test of the microfluidic fuel cell are reported.

5.1 Performance evaluation of Pd-Ni/C anode electrocatalyst: Part I

5.1.1 Physical Characterization

5.1.1.1 XRD analysis

The crystalline structure and size of the synthesized anode electrocatalyst Pd-Ni/C of different metal ratios i.e., Pd-Ni (16:4)/C, Pd-Ni (10:10)/C and Pd-Ni (4:16)/C were investigated using XRD technique as described in the chapter 'Experimental' (page no. 50). The XRD characteristics of all synthesized electrocatalysts are shown in Figure 5.1. A broad peak at about 2θ of 25^{o} to the plane (002) of hexagonal structure is related to carbon support material. The diffraction patterns show two characteristics of crystalline face centered cubic (FCC) Pd and FCC Ni with peaks corresponding to (111), (200), and (220) planes. As per JCPDS 05-0681standard the main peak for Pd nanoparticles fcc structure occur at 2θ values of 40.1^{o}, 46.7^{o} and 68.1^{o} at the corresponding plane (111), (200) and (220), respectively.

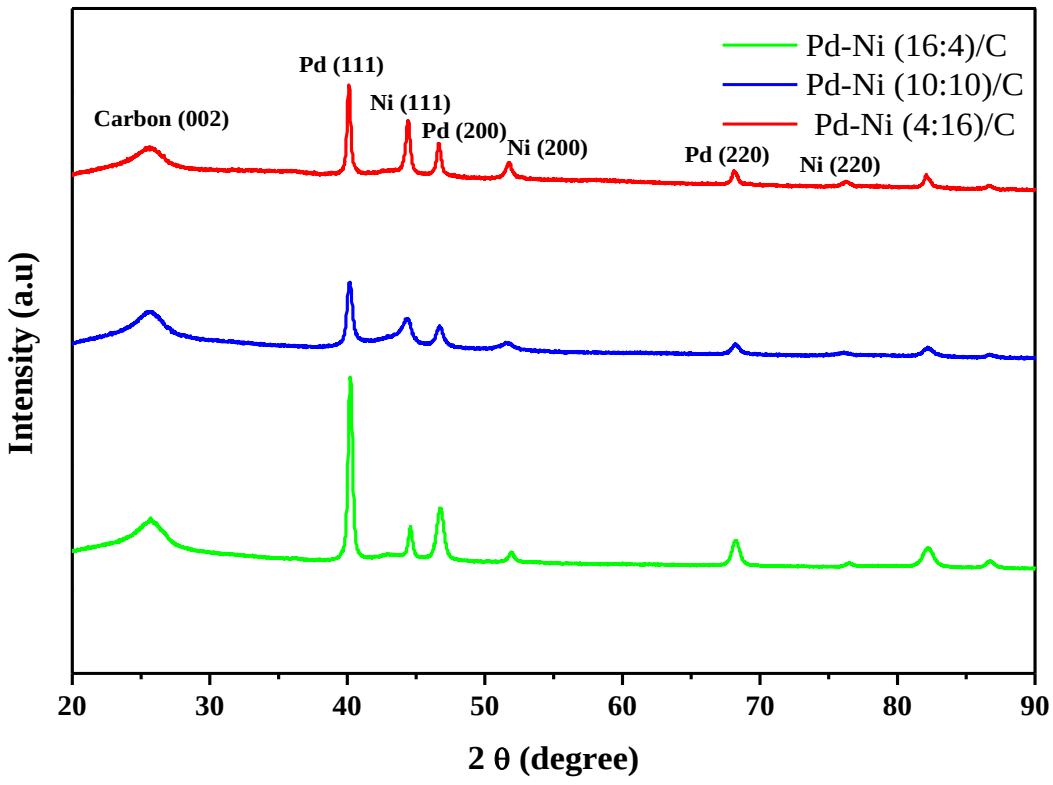

Figure 5.1 X- ray diffraction pattern of Pd-Ni/C with different weight ratios of metal.

The observed lattice parameter is 0.3890 nm. Whereas, the main peaks for Nickel (Ni) as per JCPDS 04-0850 occur at 2θ values of 44.56º, 51.76º and 76.38º at the plane of (111), (200) and (220), respectively while the lattice parameter was 0.3523 nm.

The Ni (111) peaks in the Pd-Ni electrocatalysts with rising Pd content were marginally moved to lower 2θ values of 44.58º, 44.31º and 44.27º, whereas the Pd (111) peaks shifts to the higher 2θ values of 40.19º, 40.14º and 40.1º with the addition of Ni in the Pd-Ni bimetallic as shown in Table 5.1.

Table 5.1 Crystallite size and peak position of Pd-Ni/C electrocatalyst obtained from XRD data.

Electrocatalyst type	**2θ position (deg.)**		**Crystallite size (nm)**	**Degree of alloying (%)**
	Pd (111)	**Ni (111)**	**Pd (111)**	
Pd-Ni/C (16:4)	40.19	44.48	28.5	3.8
Pd-Ni/C (10:10)	40.14	44.31	10.2	6
Pd-Ni/C (4:16)	40.10	44.27	25.7	2

This shifting in peaks change may suggest some partial alloying between Ni and Pd by integrating Pd atoms into fcc structure of Ni. The presence of fcc Pd peaks also suggests some partial alloy and bi phase particle formation (Houache et al., 2019). The peak at the plane (111) was used to find out the crystallite size of the Pd-Ni/C electrocatalyst using Scherrer's equation (Equation 5.1) and the lattice parameter was determined using Bragg's equation (Equation 5.2) (Choudhary and Pramanik 2019). Where, d_c is the calculated crystallite size, λ is the x-ray wavelength (1.54 Å), β is the width of diffraction peaks, θ (radians) is the angle between incident ray and scattering planes, n is order of diffraction and d_{hkl} is interplanar distance between two planes of miller indices (hkl). The physical parameters obtained for Pd-Ni/C from XRD pattern (Figure 5.1) is depicted in

Table 5.1. The lattice parameter of Pd-Ni/C electrocatalyst i.e., 0.3882 nm, 0.3886 nm and 0.3889 nm lie between lattice parameters of the pure metal Pd and Ni, respectively. The Pd-Ni (10:10)/C electrocatalyst have the smallest crystallite size among all the ratios as presented in Table 5.1. The degree of alloying i.e., $X_{(Ni\%)}$ for Ni in Pd-Ni/C is calculated using the given Vegard's law formula in Equation 5.3 (Dutta and Dutta 2013).

$$d_c = \frac{0.9\lambda}{\beta \cos\theta} \quad (5.1)$$

$$n\lambda = 2d_{hkl}\sin\theta \quad (5.2)$$

$$X_{(Ni\,\%)} = \frac{a - a_o}{a_{alloy} - a_o} \times 100 \quad (5.3)$$

In Equation (5.3), a represents the lattice parameter of the Pd-Ni/C electrocatalyst at different compositions, a_{alloy} is the lattice parameter of PdNi solid solution (Bagmut et al., 2010) and a_o is the lattice parameter of pure Pd. The values of degree of alloying are shown in Table 5.1. The highest degree of alloying of 6 % was observed for smaller crystallite size (10.2 nm) of alloy electrocatalyst Pd-Ni (10:10)/C. Thus, synthesized Pd-Ni (10:10)/C is expected to show excellent electrocatalytic property for glycerol electrooxidation in the half cell studies (CV analysis) and single MFC studies which are discussed in the results and discussion section "5.1.2.1 Cyclic voltammetry analysis" (page no. 76) and "5.1.4.1.2 Effect of anode electrocatalyst type" (page no. 86), respectively.

5.1.1.2 SEM-EDX analysis

The surface morphology of the prepared electrocatalyst Pd-Ni (16:4)/C, Pd-Ni (10:10)/C, Pd-Ni (4:16)/C were examined through SEM as shown in Figure 5.2a to Figure 5.2c. The SEM images of prepared electrocatalyst illustrates that the particles are uniformly distributed over the support material and of nano size range. The EDX analysis was used

to identify the chemical characterization or surface elemental composition of the synthesized electrocatalyst. The Figure 5.2a to Figure 5.2c shows the EDX pattern of the prepared electrocatalysts where the presence of Pd and Ni metals are prominent for all Pd-Ni/C electrocatalysts.

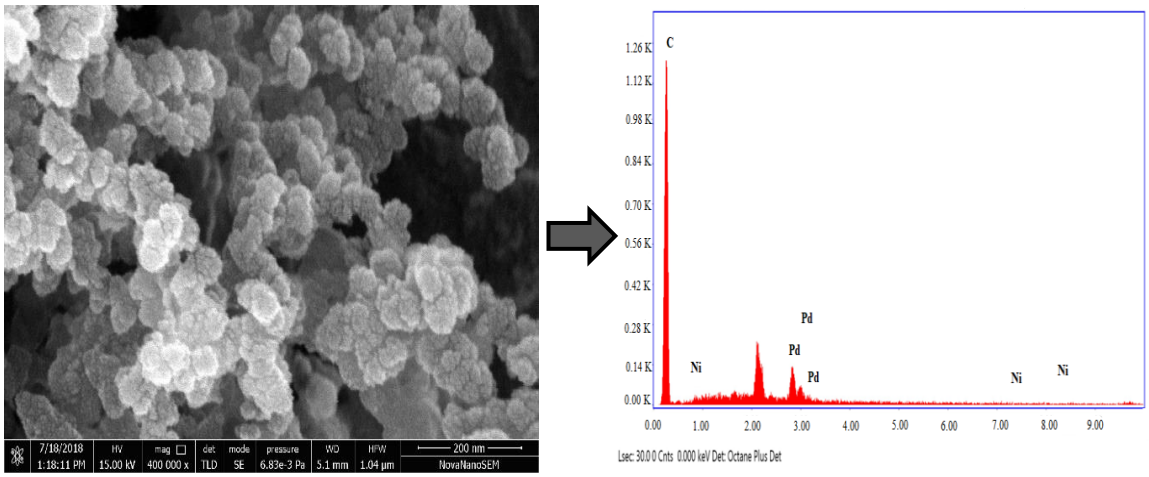

Figure 5.2a SEM-EDX images of synthesized Pd-Ni (16:4)/C electrocatalyst.

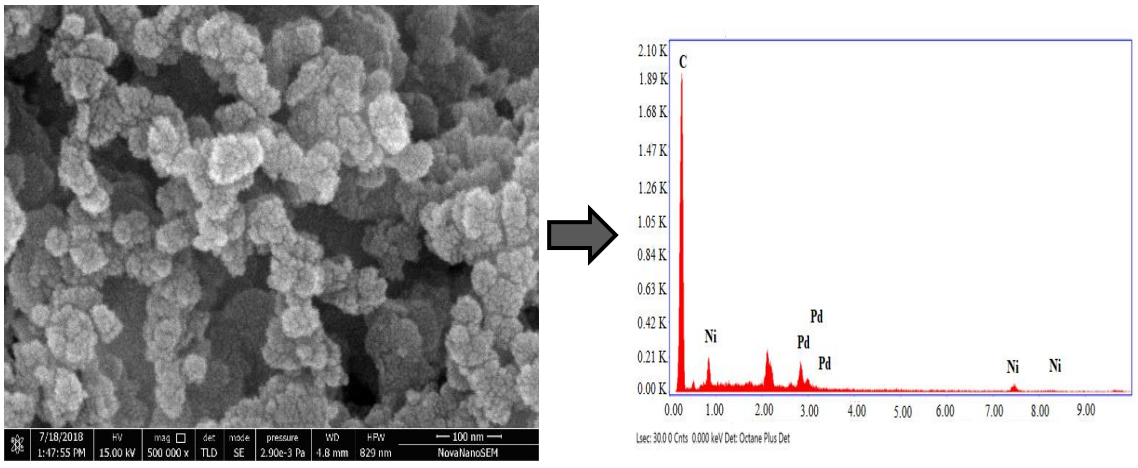

Figure 5.2b SEM-EDX images of synthesized Pd-Ni (10:10)/C electrocatalyst.

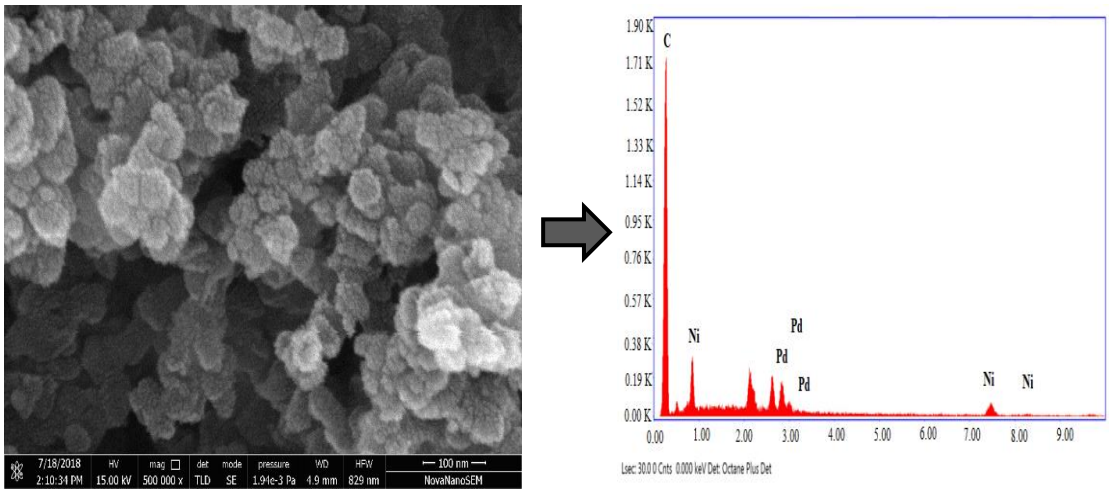

Figure 5.2c SEM-EDX images of synthesized Pd-Ni (4:16)/C electrocatalyst.

Table 5.2 shows that the electrocatalysts prepared have the same elemental compositions with some variations from the theoretical amount. Since the catalytic surface is heterogeneous, so the EDX result of elemental composition varies from point to point.

Table 5.2 Composition of electrocatalyst in weight percentage obtained from EDX.

Electrocatalyst Type	**EDX elemental compositions (wt. %)**		**Nominal compositions (wt. %)**	
	Pd	Ni	Pd	Ni
Pd-Ni (16:4)/C	11.99	3.36	16	4
Pd-Ni (10:10)/C	8.87	10.67	10	10
Pd-Ni (4:16)/C	8.42	16.09	4	16

5.1.1.3 TEM analysis

Figure 5.3a to Figure 5.3b show the TEM images and particle size histogram of the synthesized Pd-Ni (16:4)/C, Pd-Ni (10:10)/C and Pd-Ni (4:16)/C electrocatalysts. The TEM images show that the electrocatalysts are in nano sized, and reasonably dispersed on a carbon support. The electrocatalyst particle size was calculated with the help of Image J software. The particle size distributions in the histogram show that the particle size of each sample is less than 10 nm. The particle size distribution of all synthesized

electrocatalysts show that the particle sizes of electrocatalysts are 6 nm, 4.5 nm and 4.9 nm for Pd-Ni (16:4)/C Pd-Ni (10:10)/C and Pd-Ni (4:16)/C, respectively. The TEM images confirms that the particles are in spherical shape and somewhat agglomerated, due to the reduction process of the electrocatalyst by hydrogen reduction method which is a fast reduction process (Panjiara and Pramanik 2021a). The particle size obtained from the TEM analysis follows the similar trends as that of XRD crystallite size. The smaller size of electrocatalyst particles show better distribution of electrocatalyst on the electrode surface and have higher active surface area (Wang et al., 2013).

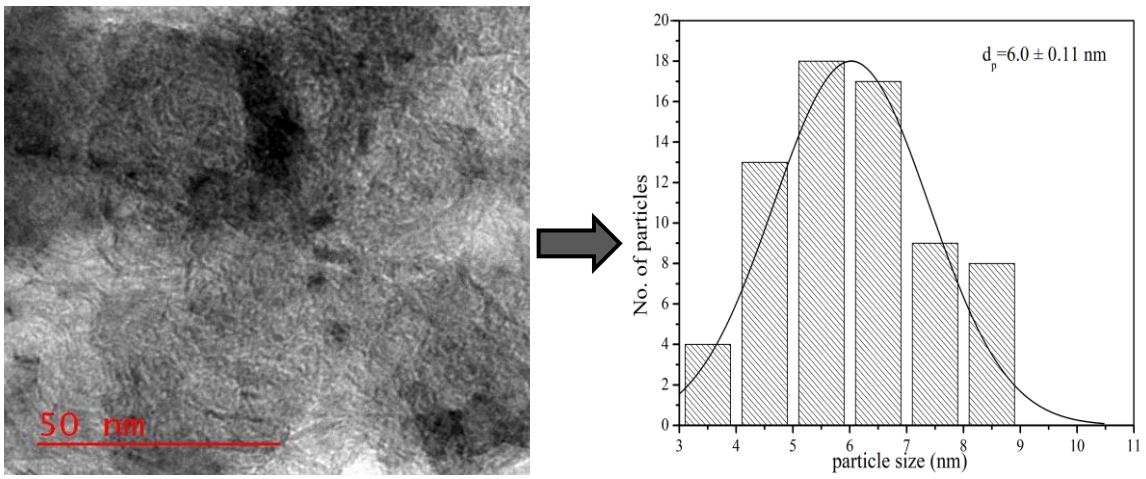

Figure 5.3a TEM images and particle size distribution histogram of synthesized Pd-Ni (16:4)/C electrocatalyst.

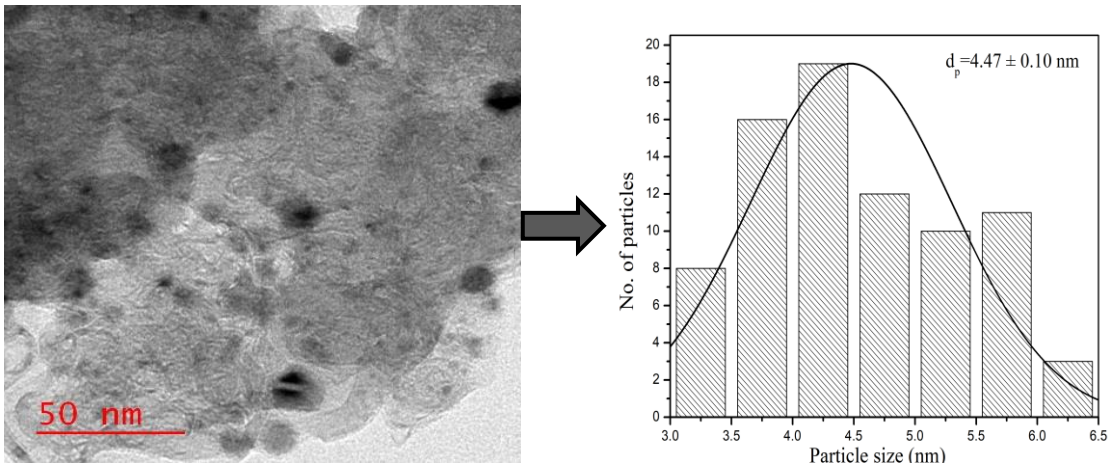

Figure 5.3b TEM images and particle size distribution histogram of synthesized Pd-Ni (10:10)/C electrocatalyst.

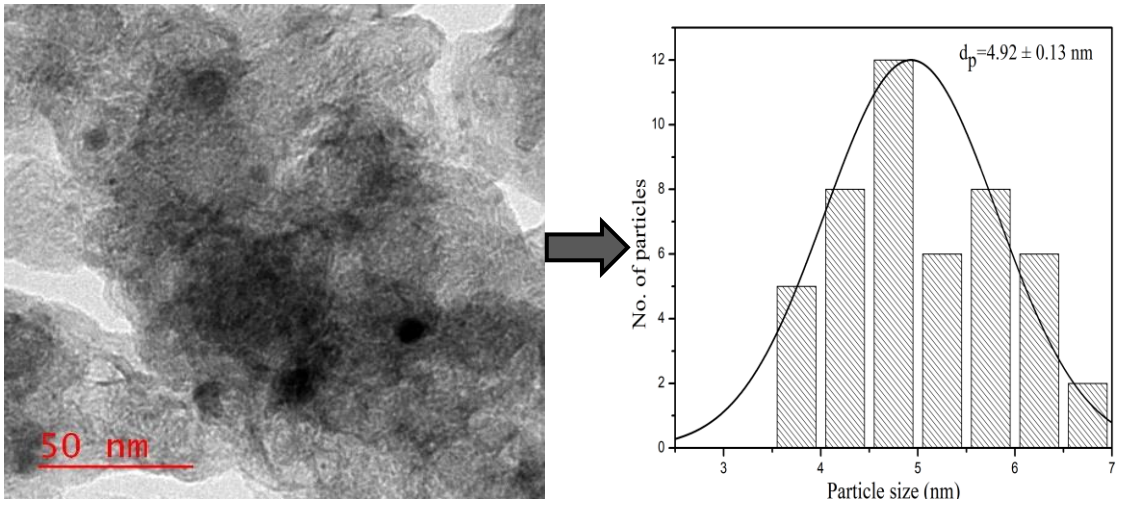

Figure 5.3c TEM images and particle size distribution histogram of synthesized Pd-Ni (4:16)/C electrocatalyst.

Similar to XRD analysis, the TEM results also suggest the better performance of Pd-Ni (10:10)/C electrocatalyst in half and single cell experiments. The XRD data in the previous section shows little higher crystallite size than the particle size obtained from TEM analysis because XRD analysis shows the crystalline particles, not the real morphology of electrocatalysts (Tayal et al., 2011). However, in TEM images utmost of the small particles are calculated, while in XRD patterns, large particles are selected for crystallite size (Tayal et al., 2011).

5.1.2 Electrochemical study of anode

5.1.2.1 Cyclic voltammetry analysis

The electrochemical characterization of the synthesized Pd-Ni (16:4)/C, Pd-Ni (10:10)/C and Pd-Ni (4:16)/C electrocatalysts were performed using CV analysis mainly for glycerol fuel after getting promising results from the physcial characterization of the synthesized electrocatalysts. Figure 5.4 shows the comparison of CV characteristics of all three bimetallic synthesized electrocatalyst Pd-Ni/C electrocatalysts which were used as electrocatalyst for working electrode fabrication. It is already mentioned in the section

experiemntal method (page no. 51) that the platinum wire and Ag/AgCl in sat. KCl were used as counter and reference electrode, respectively. The applied potential was varied from -1 V to 1 V (vs. Ag/AgCl), and the scan rate was fixed at 50 mV/sec, as the observed electrochemical peaks were prominent at this scan rate. The CV characterstics for other scan rates are presented in the Appendix C (Figure C1 to Figure C3). The peak current density of 12.75 mA/cm^2 at a peak potential of -0.174 V(vs. Ag/AgCl) was observed for glycerol electrooxidation in the forward scan when Pd-Ni (10:10)/C anode electrocatalyst was used. Whereas, Pd-Ni (16:4)/C shows electrooxidation peak current density of 19.45 mA/cm^2 at peak potential of -0.103 V(vs. Ag/AgCl).

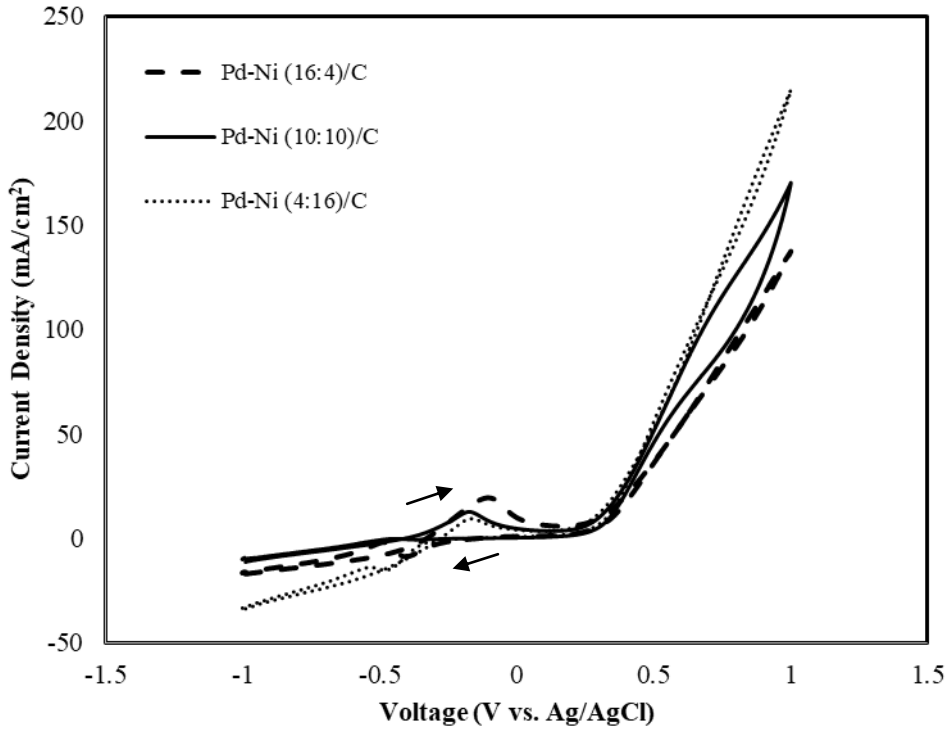

Figure 5.4 Cyclic voltammetry for different metal Pd to Ni in ratios of Pd-Ni/C anode electrocatalyst using 1 M glycerol mixed with 1 M KOH at scan rate of 50 mV/sec at a temperature of 25 ^{o}C.

The Pd-Ni (4:16)/C shows electrooxidation peak current density of 9.45 mA/cm^2 at potential of -0.168 V(vs. Ag/AgCl). It should be noted that no peak was observed in the backward scan irrespective of type of electrocatalysts. Although the peak current density

for Pd-Ni (10:10)/C electrocatalyst was little lower than the Pd-Ni (16:4)/C, the peak potential was more negative (-0.174 V) for Pd-Ni (10:10)/C than the Pd-Ni (16:4)/C (-0.103 V). Thus, it can be predicted that activation loss for the Pd-Ni (10:10)/C will be low and thus, better performance of Pd-Ni (10:10)/C is expected in single cell performance. The activation overpotential is the loss of energy due to the sluggishness of the electrochemical reactions which occurred at the electrode surface. The excellent performance of Pd-Ni (10:10)/C among all synthesized electrocatalyst was also predicted in XRD and TEM analysis earlier.

5.1.2.2 EIS analysis

The electrochemical impedance spectroscopy study of the synthesized electrocatalyst were performed using the same three electrode cell assembly in a half cell configuration as it was adopted for CV studies. The Nyquist plots of different synthesized electrodes for Pd-Ni (16:4)/C, Pd-Ni (10:10)/C and Pd-Ni (4:16)/C electrocatalyst for the 1 M glycerol mixed with 1 M KOH is shown in Figure 5.5a. The EIS plots were achieved at a frequency range of 100 kHz to 10 mHz with amplitude of 10 mV at the potential of - 0.2 V (vs Ag/AgCl). The Nyquist plots show different arc diameter for each electrocatalysts. The charge transfer resistance of the electrooxidation reaction of each electrocatalyst is depicted by the diameter of the arc (Rezaei et al., 2016). The larger arc diameter of Pd-Ni (16:4)/C electrocatalyst indicates higher charge transfer resistance compared to smaller arc diameter generated by the rest of the bimetallic electrocatalysts. Even among all the bimetallic Pd-Ni/C electrocatalysts, the Pd-Ni (10:10)/C, generates smallest arc diameter compared to other bimetallic electrocatalysts. It implies that the charge transfer resistance is lower for Pd-Ni (10:10)/C anode electrocatalyst. The equivalent circuit corresponds to the Nyquist plot is shown in the Figure 5.5b which was used to calculate the Pd-Ni (16:4)/C, Pd-Pt (10:10)/C and Pd-Ni (4:16)/C electrocatalyst charge transfer resistance.

In the equivalent circuit, the solution resistance/electrolyte resistance is represented by R_s, constant-phase element (CPE) is the double-layer capacitance at the interface of electrolyte and electrocatalyst represented by CPE, the charge-transfer resistance is represented by R_{ct} and Warburg diffusion resistance of ions in the solution is represented by W_s. The R_{ct} is the measurement of the semicircle arc diameter which is associated to the obstruction of passing of electron across the electrode area to adsorb the species and from the adsorbed species to the electrode surface. The CPE or double layer capacitance for Pd-Ni (16:4)/C, Pd-Ni (10:10)/C and Pd-Ni (4:16)/C are 2.7 mF, 2.9 mF and 3.0 mF, respectively. The Chi square fit, CPE, R_s and R_{ct} values are presented in Table 5.3.

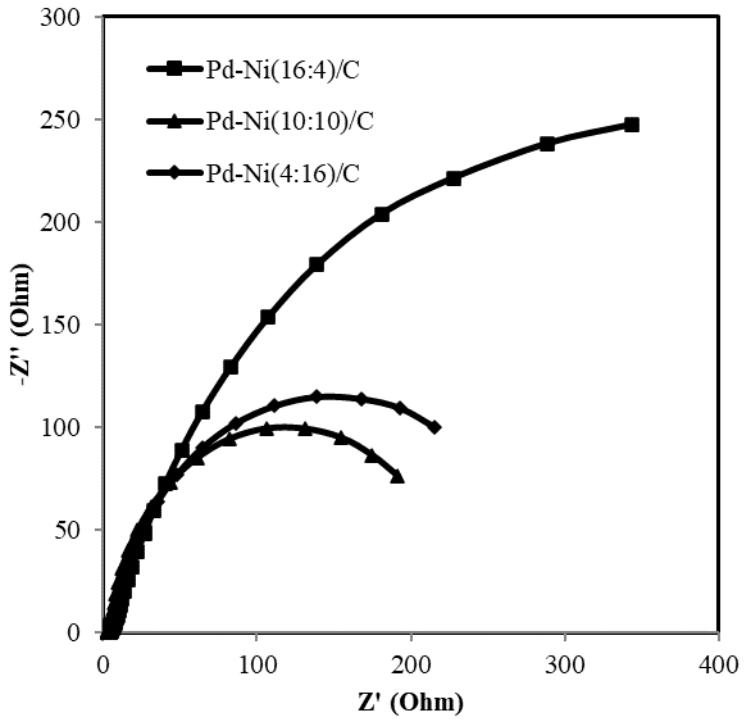

Figure 5.5a Nyquist plots of synthesized electrocatalysts recorded at - 0.2 V in 1 M glycerol mixed with 1 M KOH solution;Temperature: 25 ^{o}C

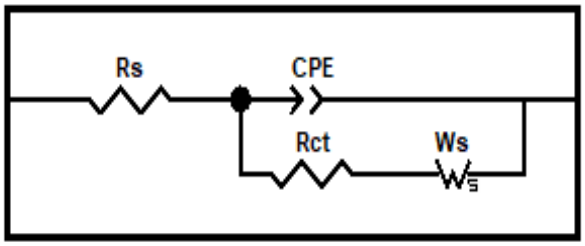

Figure 5.5b Equivalent circuit diagram corresponds to Nyquist plot.

Table 5.3 Equivalent circuit related terms for Pd-Ni/C electrocatalysts.

Electrocatalyst type	Chi square fit	R_s (ohm)	R_{ct} (ohm)	CPE (mF)
Pd-Ni (16:4)/C	0.079	5.01	1182	2.7
Pd-Ni (10:10)/C	0.074	3.51	272.6	2.9
Pd-Ni (4:16)/C	0.151	6.19	345.8	3

The conductivity is calculated using the formula $\sigma = \frac{L}{RA}$, where, σ is the conductivity, L is the thickness of the working electrode i.e., 0.016 cm, A is the area of the working electrode i.e., 0.5 cm^2 and R is the charge transfer resistance. The conductivity values for Pd-Ni (16:4)/C, Pd-Ni (10:10)/C and Pd-Ni (4:16)/C are 1.35×10^{-5} $\Omega^{-1}cm^{-1}$, 5.86×10^{-5} $\Omega^{-1}cm^{-1}$ and 4.62×10^{-5} $\Omega^{-1}cm^{-1}$ respectively. The bode phase angle at high frequency (56899 Hz) obtained from Z view software for Pd-Ni (16:4)/C, Pd-Ni (10:10)/C and Pd-Ni (4:16)/C are -24.01°, -16.67° and -23.92°, respectively. The bode magnitude for Pd-Ni (16:4)/C, Pd-Ni (10:10)/C and Pd-Ni (4:16)/C are 5.30, 3.56 and 6.33, respectively. Whereas, the charge transfer resistance R_{ct} for Pd-Ni (16:4)/C, Pd-Ni (10:10)/C and Pd-Ni (4:16)/C were 1182 Ω, 272.6 Ω and 345.8, respectively. Thus, EIS analysis shows that Pd-Ni (10:10) /C has lowest charge transfer resistance (272.6 Ω) than the other bimetallic electrocatalyst (Table 5.3). The smaller R_{ct} indicates a faster reaction rate of glycerol electrooxidation reaction.

5.1.3 Electrochemical study of cathode

5.1.3.1 Oxygen as oxidant

The oxygen reduction reaction (ORR) using cyclic voltagramm study in half cell is shown in Figure 5.6a to Figure 5.6b. The cathode electrode was made using commercial electrocatalyst Pt/C_{HSA} of 1 mg/cm^2. The data were recorded in volatge range of -1 V to 1 V vs. Ag/AgCl at a scan rate of 50 mV/sec. The ORR in nitrogen purged (Figure 5.6a) solution analysis show reduced current compared to oxygen satutaed solution (Figure 5.6b) (Yan et al., 2015). Figure 5.6a shows the CV of nitrogen purged in KOH solution. No such reduction peak is observed in the CV characterstics. Similar trend of CV was also observed by Yan et al., 2015. The oxygen reduction reaction generally occurs in one or two pathways in alkaline medium (Ortiz et al., 2003). The mechanism of cathode reduction has already been discussed in the chapter 2 (page no. 33).

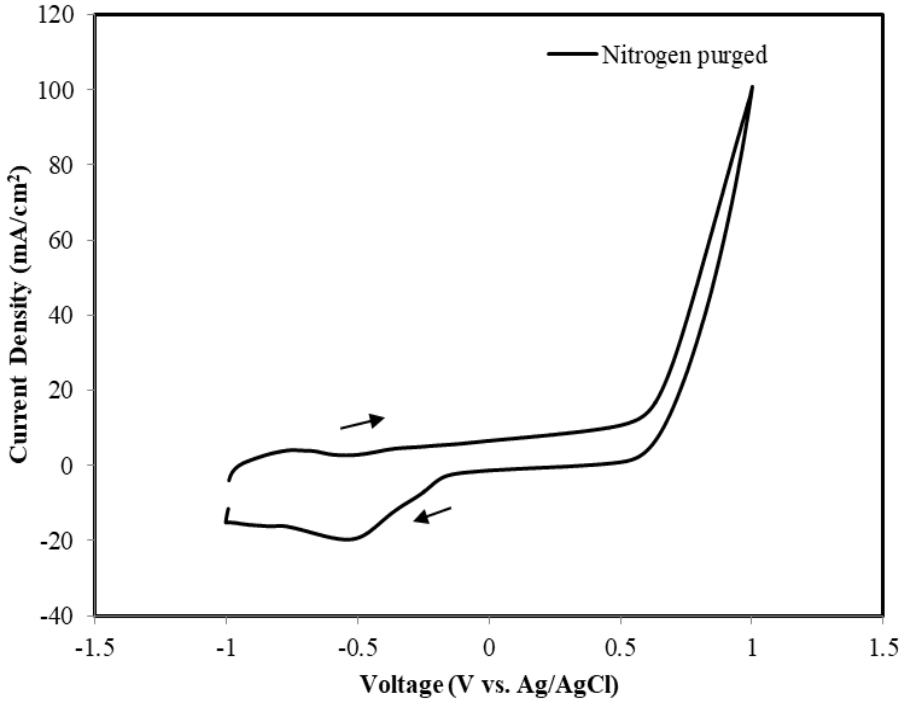

Figure 5.6a Cyclic voltammetry for 1 mg/cm^2 Pt/C_{HSA} cathode in 1 M KOH in nitrogen purged solution at 50 mV/s scan rate; Temperature. 25 ^oC.

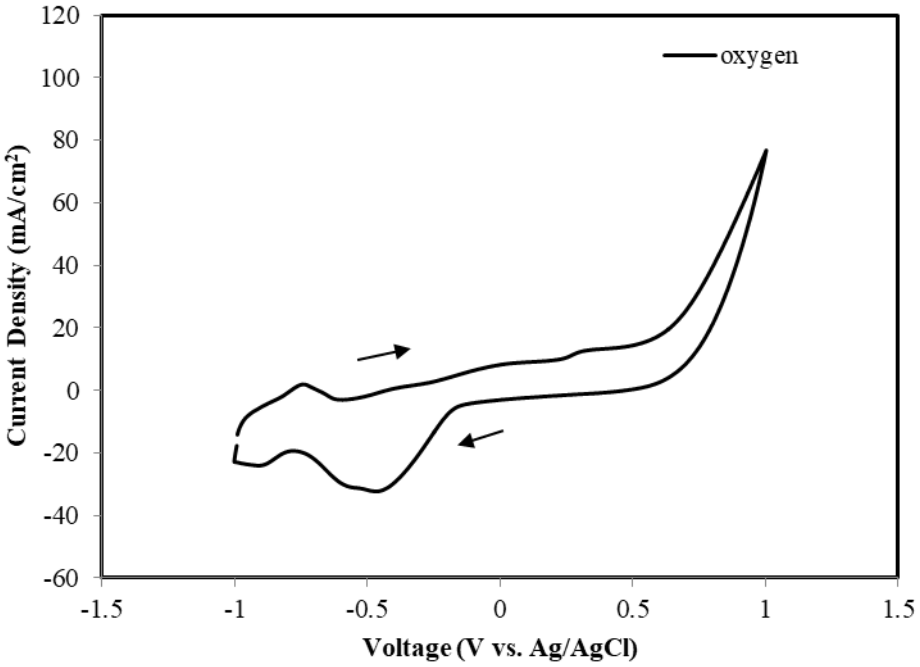

Figure 5.6b Cyclic voltammetry for 1 mg/cm^2 Pt/C_{HSA} cathode in 1 M KOH in an oxygen saturated solution at 50 mV/s scan rate; Temperature. 25 ^oC.

Figure 5.6b shows that the oxygen saturated solution genetartes two reduction peaks in the reverse scan at the potential of -0.42 V and -0.84 V. The peak current density of -30.9 mA/cm^2 at potential of -0.48 V and -21.8 mA/cm^2 at potential of -0.84 V were obtained due to oxygen reduction reaction at Pt/C_{HSA} cathode in oxygen saturated KOH electrolyte solution. The two reduction peaks shows that oxygen reduction reaction occurs in two steps 2+2 electron pathway mechanisms (page no. 34).

5.1.3.2 Mixed oxidant at cathode

The effect of mixed oxidant using oxygen saturated calcium hypochlorite in cyclic voltammetry study is shown in Figure 5.7. The cathode was made of 1 mg/cm^2 of Pt/C_{HSA} electrode and the electrolyte solution was 1.5 M calcium hypochlorite mixed with 1 M KOH in an oxygen saturated solution which was designated as mixed oxidant. The data were recorded in the voltage range from -1 V to 1 V vs. Ag/AgCl at a 50 mV/s scan rate. The mixed oxidant reduction reaction also occurs via two steps 2+2 electrons mechanism.

The first peak of pure oxygen reduction shifts from -0.42 V to -0.27 V towards less negative potential when oxygen saturated calcium hypochlorite solution (Figure 5.7) was used as oxidant. The second reduction peak was observed at the potential of -0.51 V for oxygen saturated mixed oxidant conditions (Figure 5.7).

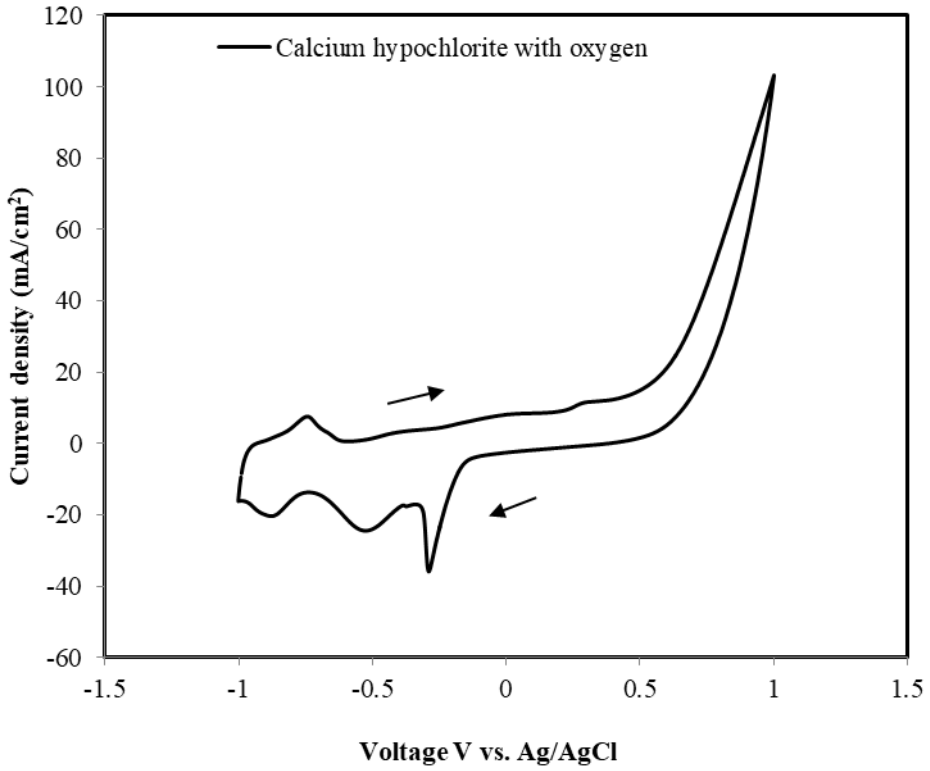

Figure 5.7 cyclic voltammetry for 1 mg/cm^2 Pt/C_{HSA} cathode in 1 M KOH in with 1.5 M calcium hypochlorite mixed with oxygen saturated solution at 50 mV/s scan rate; Temperature. 25 ^oC.

The shifting of first reduction peak from -0.42 V to -0.27 V (towards less negative potential) shows that calcium hypochlorite mixed with oxygen saturated solution reduce activation loss due to the increase in the concentration of oxidant at cathode electrocatalyst sites. This mixed oxidant reduces the mass transfer losses at high current density (Figure 5.7).

5.1.4 Performance evaluation of Pd-Ni/C anode electrocatalyst in MFC

5.1.4.1 Y-shaped air breathing MFC

5.1.4.1.1 Effect of flow rate at anode and cathode

The flow rate of glycerol and electrolyte stream is one of the key factors that influence MFC performance. Thus, it is important to optimize the flow rates of fuel and electrolyte streams. Figure 5.8a to Figure 5.8b represents the effect of flow rates of fuel and electrolyte streams in the Y-shaped air breathing MFC performance for varying flow rates ranging from 0.3 ml/min to 1.5 ml/min in both fuel and electrolyte streams. The anode fuel glycerol of 0.5 M mixed with 0.5 M KOH was fed at anode whereas atmospheric oxygen was used as cathode.

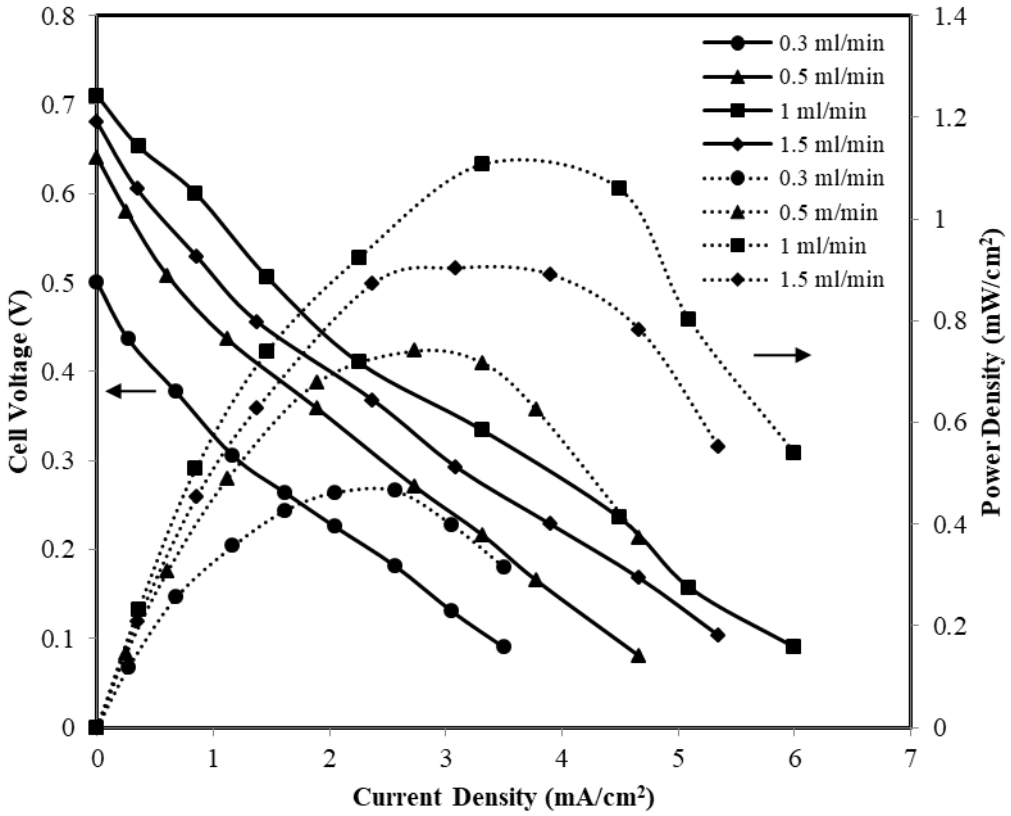

Figure 5.8a Polarization and power density curves of MFC for 0.5 M glycerol mixed with 0.5 M KOH at anode and cathode electrolyte of 0.5 M KOH using (a) varying flow rate at anode and fixed flow rate 1 ml/min at cathode; Anode: Pd-Ni (10:10)/C of 1 mg/cm^2 and cathode: Pt/C_{HSA} of 1 mg/cm^2, MFC temperature: 35 ^oC; Dotted line – power density curves; Solid lines – polarization curves.

To check the effect of flow rates, at first anode stream was studied at the flow rates of 0.3 ml/min, 0.5ml/min, 1 ml/min, and 1.5 ml/min while, fixed flow rate of 1 ml/min was kept for the cathode stream. It is seen from the Figure 5.8a that the cell performance in terms of open circuit voltage (OCV) and power density increases with the increase in anode flow rate upto 1 ml/min and further increase in the flow rate beyond 1 ml/min, the cell performance decreases drastically (Figure 5.8a). The OCV of 0.71 V and maximum power density of 1.1 mW/cm^2 at a current density of 3.31 mA/cm^2 were achieved at a flow rate of 1 ml/min at the anode side.

Whereas maximum power density of 0.46 mW/cm^2, 0.74 mW/cm^2 and 0.9 mW/cm^2 at a current density of 2.56 mA/cm^2, 2.74 mA/cm^2 and 3.08 mA/cm^2 were obtained from the flow rate of 0.3 ml/min, 0.5 ml/min and 1.5 ml/min, respectively.

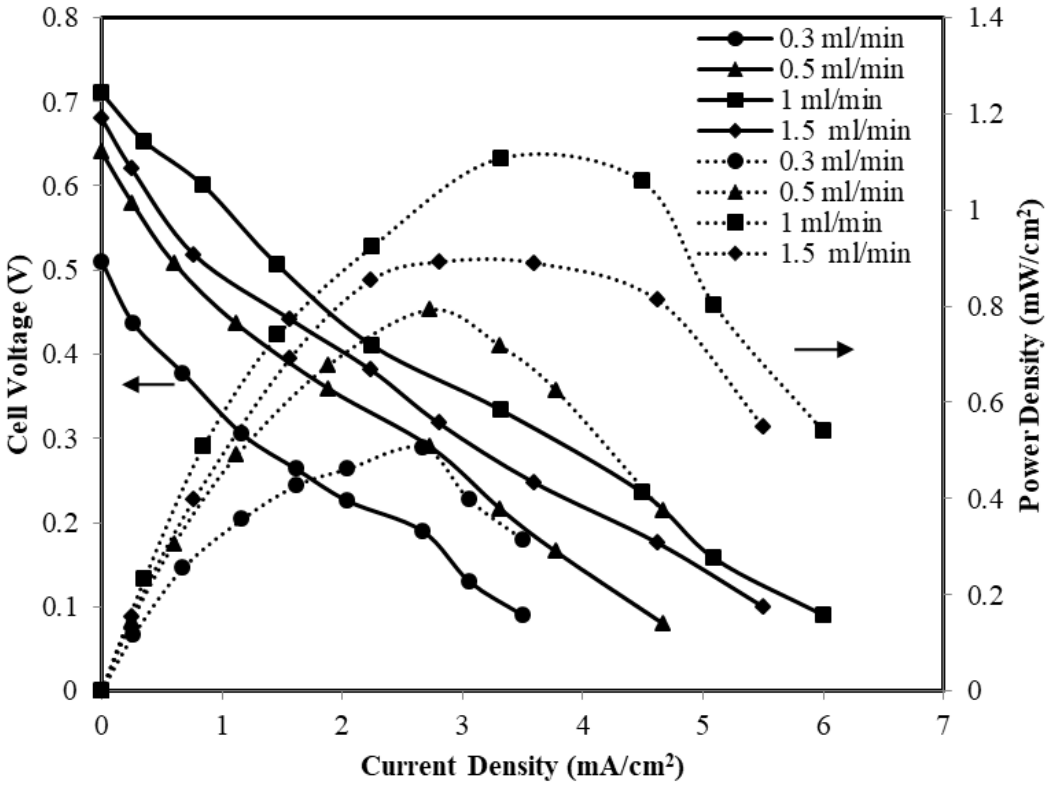

Figure 5.8b Polarization and power density curves of MFC for 0.5 M glycerol mixed with 0.5 M KOH at anode and cathode electrolyte of 0.5 M KOH using varying flow rate at cathode and optimum flow rate at anode (1 ml/min); Anode: Pd-Ni (10:10)/C of 1 mg/cm^2 and cathode: Pt/C_{HSA} of 1 mg/cm^2, MFC temperature: 35 ^oC; Dotted line – power density curves; Solid lines – polarization curves.

After optimizing the flow rate at anode, the cathode side flow rate was varied as shown in Figure 5.8b. The cathode stream flow rates of 0.3 ml/min, 0.5 ml/min, 1 ml/min and 1.5 ml/min were maintained to evaluate the optimum cathode flow rate keeping the anode flow rate at optimum value of 1 ml/min. The MFC performance increases with the increase in cathode flow rate upto 1 ml/min and further increase in flow rate beyond 1 ml/min, the cell performance decreases (Figure 5.8b). The maximum OCV of 0.71 V and maximum power density 1.1 mW/cm^2 at a current density of 3.31 mA/cm^2 were obtained at cathode flow rate of 1 ml/min and anode flow rate of 1 ml/min (Figure 5.8b). Whereas, the maximum power density of 0.48 mW/cm^2, 0.76 mW/cm^2 and 0.88 mW/cm^2 at a current density of 2.6 mA/cm^2, 2.73 mA/cm^2 and 2.8 mA/cm^2 were obtained at flow rate of 0.3 ml/min, 0.5 ml/min and 1.5 ml/min, respectively.

At higher flow rates of streams, hydrodynamic instability causes the streams to oscillate which leads to disrupt the interface between two streams (Liu et al., 2019). On the other side at slower flow rate of streams caused fuel crossover by diffusion which results in mixed potential at the cathode and thus MFC performance get reduced (Choban et al., 2004). The fuel crossover from anode to cathode becomes easy because of the broadening of the inter diffusion layer between the fuel and the electrolyte streams at lower flow rate. The thinner diffusion zones between the two streams reduce the mixed potential at cathode due to fuel crossover in the MFC device (Chang et al., 2006).

5.1.4.1.2 Effect of anode electrocatalyst type

Figure 5.9 shows the performance characteristics of the air breathing microfluidic fuel cell operated with synthesized Pd-Ni (16:4)/C, Pd-Ni (10:10)/C and Pd-Ni (4:16)/C anode electrocatalysts, respectively. The cathode electrocatalysts was commercial Pt/C_{HSA}. Both the electrodes were constructed with the same electrocatalysts loading of 1 mg/cm^2. The anode fuel glycerol of 0.5 M mixed with 0.5 M KOH was fed at anode, whereas

atmospheric oxygen was used as oxidant at cathode. The anode and cathode streams were fixed at the optimum flow rates of 1 ml/min in the subsequent experiments in Y-shaped MFC. The highest OCV of 0.71 V and power density 1.1 mW/cm^2 at a current density of 3.3 mA/cm^2 was obtained for synthesized bimetallic Pd-Ni (10:10)/C. Whereas, OCV of 0.65 V and maximum power density of 1.03 mW/cm^2 at a current density of 3.13 mA/cm^2 was obtained for Pd-Ni (16:4)/C anode electrocatalyst. The Pd-Ni (4:16)/C electrocatalysts produces lowest OCV of 0.6 V and lowest power density of 0.73 mW/cm^2 at a current density of 2.23 mA/cm^2 for glycerol electrooxidation. The reason for best performance of Pd-Ni (10:10)/C may be due to higher degree of alloying and low overpotential as already discussed in XRD (page no. 70) and CV observation (page no. 76), respectively.

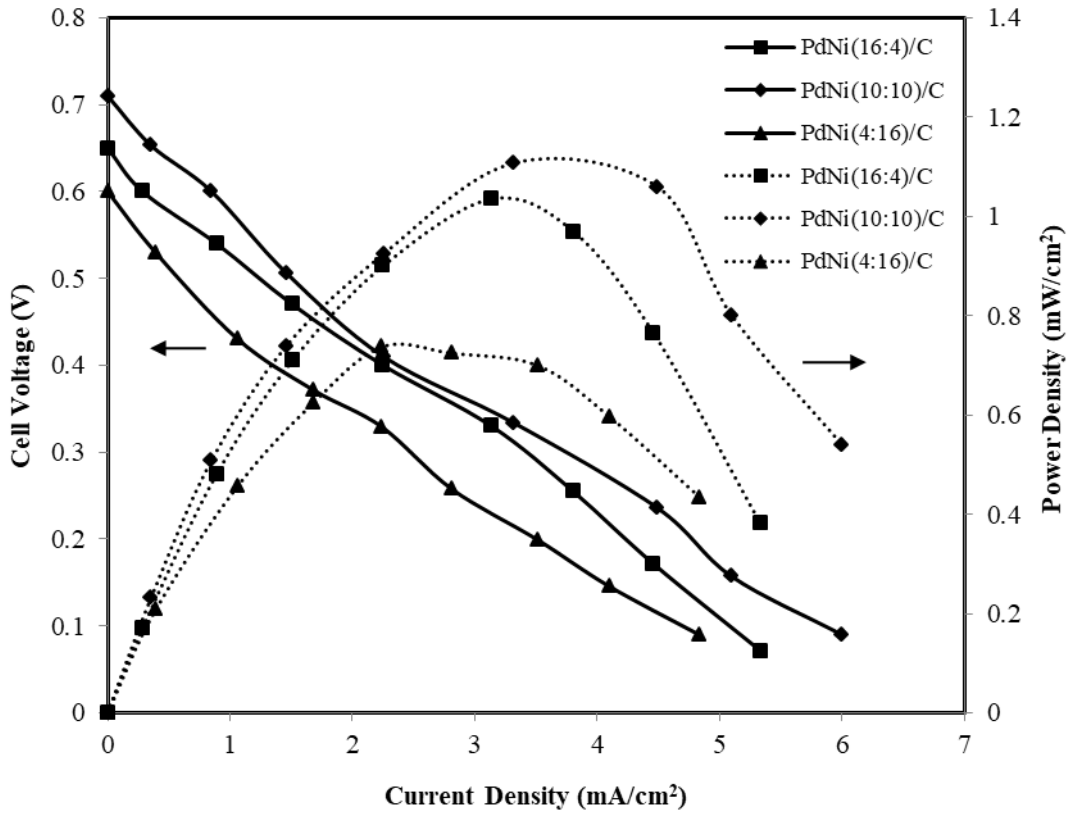

Figure 5.9 Polarization and power density curves of MFC for the different types of anode electrocatalyst using anode fed of 0.5 M glycerol mixed with 0.5 M KOH and cathode electrolyte of 0.5 M KOH; Cathode: Pt/C_{HSA} of 1 mg/cm^2, MFC temperature: 35 ^oC; Dotted line – power density curves; Solid lines – polarization curves.

5.1.4.1.3 Effect of anode electrocatalyst loading

The single cell study using various types anode electrocatalyst shows that the synthesized Pd-Ni (10:10)/C electrocatalyst performs better among all tested electrocatalysts. Thus, the anode loading was varied in the Y-shaped air breathing MFC using synthesized Pd-Ni (10:10)/C to get highest cell performance at the optimum anode loading. The anode fuel glycerol of 0.5 M mixed with 0.5 M KOH was fed at anode whereas atmospheric oxygen was used as oxidant at cathode. Figure 5.10 shows the performance characteristics of air breathing MFC for different loading of Pd-Ni (10:10)/C electrocatalyst at anode varying from 1 mg/cm^2 to 2.5 mg/cm^2. The electrocatalyst loading at cathode Pt/C_{HSA} was kept 1 mg/cm^2 same for each set of experiments.

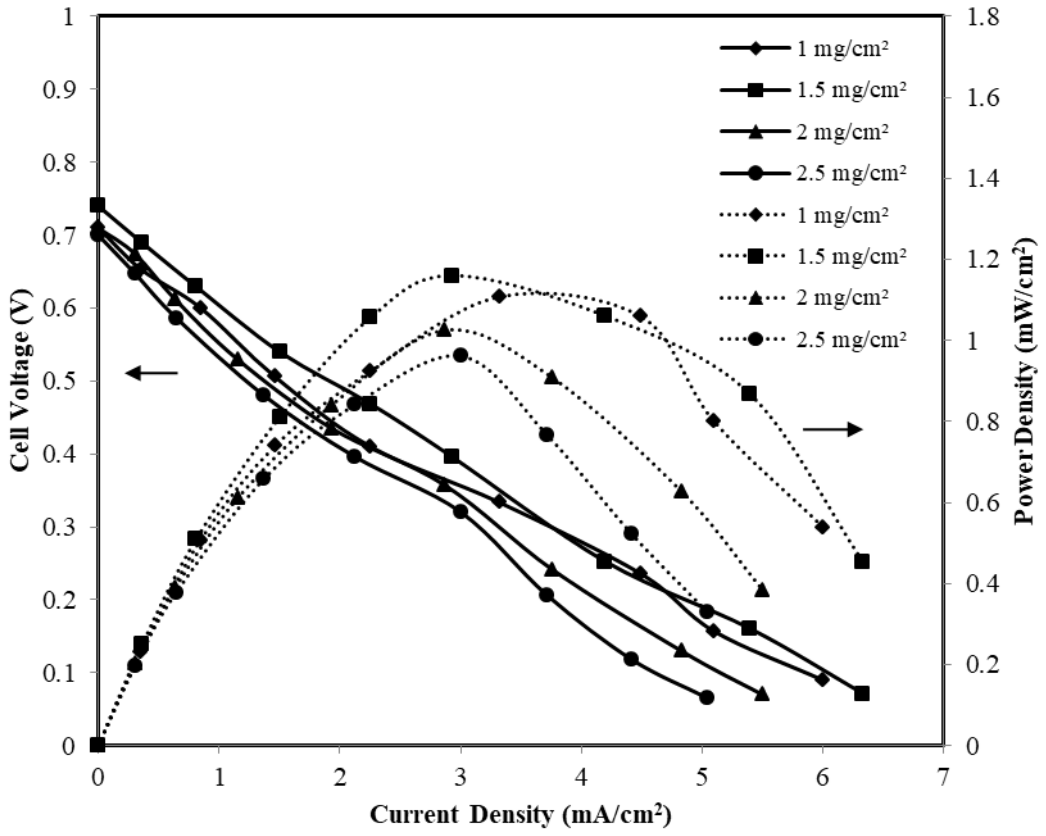

Figure 5.10 Polarization and power density curves of MFC for different loading of anode electrocatalyst and fixed cathode loading of 1 mg/cm^2 Pt/C_{HSA} using anode fed of 0.5 M glycerol mixed with 0.5 M KOH and cathode electrolyte of 0.5 M KOH; MFC temperature: 35 ^oC; Dotted line – power density curves; Solid lines – polarization curves.

It is seen from the Figure 5.10 that the cell performance increases with the increase in electrocatalyst loading from 1 mg/cm^2 to 1.5 mg/cm^2. Further increase in loading beyond 1.5 mg/cm^2, the cell performance decreases. The highest power density of 1.16 mW/cm^2 at a current density of 2.92 mA/cm^2 was obtained for 1.5 mg/cm^2 electrocatalyst loading. At the lowest electrocatalyst loading of 1 mg/cm^2 the maximum power density was 1.1 mW/cm^2 at a current density of 3.3 mA/cm^2. The recorded power densities for the loading of 2 mg/cm^2 and 2.5 mg/cm^2 were very low i.e., giving the maximum power density of 1.02 mW/cm^2 at a current density of 2.86 mA/cm^2 and 0.96 mW/cm^2 at a current density of 3 mA/cm^2, respectively. It shows that even very high loading resulting in very low power density. The active site of electrocatalysts increases with the increase in electrocatalyst loading. Thus, more fuel molecules and OH^- ions interact with the electrocatalyst surface resulting in more electrooxidation reaction which gives more current density and power density. However, increase in loading beyond the optimum loading, the electrocatalyst particles starts to agglomerated at the electrode surface and make it more compact. It creates hindrance for the diffusion of fuel molecules and OH^- ions at the electrode surface which reduces the cell performance.

5.1.4.1.4 Effect of cathode electrocatalyst loading

After optimizing anode electrocatalyst loading at anode, the cathode side loading was also optimized to obtain highest performance from the Y-shaped air breathing MFC. The anode fuel glycerol of 0.5 M mixed with 0.5 M KOH was fed at anode whereas atmospheric oxygen was used as cathode. Figure 5.11 shows the polarization characteristics of MFC using varying cathode electrocatalyst loading of Pt/C_{HSA} ranging from 1 mg/cm^2 to 2.5 mg/cm^2 keeping anode electrocatalyst fixed at the optimum loading of 1.5 mg/cm^2 of Pd-Ni (10:10)/C.

It is seen from Figure 5.11 that the cell performance increases with the increase in the electrocatalyst loading upto 1.5 mg/cm^2 of Pt/$_{CHSA}$ and further increase in loading beyond 1.5 mg/cm^2, the cell performance decreases. The highest power density of 1.16 mW/cm^2 at a current density of 2.92 mA/cm^2 was obtained at the electrocatalyst loading of 1.5 mg/cm^2.

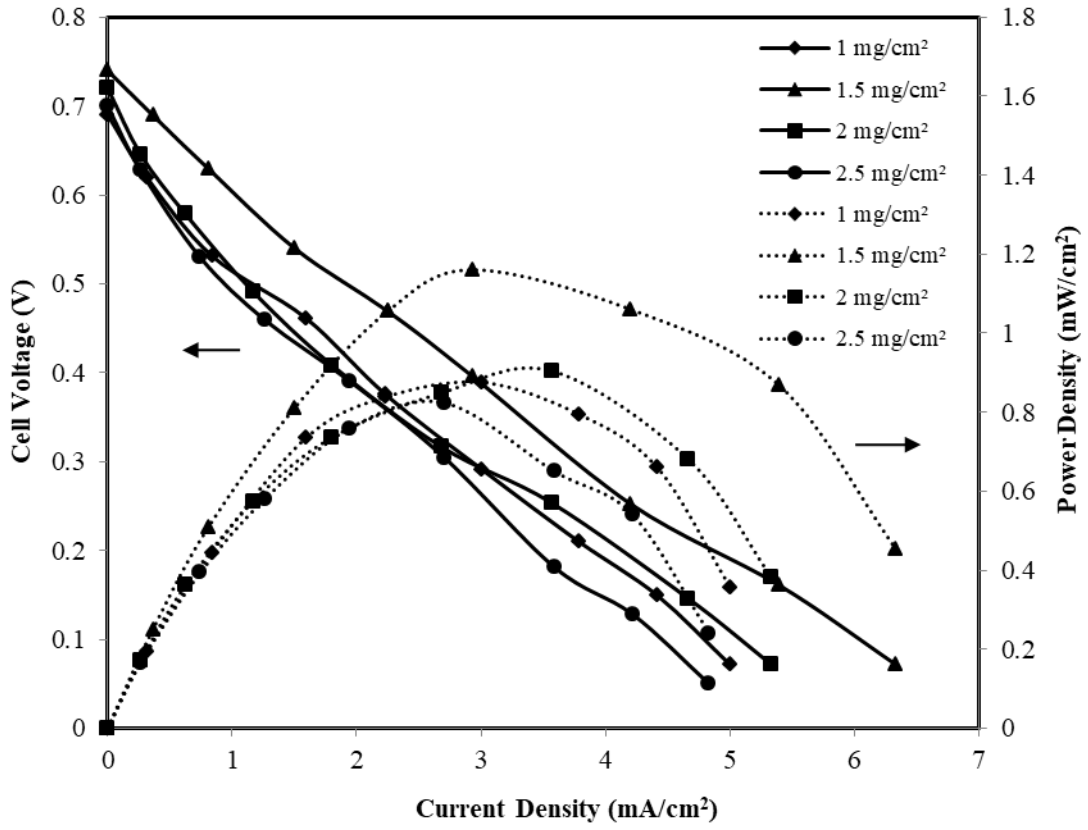

Figure 5.11 Polarization and power density curves of MFC for different loading of cathode electrocatalyst and anode loading of 1.5 mg/cm^2 Pd-Ni (10:10)/C using anode fed of 0.5 M glycerol mixed with 0.5 M KOH and cathode electrolyte of 0.5 M KOH; MFC temperature: 35 ^{o}C ; Dotted line – power density curves; Solid lines – polarization curves.

Whereas, Pt/C_{HSA} of 2 mg/cm^2 and 2.5 mg/cm^2 loading produced power density of 0.9 mW/cm^2 and 0.82 mW/cm^2 at a current density of 3.56 mA/cm^2 and 2.7 mA/cm^2, respectively. At low electrocatalyst loading of 1 mg/cm^2, the MFC produced power density of 0.87 mW/cm^2 at a current density of 3 mA/cm^2.

The highest power density (1.16 mW/cm^2) at 1.5 mg/cm^2 Pt/C_{HSA} was due to optimal compromise between the available surface and particle available without any agglomeration as it has already been discussed in the previous section "5.1.4.1.3 Effect of anode electrocatalyst loading" (page no. 88)

5.1.4.1.5 Effect of anode KOH electrolyte concentration

The effect of electrolyte concentration on the performance of Y-shaped air breathing MFC is shown in Figure 5.12. The anode and cathode were fabricated using optimum loading of 1.5 mg/cm^2 synthesized Pd-Ni (10:10)/C and commercial Pt/C_{HSA} cathode electrocatalyst both. The electrolyte (KOH) concentration was varied from 0.3 M to 1.5 M, while the glycerol concentration was kept fixed at 0.5 M. The electrolyte provides ionic mobility of the OH^- ions and reduces the ohmic loss and thus, increase in electrolyte concentration increases the movements of anions upto KOH concentration of 0.5 M. Further increase in electrolyte concentration beyond 0.5 M KOH, the glycerol molecules get replaced by the OH^- ions at the electrode surface thus, cell performance fall down.

As per anode reaction Equation (1.1) (page no. 9), the presence of glycerol and OH^- ions both are required. A delicate balance between glycerol and OH^- ions will ensure the highest cell performance of MFC which is achieved at the anode KOH concentration of 0.5 M. The optimum concentration of KOH electrolyte was recorded 0.5 M at which the maximum power density 1.16 mW/cm^2 at a current density of 2.92 mA/cm^2 was generated by the cell. At low concentration of 0.3 M KOH, the maximum power density of 0.78 mW/cm^2 at a current density of 2.82 mA/cm^2 was obtained. Moreover, at higher concentration of 1 M and 1.5 M KOH beyond the optimum concentration the power density were 0.96 mW/cm^2 and 0.87 mW/cm^2 at a current density of 2.95 mA/cm^2 and 2.86 mA/cm^2, respectively.

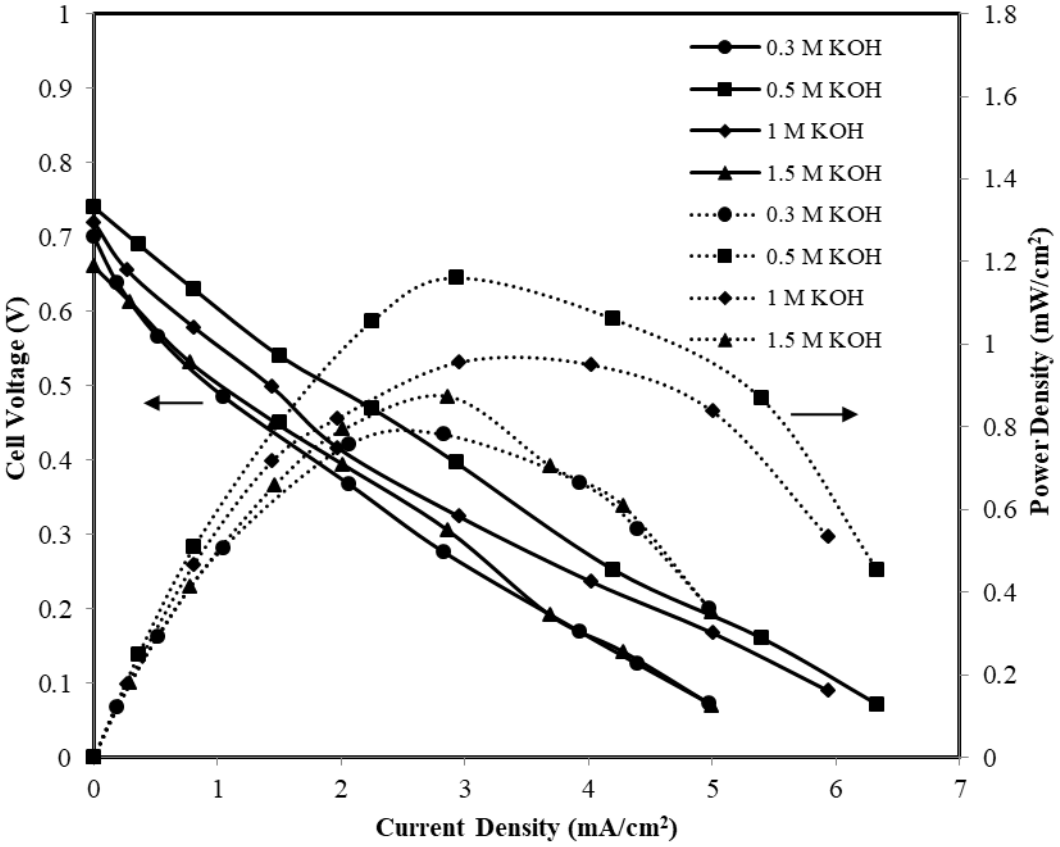

Figure 5.12 Polarization and power density curves of MFC for different anode side KOH concentration mixed with 0.5 M glycerol at anode and cathode electrolyte of 0.5 M KOH; Anode: Pd-Ni (10:10)/C of 1.5 mg/cm^2 and cathode: Pt/C_{HSA} of 1.5 mg/cm^2; MFC temperature: 35 ^oC; Dotted line – power density curves; Solid lines – polarization curves.

5.1.4.1.6 Effect of cathode KOH electrolyte concentration

After optimizing the anode side KOH electrolyte concentration, the cathode side KOH electrolyte concentration was optimized to achieve highest power density form the Y-shaped air breathing MFC. Figure 5.13 shows the effect of cathode electrolyte concentration on polarization and power density curves. The KOH electrolyte concentration of 0.3 M, 0.5 M, 1 M and 1.5 M KOH were used at cathode site for each set of experiments keeping the anode electrolyte concentration at optimum value of 0.5 M KOH. The glycerol of 0.5 M was fed at the anode of MFC. The oxidant at cathode was atmospheric oxygen.

It is seen from the Figure 5.13 that the polarization and power density curves shifted to upward direction when KOH concentration at cathode was increased from 0.3 M to 0.5 M. Further increase in KOH concentration beyond 0.5 M, both the curves decreased due to replacement of water molecules by OH^- ions and thereby reducing water molecules at active electrocatalysts sites of cathode. As shown in Equation (1.2) (page no. 9), the water molecules are essential for the completion of cathodic reaction. Thus, performance of MFC get hindered due to slowness of cathode reaction kinetics.

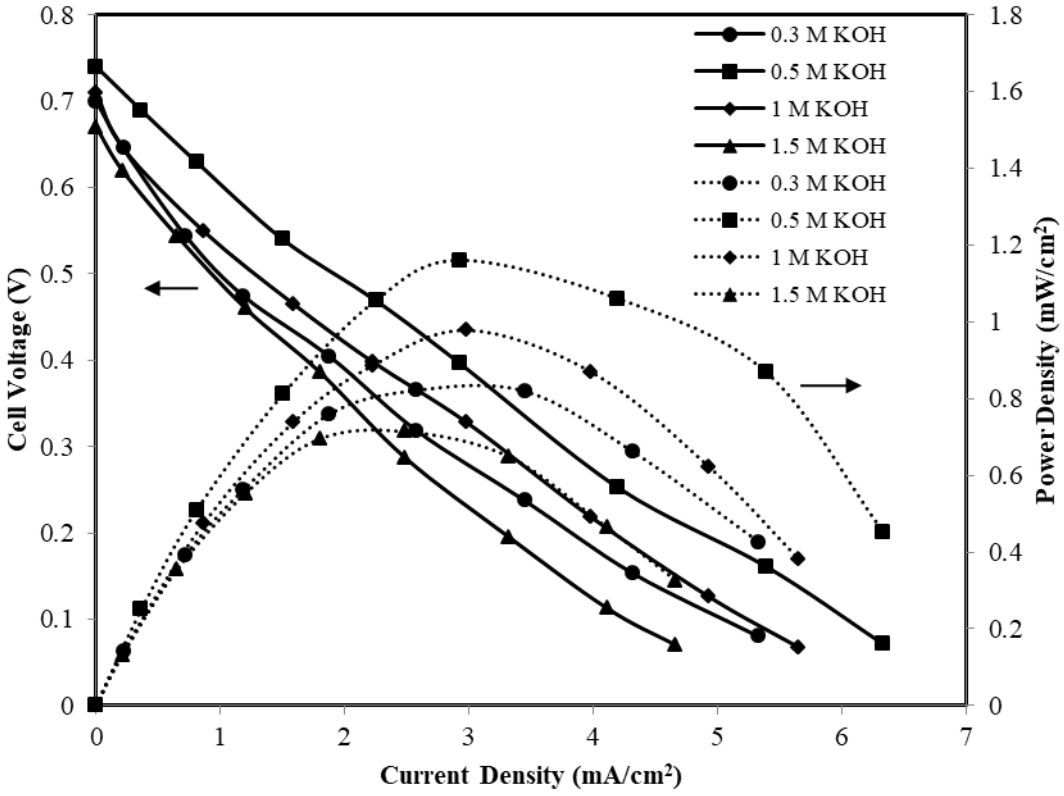

Figure 5.13 Polarization and power density curves of MFC for different cathode side KOH concentration and 0.5 M glycerol mixed with anode KOH electrolyte of 0.5 M KOH; Anode: Pd-Ni (10:10)/C of 1.5 mg/cm^2 and cathode: Pt/C_{HSA} of 1.5 mg/cm^2; MFC temperature: 35 ^oC ; Dotted line – power density curves; Solid lines – polarization curves.

The highest power density of 1.16 mW/cm^2 at a current density of 2.92 mA/cm^2 was obtained at 0.5 M KOH concentration at cathode. While, maximum power density of 0.82 mW/cm^2 at a current density of 2.57 mA/cm^2 for lower concentration of 0.3 M KOH. The

KOH concentration of 1 M and 1.5 M produced low power density of 0.97 mW/cm^2 at a current density of 2.98 mA/cm^2 and 0.71 mW/cm^2 at a current density of 2.48 mA/cm^2, respectively.

5.1.4.1.7 Effect of glycerol concentration

The effect of glycerol concentration on the performance characteristics i.e., polarization and power density curves of Y-shaped air breathing MFC is presented in Figure 5.14. The glycerol concentration was varied from 0.3 M to 1.5 M keeping the anode and cathode electrolyte concentration both fixed at the optimum value of 0.5 M KOH. It is seen in the Figure 5.14, the cell performance increases with the increase in glycerol concentration upto 0.5 M and further increase in glycerol concentration beyond 0.5 M, the cell performance decreases. This decreasing trend in the cell performance was recorded upto 1.5 M of glycerol concentration. It may be due to the increase in glycerol concentration, electrolyte KOH concentration get decreased at the electrocatalysts surface which is unfavourable for the anode electrooxidation reaction.

As per the reaction anode scheme (Equation 1.1), a delicate balance is required between glycerol and OH^- ions at the anode electrocatalysts sites (page no. 9). This has already been discussed in the section "5.1.4.1.5 Effect of anode KOH electrolyte concentration" (page no.91). The maximum power density 1.16 mW/cm^2 at a current density of 2.92 mA/cm^2 was obtained for 0.5 M glycerol concentration mixed with optimum KOH concentration of 0.5 M. The cell performance was very low at 0.3 M glycerol concentration. At this concentration, the maximum power density of 0.88 mW/cm^2 at a current density of 2.55 mA/cm^2 was obtained, due to less availability of OH^- ions relative to glycerol molecules at the surface of electrode.

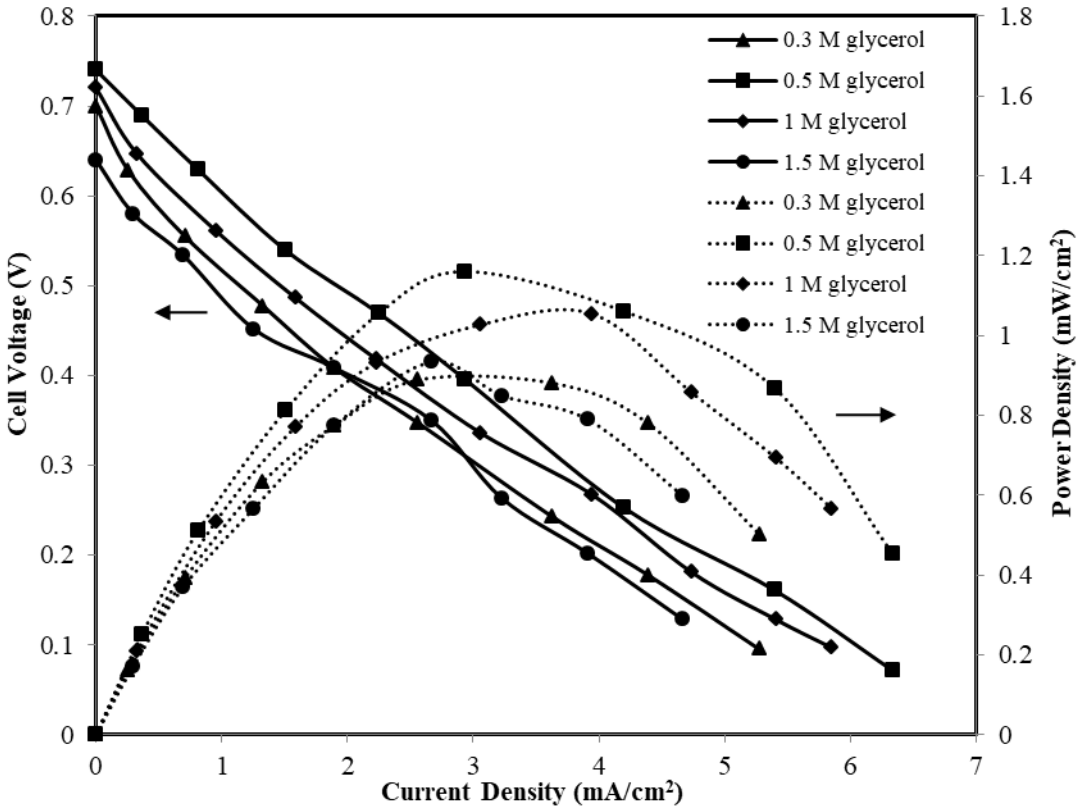

Figure 5.14 Polarization and power density curves of MFC for different glycerol concertation mixed with 0.5 M KOH electrolyte at anode side and cathode electrolyte of 0.5 M KOH; Anode: Pd-Ni (10:10)/C of 1.5 mg/cm^2 and cathode: Pt/C_{HSA} of 1.5 mg/cm^2; MFC temperature: 35 ^oC; Dotted line – power density curves; Solid lines – polarization curves.

On the other side, the relative concentration OH^- ions at the surface of electrocatalysts get decreased at very high concentration of 1 M and 1.5 M glycerol which results lower cell performance in terms of power density 1.05 mW/cm^2 at a current density of 3.94 mA/cm^2 and 0.93 mW/cm^2 at a current density of 2.66 mA/cm^2 were obtained for 1 M and 1.5 M glycerol, respectively.

5.1.4.1.8 Effect of cell temperature

Figure 5.15 shows the polarization and power density curves of Y-shaped air breathing MFC for the varying temperature from 35 ^oC to 95 ^oC using 0.5 M glycerol (optimum) mixed with 0.5 M KOH (optimum) at anode and 0.5 M KOH (optimum) at cathode. The oxidant at cathode was atmospheric oxygen. The maximum cell temperature of 95 ^oC was

maintained keeping in mind the boiling point of water (100 ^{o}C) and avoid two phase flow which would hinder the flow dynamics in the microchannel (Wang et al., 2019). It is seen from the Figure 5.15, the cell performance increases with increase in cell temperature upto 75 ^{o}C. Further increase in temperature beyond 75 ^{o}C, the cell performance decreased rapidly. It may be due to increase in KOH solution conductivity with the increase in temperature for increased mobility of the ions in the solution (Gilliam et al., 2007). It also reduces the ohmic resistance. The maximum OCV of 0.8 V and power density of 1.6 mW/cm^2 at a current density of 5.5 mA/cm^2 was obtained at the temperature of 75 ^{o}C. While, at lower temperature of 35 ^{o}C and 55 ^{o}C, the power density were 1.16 mW/cm^2 at a current density of 2.92 mA/cm^2 and 1.24 mW/cm^2 at a current density of 4.36 mA/cm^2, respectively.

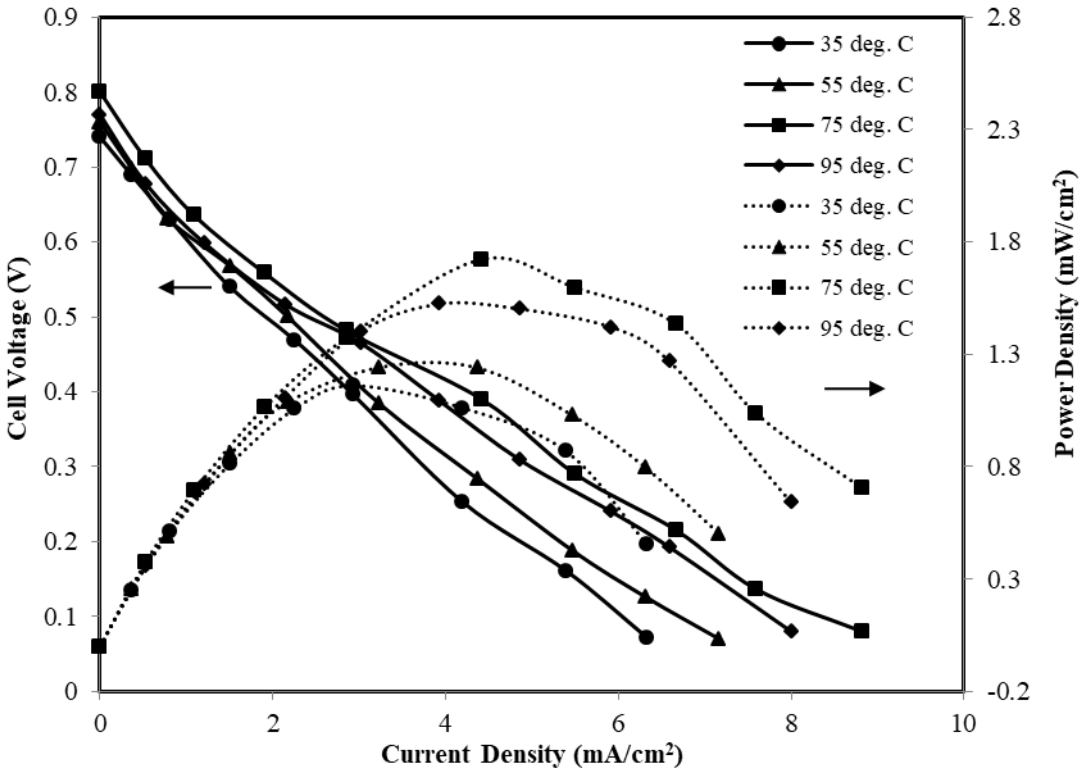

Figure 5.15 Polarization and power density curves of MFC for different cell temperature with 0.5 M glycerol mixed with 0.5 M KOH electrolyte at anode and cathode electrolyte of 0.5 M KOH; Anode: Pd-Ni (10:10)/C of 1.5 mg/cm^2 and cathode: Pt/C_{HSA} of 1.5 mg/cm^2; MFC temperature: 35 ^{o}C ; Dotted line – power density curves; Solid lines – polarization curves.

Whereas, very high cell temperature of 95 ^{o}C, produce the maximum power density of 1.52 mW/cm^2 at a current density of 3.92 mA/cm^2 which is lower than the maximum power density obtained 75 ^{o}C (1.6 mW/cm^2). The power density increased by 37.93 % for the rise in cell temperature from 35 ^{o}C to 75 ^{o}C.

Though, the conductivity of KOH solution has a higher value at an optimum KOH concentration (0.5 M) and it start to decreases for higher concentration due to increase in solution viscosity. The another reason may be due to an increase in water vapor partial pressure, which accelerates the vaporization process of solution, even though the boiling point of water increases by the presence of KOH (Nascimento et al., 2014). The increase in temperature also improves the electrooxidation rate of glycerol molecules at the electrode surface resulting in high current density due to better reaction kinetics (Zhang et al., 2012).

5.1.4.2 T-shaped air breathing MFC

5.1.4.2.1 Effect of flow rate at anode and cathode

As already mentioned in the section "5.1.4.1 Y-shaped air breathing MFC" (page no. 84) that the flow rate of fuel and electrolyte stream is one of the key factors that influence cell performance. Thus, flow rates for both the streams were optimized to achieve highest cell performance. Figure 5.16a represents the effect of the different flow rates of fuel and electrolyte streams for T-shaped air breathing MFC. The flow rate was varied from 0.5 ml/min to 1.6 ml/min in both fuel and electrolyte streams. At first, anode stream was studied at the flow rates of 0.5 ml/min, 0.8 ml/min, 1 ml/min, 1.2 ml/min and 1.6 ml/min keeping the cathode flow rate fixed at 1 ml/min. The cell performance in terms of OCV and power density increases with the increase in anode flow rate upto 1.2 ml/min and further increase in the flow rate beyond 1.2 ml/min, the cell performance decreases drastically.

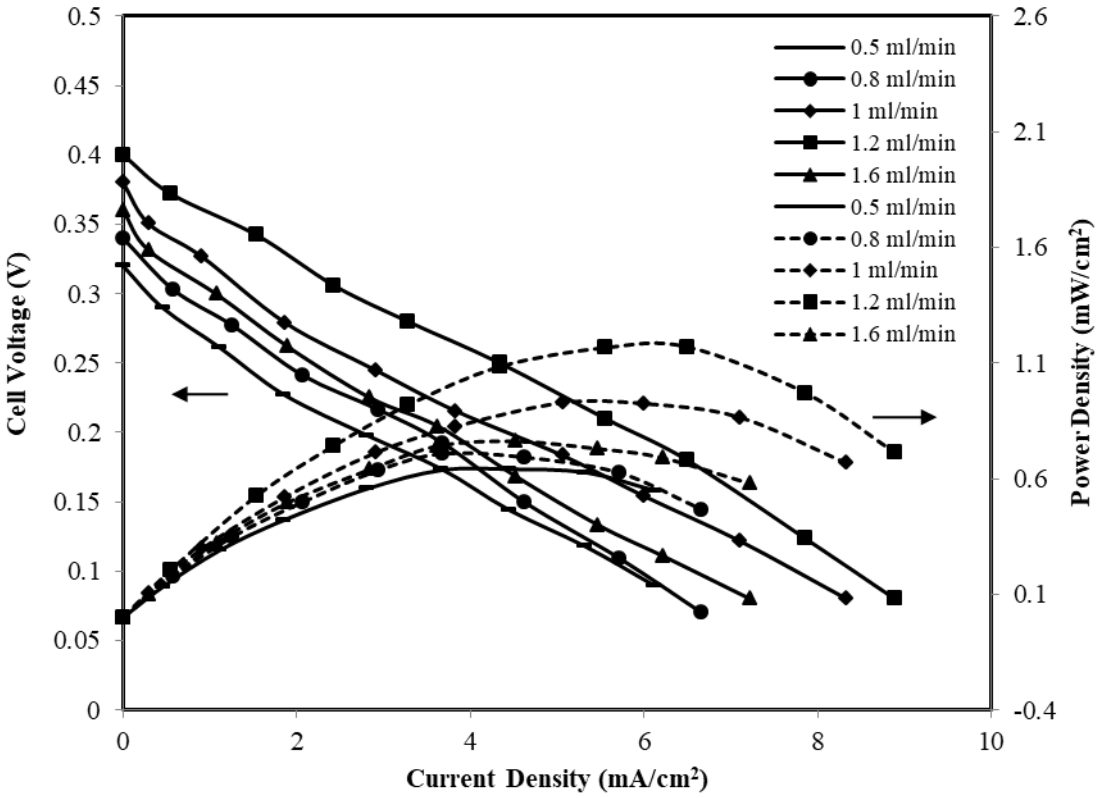

Figure 5.16a Polarization and power density curves of MFC for 1 M glycerol mixed with 1 M KOH at anode and cathode electrolyte of 0.5 M KOH using varying flow rate at anode and fixed flow rate at cathode of 1 ml/min; Anode: Pd-Ni (10:10)/C of 1 mg/cm^2 and cathode: Pt/C_{HSA} of 1 mg/cm^2, MFC temperature: 35 ^oC; Dotted line – power density curves; Solid lines – polarization curves.

The reason for decrease in OCV at low flow rate is due to induces transverse diffusion of the anode and cathode streams. Moreover, at higher flow rate mixing of anode and cathode stream causes decrease in OCV (Liu et al., 2019). The similar trend of power density curves with flow rates were observed as it was seen in the case of Y-shaped air breathing MFC.

After optimizing the anode side flow rate, the cathode side flow rate was varied and optimized in similar way. The cathode stream flow rates of 0.5 ml/min, 0.8 ml/min, 1 ml/min, 1.2 ml/min and 1.6 ml/min were maintained to evaluate the optimum cathode flow rate keeping the anode flow rate at optimum value of 1.2 ml/min.

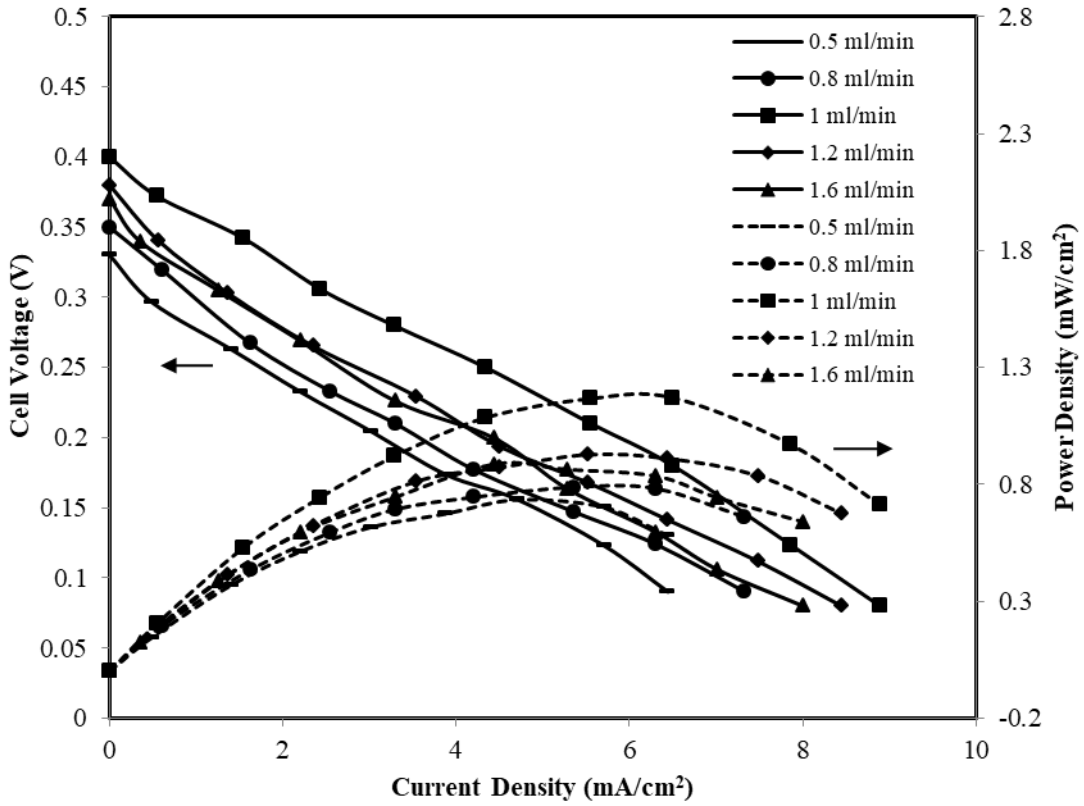

Figure 5.16b Polarization and power density curves of MFC for 1 M glycerol mixed with 1 M KOH at anode and cathode electrolyte of 0.5 M KOH using varying flow rate at cathode and fixed flow rate at anode (1.2 ml/min); Anode: Pd-Ni (10:10)/C of 1 mg/cm^2 and cathode: Pt/C_{HSA} of 1 mg/cm^2, MFC temperature: 35 ^oC; Dotted line – power density curves; Solid lines – polarization curves.

The highest power density of 1.17 mW/cm^2 at a current density of 6.5 mA/cm^2 was obtained for the cathode flow rate of 1 ml/min. Whereas, the maximum power density was 0.70 mW/cm^2, 0.78 mW/cm^2, 0.91 mW/cm^2 and 0.88 mW/cm^2 at a current density current density of 5.7 mA/cm^2, 6.3 mA/cm^2, 5.5 mA/cm^2 and 4.44 mA/cm^2 were obtained at flow rate of 0.5 ml/min, 0.8 ml/min, 1.2 ml/min and 1.6 ml/min, respectively. The reason for such trend in cell performance have already been discussed in earlier (page no. 84) for the Y-shaped air breathing MFC.

At higher flow rates of streams, hydrodynamic instability causes the streams to oscillate which leads to disrupt the interface between two streams (Liu et al., 2019). However, at a slower flow rate of streams causes fuel crossover by diffusion, which results in a mixed

potential at the cathode and lowers the cell performance (Choban et al., 2004). The fuel crossover from anode to cathode becomes easy because of the broadening of the inter diffusion layer between the fuel and the electrolyte streams. The maximum cell performance was observed at an anode flow rate of 1.2 ml/min and cathode flow rate of 1 ml/min with OCV of 0.4 V and maximum power density 1.17 mW/cm^2 at a current density of 6.5 mA/cm^2.

5.1.4.2.2 Effect of anode electrocatalyst type

Figure 5.17 represents the performance characteristics of the T-shaped air breathing MFC for the synthesized Pd-Ni (16:4)/C, Pd-Ni (10:10)/C and Pd-Ni (4:16)/C anode electrocatalyst, respectively. The cathode electrocatalysts was commercial Pt/C_{HSA}. Both the electrodes were constructed with the electrocatalyst loading of $1mg/cm^2$. The anode fuel glycerol of 1 M mixed with 1 M KOH was fed at anode whereas atmospheric oxygen was used as cathode with 0.5 M KOH electrolyte. The anode and cathode streams flow rates were fixed at optimum conditions i.e., 1.2 ml/min at anode and 1 ml/min at cathode in the subsequent experiments of T-shaped air breathing MFC. The highest OCV 0.4 V and power density of 1.17 mW/cm^2 at a current density of 6.5 mA/cm^2 was obtained for synthesized bimetallic Pd-Ni (10:10)/C. Whereas, OCV of 0.35 V and maximum power density of 1.04 mW/cm^2 at a current density of 5.3 mA/cm^2 was obtained for Pd-Ni (16:4)/C anode electrocatalyst. The Pd-Ni (4:16)/C electrocatalysts produces lowest OCV of 0.32 V and lowest power density of 0.65 mW/cm^2 at a current density of 4.33 mA/cm^2 for glycerol electrooxidation. The reason for best performance of Pd-Ni (10:10)/C may be due to higher degree of alloying and low overpotential as already discussed in XRD (page no. 70) and CV studies (page no. 76), respectively.

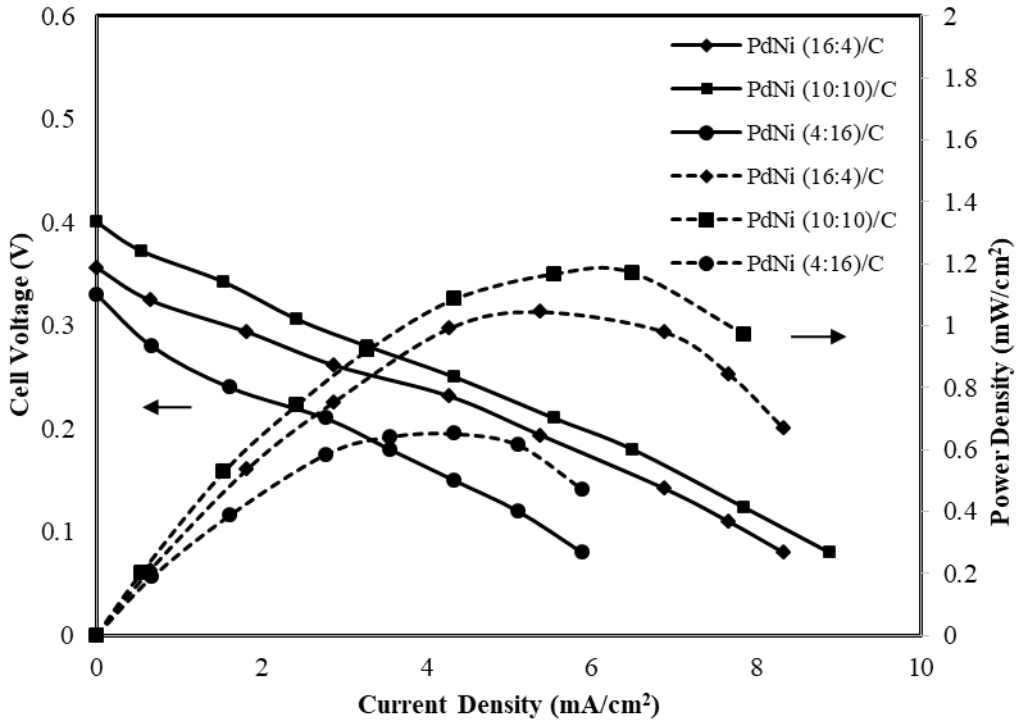

Figure 5.17 Polarization and power density curves from air breathing MFC for the different types of anode electrocatalyst using anode fed of 1 M glycerol mixed with 1 M KOH and cathode electrolyte of 0.5 M KOH with atmospheric air as oxidant; cathode: Pt/C_{HSA} of 1 mg/cm^2; MFC temperature: 35 ^oC; Dotted line – power density curves; Solid lines – polarization curves.

5.1.4.2.3 Effect of anode electrocatalyst loading

The single cell study using various types anode electrocatalyst shows that the synthesized Pd-Ni (10:10)/C electrocatalyst performs better among all tested electrocatalysts. Thus, the anode loading was varied in the T-shaped air breathing MFC using synthesized Pd-Ni (10:10)/C to get highest cell performance at the optimum anode loading. The anode fuel glycerol of 1 M mixed with 1 M KOH was fed at anode whereas atmospheric oxygen was used as cathode oxidant along with 0.5 M KOH. Figure 5.18 shows the performance characteristics of air breathing MFC for different loading of Pd-Ni (10:10)/C electrocatalyst at anode varying from 0.5 mg/cm^2 to 2 mg/cm^2. The electrocatalyst loading at cathode Pt/C_{HSA} was kept 1 mg/cm^2 same for each set of experiments. It is seen from the Figure 5.18 that the cell performance increases with the increase in loading from

0.5 mg/cm^2 to 1 mg/cm^2. Further increase in loading beyond 1 mg/cm^2, the cell performance decreases. The maximum OCV of 0.4 V and maximum power density of 1.17 mW/cm^2 at a current density of 6.5 mA/cm^2 was obtained for 1 mg/cm^2 electrocatalyst loading. At the lowest electrocatalyst loading of 0.5 mg/cm^2 the maximum power density was 0.86 mW/cm^2 at a current density of 5.2 mA/cm^2. The recorded power densities for the loading of 1.5 mg/cm^2 and 2 mg/cm^2 were very low i.e., giving the maximum power density of 0.72 mW/cm^2 at a current density of 4.70 mA/cm^2 and 0.66 mW/cm^2 at a current density of 4.3 mA/cm^2, respectively. It shows that even very high loading resulting in very low power density.

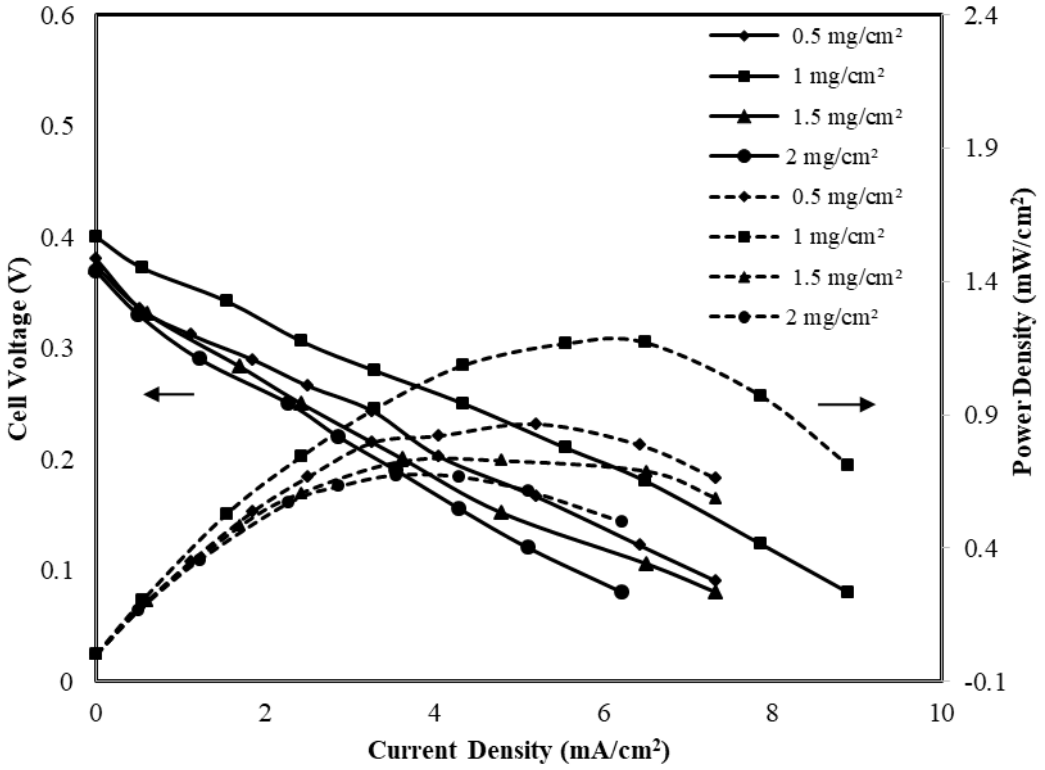

Figure 5.18 Polarization and power density curves from air breathing MFC for varying loading of anode electrocatalyst Pd-Ni (10:10/C) and fixed cathode loading of 1 mg/cm^2 Pt/C_{HSA} using anode fed of 1 M glycerol mixed with 1 M KOH and cathode electrolyte of 0.5 M KOH with atmospheric air as oxidant; MFC temperature: 35 ^oC ; Dotted line – power density curves; Solid lines – polarization curves.

It may be due to the increase in the active site of electrocatalyst with the increase in electrocatalyst loading. Thus, more fuel molecules and OH^- ions interact with the electrocatalyst surface resulting in more electrooxidation reaction which gives more current density and power density. However, increase in loading beyond the optimum loading, the electrocatalyst particles starts to agglomerated at the electrode surface and make it more compact. It creates hindrance for the diffusion of fuel molecules and OH^- ions at the electrode surface which reduces the cell performance and it has already been discussed earlier for the Y-shaped MFC (page no. 88).

5.1.4.2.4 Effect of cathode electrocatalyst loading

After optimizing anode electrocatalyst loading at anode, the cathode side loading was also optimized to obtain highest performance from the T-shaped air breathing MFC. The anode fuel glycerol of 1 M mixed with 1 M KOH was fed at anode whereas atmospheric oxygen was used as oxidant at cathode along with 0.5 M KOH. Figure 5.19 shows the polarization characteristics of MFC using varying cathode electrocatalyst loading of Pt/C_{HSA} ranging from 0.5 mg/cm^2 to 2 mg/cm^2 keeping anode electrocatalyst fixed at the optimum loading of 1 mg/cm^2 of Pd-Ni(10:10)/C. It is seen from Figure 5.19 that the cell performance increases with the increase in the electrocatalyst loading upto 1 mg/cm^2 of $Pt/_{CHSA}$ and further increase in loading beyond 1 mg/cm^2, the cell performance decreases. The maximum OCV of 0.4 V and maximum power density of 1.17 mW/cm^2 at a current density of 6.5 mA/cm^2 was obtained at the electrocatalyst loading of 1 mg/cm^2. Whereas, Pt/C_{HSA} of 1.5 mg/cm^2 and 2 mg/cm^2 loading produced power density of 0.86 mW/cm^2 and 0.85 mW/cm^2 at a current density of 4.8 mA/cm^2 and 4.9 mA/cm^2, respectively. At low electrocatalyst loading of 0.5 mg/cm^2 produced power density of 0.82 mW/cm^2 at a current density of 5.17 mA/cm^2. The highest power density of 1.17 mW/cm^2 at the cathode loading of 1 mg/cm^2 Pt/C_{HSA} was due to optimal compromise between the

available surface and particle available without any agglomeration as already been discussed in the previous section "5.1.4.2.3 Effect of anode electrocatalyst loading" (page no. 101).

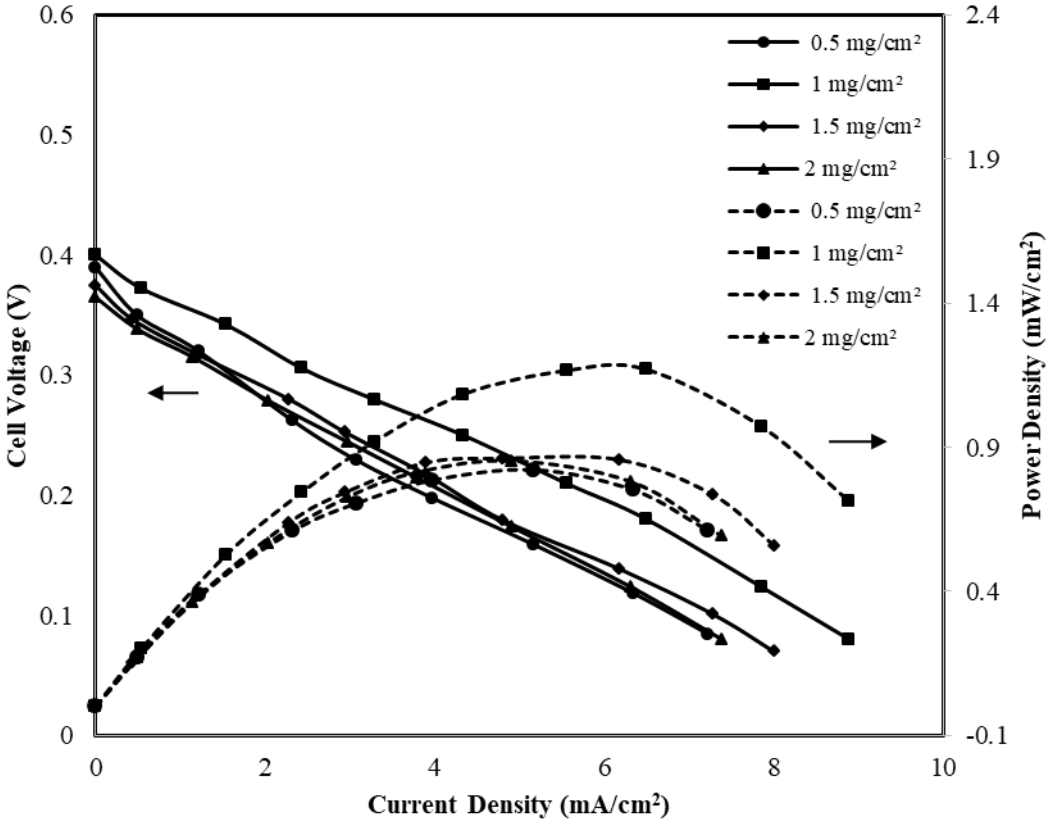

Figure 5.19 Polarization and power density curves from air breathing MFC for varying loading of cathode electrocatalyst and optimum anode loading of 1 mg/cm^2 Pd-Ni (10:10)/C using anode fed of 1 M glycerol mixed with 1 M KOH and cathode fed of 0.5 M KOH electrolyte with atmospheric air as oxidant; MFC temperature: 35 ^{o}C; Dotted line – power density curves; Solid lines – polarization curves.

5.1.4.2.5 Effect of glycerol concentration

The effect of glycerol concentration on the performance characteristics i.e., polarization and power density curves of T-shaped air breathing MFC is presented in Figure 5.20. The glycerol concentration was varied from 0.5 M to 2 M keeping the anode and cathode electrolyte concentration both fixed at the optimum value of 0.5 M KOH. It is seen in the Figure 5.20, the cell performance increases with the increase in glycerol concentration upto 1 M and further increase in glycerol concentration beyond 1 M, the cell performance

decreases. This decreasing trend in the cell performance was recorded upto 2 M of glycerol concentration. It may be due to the increase in glycerol concentration, electrolyte KOH concentration get decreased at the electrocatalysts surface which is unfavourable for the anode electrooxidation reaction.

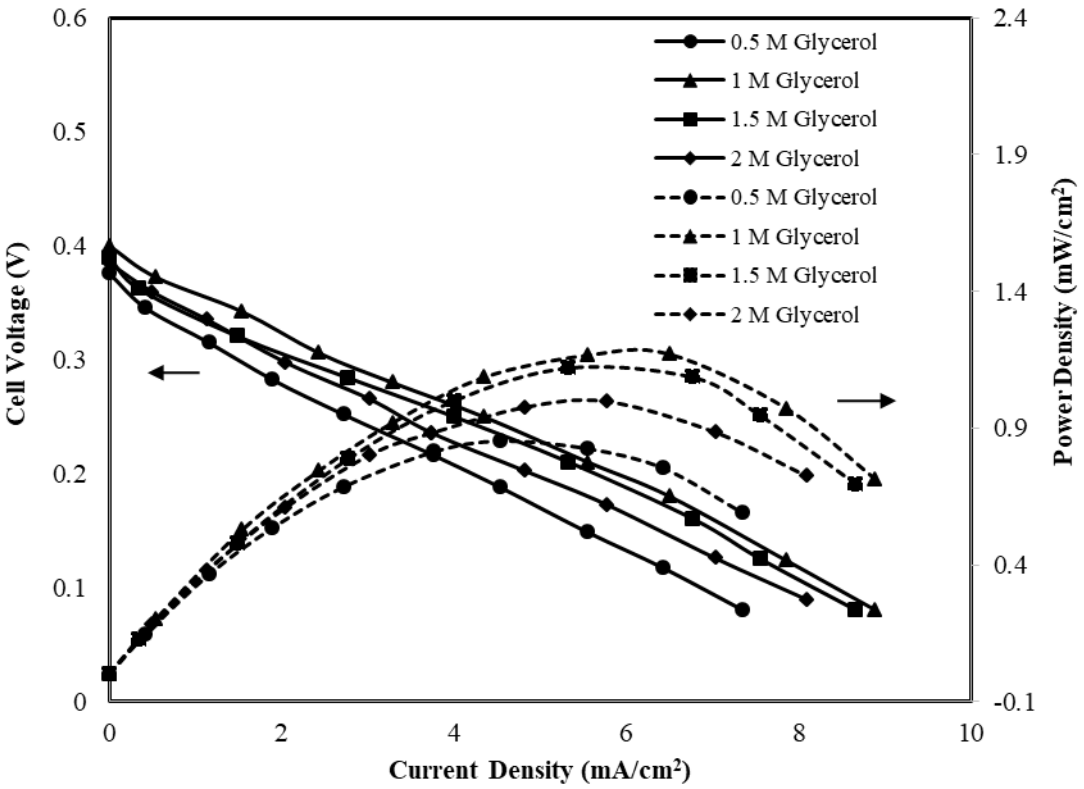

Figure 5.20 Polarization and power density curves from air breathing MFC for varying glycerol concentration mixed with 1 M KOH electrolyte at anode side and 0.5 M KOH electrolyte with atmospheric air as oxidant at cathode side. Anode electrocatalyst was optimum 1 mg/cm^2 Pd-Ni (10:10)/C; Cathode electrocatalyst was optimum 1 mg/cm^2 Pt/C_{HSA}; MFC temperature: 35 ^oC; Solid lines – polarization curves; Dotted lines – power density curves.

As per the reaction anode scheme (Equation 1.1), a delicate balance is required between glycerol and OH^- ions at the anode electrocatalysts sites (page no. 9). The maximum OCV 0.4 V and power density 1.17 mW/cm^2 at a current density of 6.5 mA/cm^2 was obtained for 1 M glycerol concentration mixed with KOH concentration of 1 M. The cell performance was very low at 0.5 M glycerol concentration. At this concentration, the maximum power density of 0.85 mW/cm^2 at a current density of 6.5 mA/cm^2 was

obtained, due to less availability of OH^- ions relative to glycerol molecules at the surface of electrode. On the other side, the relative concentration OH^- ions at the surface of electrocatalysts get decreased at very high concentration of 1.5 M and 2 M glycerol which results lower cell performance in terms of power density of 1.12 mW/cm^2 at a current density of 5.3 mA/cm^2 and 1 mW/cm^2 at a current density of 5.7 mA/cm^2 were obtained for 1.5 M and 2 M glycerol, respectively.

5.1.4.2.6 Effect of anode KOH concentration

The effect of electrolyte concentration on the performance of Y-shaped air breathing MFC is shown in Figure 5.21. The anode and cathode were fabricated using optimum loading of 1 mg/cm^2 synthesized Pd-Ni (10:10)/C and commercial Pt/C_{HSA} cathode electrocatalyst both. The electrolyte (KOH) concentration was varied from 0.5 M to 2 M, while the glycerol concentration was kept fixed at optimum 1 M. The electrolyte provides ionic mobility of the OH^- ions and reduces the ohmic loss and thus, increase in electrolyte concentration increases the movements of anions increases upto KOH concentration of 1 M. Further increase in electrolyte concentration beyond 0.5 M KOH, the glycerol molecules get replaced by the OH^- ions at the electrode surface thus, cell performance fall down. As per anode reaction Equation (1.1) (page no. 9), the presence of glycerol and OH^- ions both are required. As already discussed, a delicate balance between glycerol and OH^- ions will ensure the highest cell performance of MFC which reached at the anode KOH concentration of 1 M. The optimum concentration of KOH electrolyte was recorded 1 M at which the maximum power density 1.17 mW/cm^2 at a current density of 6.5 mA/cm^2 was generated by the cell.

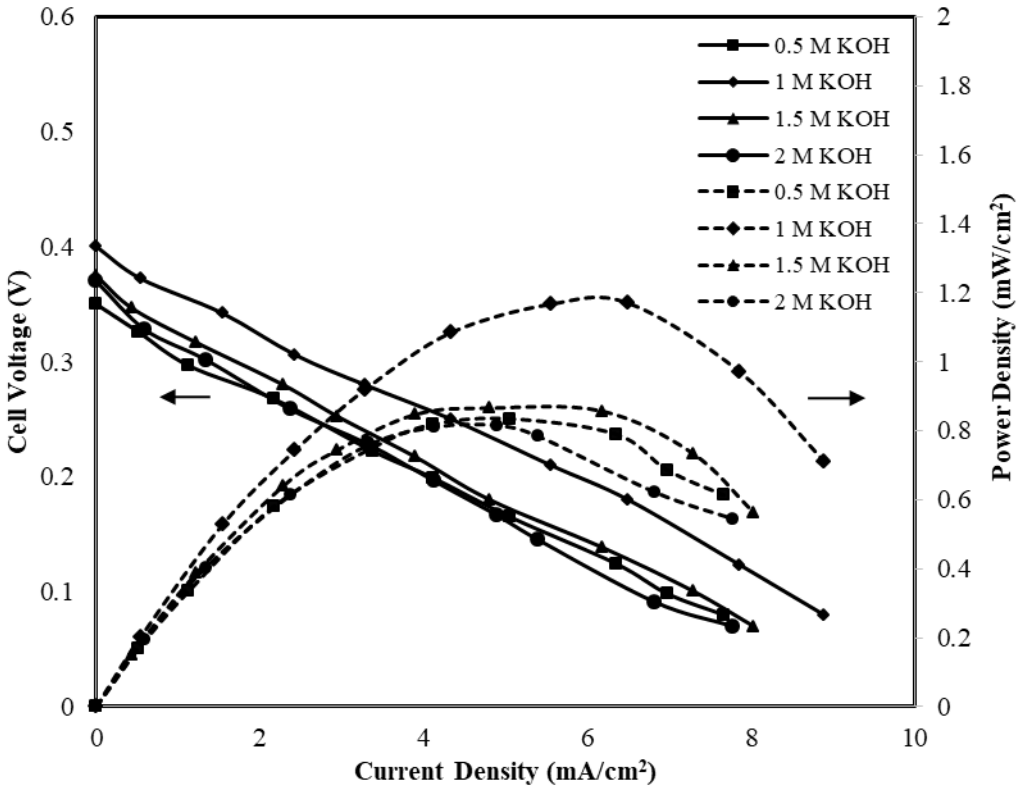

Figure 5.21 Polarization and power density curves for varying concentration of KOH electrolyte at anode side mixed with optimum 1 M glycerol and 0.5 M KOH electrolyte with atmospheric air as oxidant at cathode side. Anode electrocatalyst was optimum 1 mg/cm^2 Pd-Ni (10:10)/C; Cathode electrocatalyst was optimum 1 mg/cm^2 Pt/C_{HSA}; MFC temperature: 35 ^oC; Solid lines – polarization curves; Dotted lines – power density curves.

At low concentration of 0.5 M KOH, the maximum power density of 0.83 mW/cm^2 at a current density of 5.05 mA/cm^2 was obtained. Moreover, at higher concentration of 1.5 M and 2 M KOH beyond the optimum concentration (1 M) the power density were 0.86 mW/cm^2 and 0.81 mW/cm^2 at a current density of 4.8 mA/cm^2 and 4.89 mA/cm^2, respectively.

5.1.4.2.7 Effect of cathode KOH concentration

After optimizing the anode side KOH electrolyte concentration, the cathode side KOH electrolyte concentration was optimized to achieve highest power density form the T-shaped air breathing MFC. Figure 5.22 shows the effect of cathode electrolyte concentration on polarization and power density curves. The KOH electrolyte

concentration of 0.3 M, 0.5 M, 1 M and 1.5 M KOH were used at cathode site for each set of experiments keeping the anode electrolyte concentration at optimum value of 1 M KOH. The glycerol of 1 M was fed at the anode of MFC. It is seen from the Figure 5.22 that the polarization and power density curves shifted to upward direction when KOH concentration at cathode was increased from 0.3 M to 1 M. Further increase in KOH concentration beyond 1 M, both the curves shifted downward due to replacement of water molecules by OH^- ions and thereby reducing water molecules at active electrocatalysts sites of cathode.

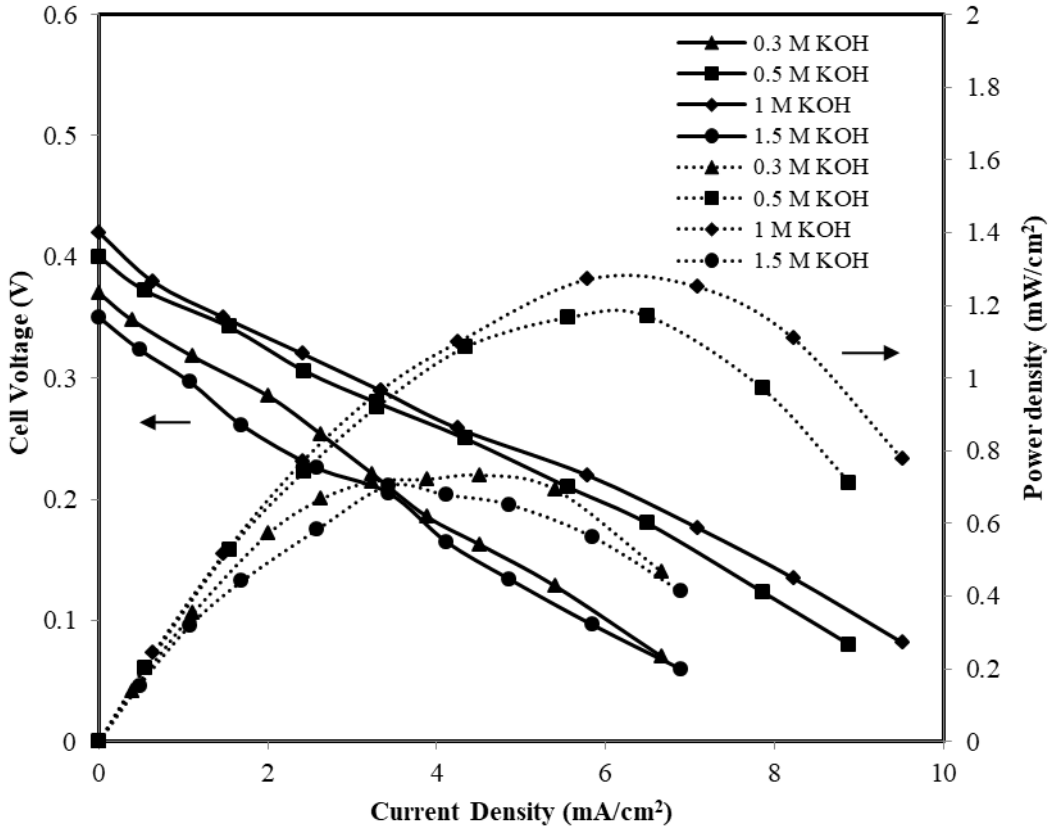

Figure 5.22 Polarization and power density curves for varying concentration of KOH electrolyte with atmospheric air as oxidant at cathode side and optimum 1 M glycerol and 1 M KOH electrolyte at anode side. The anode electrocatalyst was optimum loading 1 mg/cm^2 of Pd-Ni(16:4)/C and cathode electrocatalyst was optimum loading 1 mg/cm^2 of Pt/C_{HSA} for both cases; MFC temperature: 35 ^oC; Solid lines – polarization curves; Dotted lines – power density curves.

As shown in Equation (1.2) (page no. 9), the water molecules are essential for the completion of cathodic reaction. Thus, performance of MFC hindered due to slowness of cathode reaction kinetics. The oxidant at cathode was atmospheric oxygen. The highest power density of 1.27 mW/cm^2 at a current density of 5.77 mA/cm^2 was obtained at 1 M KOH concentration at cathode. While, maximum power density of 0.73 mW/cm^2 at a current density of 4.5 mA/cm^2 for lower concentration of 0.3 M KOH. The KOH concentration of 0.5 M and 1.5 M produced power density of 1.17 mW/cm^2 at a current density of 6.5 mA/cm^2 and 0.7 mW/cm^2 at a current density of 3.42 mA/cm^2, respectively.

5.1.4.2.8 Effect of cell temperature

Figure 5.23 shows the polarization and power density curves of T-shaped air breathing MFC for the varying temperature from 35 ^oC to 95 ^oC using 1 M glycerol (optimum) mixed with 1 M KOH (optimum) at anode and 1 M KOH at cathode. The oxidant at cathode was atmospheric oxygen. The optimum flow rates of 1.2 ml/min and 1 ml/min were maintained at anode and cathode stream, respectively. As mentioned earlier, the MFC was operated at the maximum temperature of 95 ^oC was maintained keeping in mind the boiling point of water (100 ^oC) and avoid two phase flow which would hinder the flow dynamics in the microchannel (Wang et al., 2019). It is seen from the Figure 5.23, the cell performance increases with increase in temperature upto 75 ^oC. Further increase in temperature beyond 75 ^oC, the cell performance decreases rapidly. It may be due to increase in KOH solution conductivity with the increase in temperature for increased mobility of the ions in the solution (Gilliam et al., 2007). It also reduces the ohmic resistance. Thus, the highest cell performance was obtained at the temperature of 75 ^oC. The maximum power density of 2.14 mW/cm^2 at a current density of 8.96 mA/cm^2

was obtained at the temperature of 75 ^{o}C. While, at lower temperature of 35 ^{o}C and 55 ^{o}C, the power density were 1.27 mW/cm^2 at a current density of 6.7 mA/cm^2 and 1.46 mW/cm^2 at a current density of 6.7 mA/cm^2, respectively.

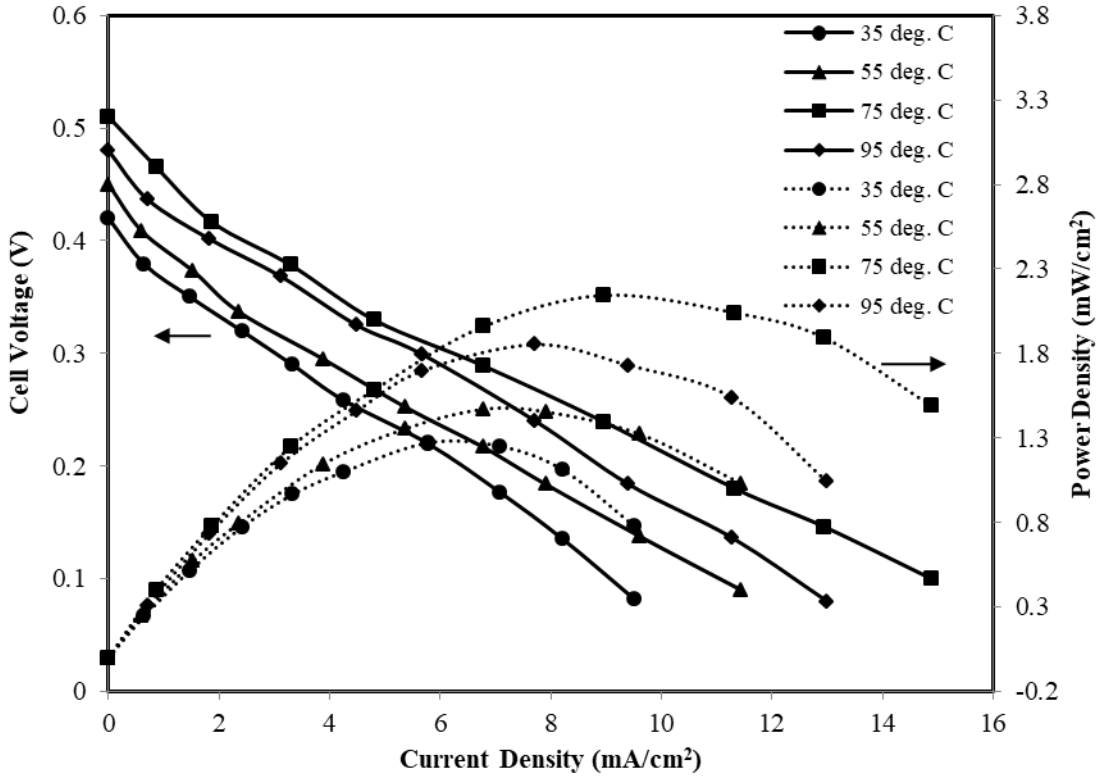

Figure 5.23 Polarization and power density curves of MFC for different cell temperature with 1 M glycerol mixed with 1 M KOH electrolyte at anode and cathode electrolyte of 1 M KOH; Anode: Pd-Ni (10:10)/C of 1 mg/cm^2 and cathode: Pt/C_{HSA} of 1 mg/cm^2; MFC temperature: 35 ^{o}C; Dotted line – power density curves; Solid lines – polarization curves.

Whereas, very high cell temperature of 95 ^{o}C, produce the maximum power density of 1.85 mW/cm^2 at a current density of 7.71 mA/cm^2 which is lower than the maximum power density obtained at the temperature of 75 ^{o}C (2.14 mW/cm^2). The power density increased by 68.50 % for the rise in cell temperature from 35 ^{o}C to 75 ^{o}C. The reason for the dependency of MFC performance on cell temperature have already been discussed in Y-shaped MFC performance (page no. 95-97).

5.1.4.2.9 Bleaching and air as mixed oxidant for air breathing MFC

Figure 5.24 shows the polarization and power density characteristics of different concentration of calcium hypochlorite/$Ca(OCl)_2$ in presence of air at the room temperature of 35 ^{o}C. The purpose of using mixed oxidant was to study the effect of calcium hypochlorite along with atmospheric oxygen as oxidant in MFC. The calcium hypochlorite of varying concentrations was mixed with optimum electrolyte concentration of 1 M KOH before the solutions fed to the cathode side of the MFC. As proposed by Momoh, (2011) in the Equation (5.4), calcium hypochlorite reacts with water to form hypochorous acid and calcium hydroxide. The formed calcium hydroxide settle down in the beaker and rest of the liquid was used as oxidant for the MFC experiment. In alkaline medium, hypochlorous acid is converted into hypochlorite ions as shown in Equation (5.5). The reaction from the conversion of calcium hypochlorite to hypochlorite ion is given in Equation (5.6), and the overall cathode side reaction is given by Equation (5.7) (Martins et al., 2018).

$$Ca(OCl)_2 + 2\,H_2O \rightarrow 2\,HOCl + Ca(OH)_2 \quad (5.4)$$

$$2\,HOCl + 2\,OH^- \rightarrow 2\,OCl^- + 2\,H_2O \quad (5.5)$$

$$Ca(OCl)_2 + 2\,OH^- \rightarrow 2\,OCl^- + Ca(OH)_2 \quad (5.6)$$

$$2\,ClO^- + H_2O + 2e^- \rightarrow 2\,Cl^- + 2OH^- \quad (5.7)$$

The combined effect of mixed oxidant air and hypochlorite ion is shown in cathode reduction in Equation (1.2) (page no. 9) and Equation (5.7), enhanced the MFC performance significantly. The CV study of the cathode in the half cell using mixed oxidant calcium hypochlorite and oxygen also showed better performance in comparison to only oxygen as oxidant (page no. 82).

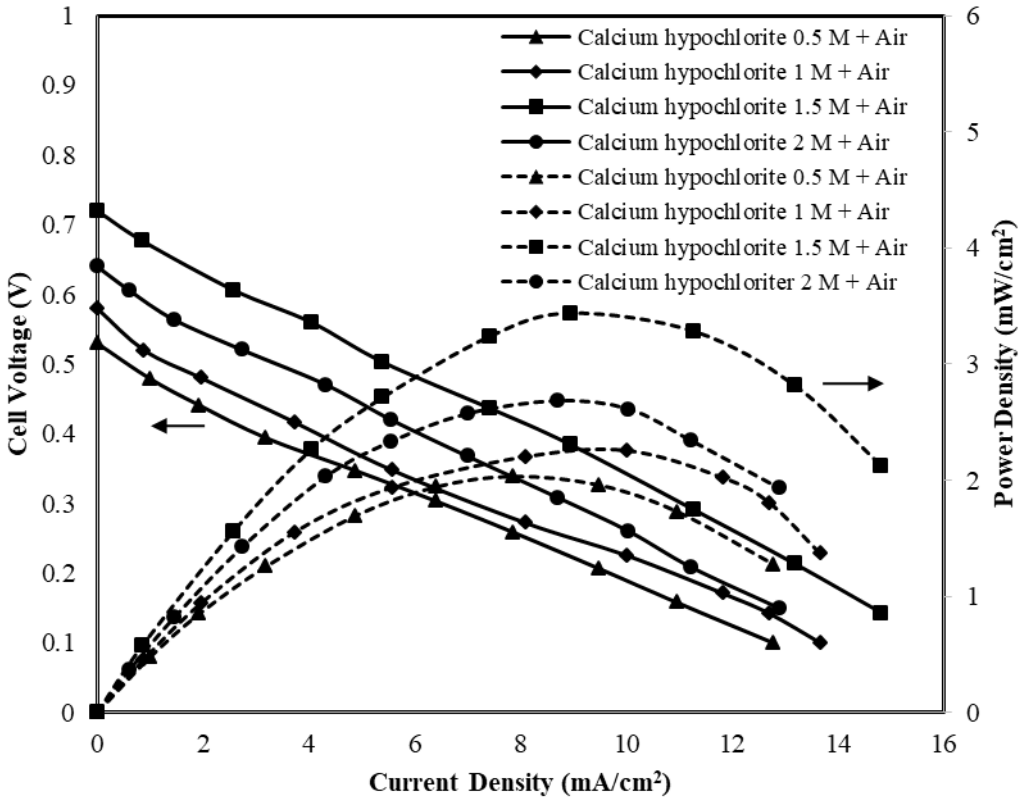

Figure 5.24 Polarization and power density curves from air breathing MFC for varying concentrations of calcium hypochlorite and atmospheric air as mixed oxidant as catholyte and optimum 1 M glycerol mixed with 1 M KOH electrolyte as anolyte. The anode electrocatalyst was 1 mg/cm^2 of Pd-Ni (10:10)/C and cathode electrocatalyst was 1 mg/cm^2 of Pt/C_{HSA}. MFC temperature: 35 ^oC; Solid lines – polarization curves; Dotted lines – power density curves.

The cathode peak shifted towards more positive potential (-0.27 V) for the mixed oxidant condition. It is seen from the Figure 5.24 that MFC performace increases with the increase in $Ca(OCl)_2$ concentration upto 1.5M and futher increase in oxidant concentration 2M, the cell performance decreases. It may be due to the less avialability of water molecules at the active catalysts sites at higher oxidant concentration and thus, the cell performace reduces in terms of OCV and power density. The oxidant/$Ca(OCl)_2$ concentration of 1.5 M and air produced very high OCV of 0.72 V with highest power density of 3.43 mW/cm^2 at a current density of 8.93 mA/cm^2. Whereas, OCV of 0.53 V was found at oxidant concentration of 0.5 M with a maximum power density of 2.03 mW/cm^2 at the current density of 7.86 mA/cm^2. At, oxidant/$Ca(OCl)_2$ concentration of 1

M and air produced OCV of 0.58 V with highest power density of 2.25 mW/cm^2 at a current density of 10.01 mA/cm^2. Very high concentration of oxidant/$Ca(OCl)_2$ of 2 M and air produced low OCV of 0.62 V and maximum power density was also reduced to 2.68 mW/cm^2.

It should be noted that the performance of MFC was found highest for the mixed oxidant condition using 1.5M of $Ca(OCl)_2$ in presence of air. At this condition a delicate balance is establish between water molecules, OCl^- ions and oxygen which are essential to complete the ctahode reations at the active sites of the Pt/C_{HSA} electrocatalysts.

5.1.4.2.10 Effect of different types of oxidants at cathode

The performance MFC using mixed oxidant calcium hypochlorite and air was compared with another popular hypochlorite i.e., sodium hypochlorite and air as mixed oxidant. Figure 5.25 shows the performance characteristics of glycerol based MFC using the above combination of cathode oxidants. All the parameters used at anode were optimum conditions obtained using T-shaped air breathing MFC reported earlier. It is clearly seen from Figure 5.25 that only air as oxidant produced lowest power density of 1.27 mW/cm^2 at a current density of 5.77 mA/cm^2. The power density increased significantly and reached to highest value (3.43 mW/cm^2) when mixed oxidant $Ca(OCl)_2$ and air was used at cathode. The other oxidant NaOCl and air mixture produced moderate power density of 1.52 mW/cm^2 which is lower than $Ca(OCl)_2$ based mixed oxidant. The reason for higher cell performance in terms of OCV and current density using calcium hypochlorite is the pH value. As reported in literature, the oxygen reduction reaction kinetics improves at higher pH value (Osmieri et al., 2017). The pH value for the concentration of 1.5 M sodium hypochlorite is 9.74, while 1.5 M calcium hypochlorite is 11.61.

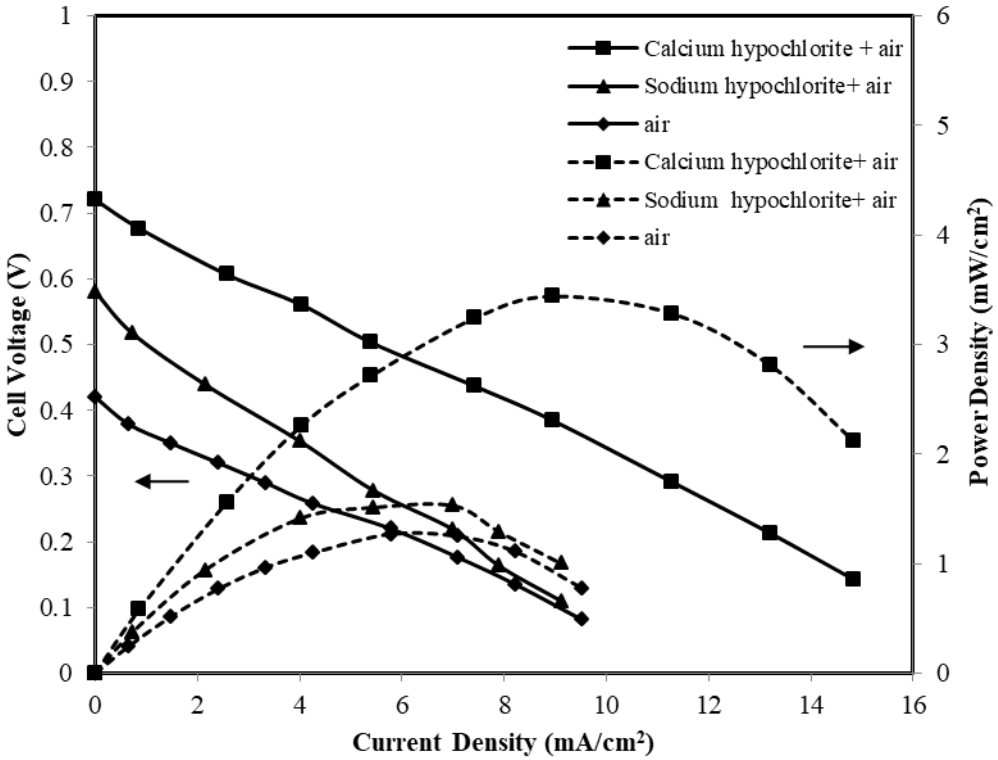

Figure 5.25 Comparison of polarization and power density curves for different types of hypochlorite with air as mixed oxidant and atmospheric air oxidant in air breathing MFC. Anolyte: 1 M glycerol mixed with optimum concentration of 1 M KOH; Catholyte: 1 M KOH. Pd-Ni (10:10)/C anode electrocatalyst of 1 mg/cm^2 and Pt/C_{HSA} cathode electrocatalyst of 1 mg/cm^2. MFC temperature: 35°C. Solid line – polarization curves; Dotted line – power density curves.

5.2 Performance evaluation of Pd-Pt/C anode electrocatalyst: Part II

5.2.1 Physical characterization

5.2.1.1 XRD analysis

The XRD analysis of synthesized electrocatalyst Pd/C and bimetallic Pd-Pt (16:4)/C, Pd-Pt (10:10)/C, and Pd-Pt (4:16)/C of various compositions are shown in Figure 5.26. The peak value at 2θ position of 25^{o} to the plane (002) of a hexagonal structure is related to the carbon support material. The diffraction patterns show the characteristics of crystalline face-centered cubic (FCC) Pd, with all peaks corresponding to (111), (200), and (220) planes. The main peaks for pure Pd appear at 2θ values of 40.1° (111), 46.7° (200) and 68.1° (220) comply with the standard of JCPDS (05 0681) (Panjiara and Pramanik 2020a). The main peaks (JCPDS 040802) for pure Pt appear at 2θ values of 39.76^{o} (111), 46.27^{o} (200) and 67.5° (220). The average crystallite sizes were determined using Scherrer's equation (Equation 5.1) on the diffraction peak at the plane (111) and the lattice parameter was calculated using Bragg's equation (Equation 5.2) (Choudhary and Pramanik 2019).

The diffraction peaks of Pd-Pt/C are shifted to lower 2θ values compared to Pd/C as shown in Table 5.5 distinctly for the plane (111). The 2θ values at (111) plane for the synthesized Pd-Pt (16:4)/C, Pd-Pt (10:10)/C, Pd-Pt (4:16)/C were 40.08^{o}, 40.08^{o} and 40.04^{o}, respectively. All the 2θ values are lower than the 2θ value of Pd/C (40.09^{o}). The lattice parameters of all Pd-Pt/C alloy electrocatalysts, (0.3891, 0.3892, 0.3893 and 0.3896 nm) are smaller than the value for pure Pt (0.3923 nm) but higher than that of pure Pd (0.3890 nm) (Maghsodi et al., 2011). It indicates the decrease in the lattice is due to the particle replacement of Pt by Pd in the structure of the Pd-Pt alloy (Lopes et al., 2008; Nishanth et al., 2011). The crystalline size of Pd-Pt/C was strongly affected by the addition of Pt element on the electrocatalyst (Li et al., 2007). In general, crystalline size

of carbon supported metal crystallite size decreases in the order of Pt < Pd-Pt/C < Pd (Li et al., 2004; Joo et al., 2008). Garcia et al., (2008) observed that the metal particle sizes estimated from the XRD data exhibit that the sizes are smaller at higher concentrations of Pt in Pd-Pt electrocatalyst. The similar trend was also found in the present study in XRD analyses (Table 5.4) (Garcia et al., 2008; Choudhary and Pramanik 2019). Choudhary and Pramanik (2019) reported the synthesis of HNO_3-functionalized acetylene black carbon supported Pt-Ru/C_{AB} nano electrocatalysts for ethanol electrooxidation, where larger crystallite size of the Pt-Ru/C_{AB} electrocatalysts comes up with higher degree of alloying. The alloying of Ru with Pt atom plays a very crucial role in electrooxidation of ethanol fuel. Thus, it could concluded that the higher crystallite size might results in high degree of alloying.

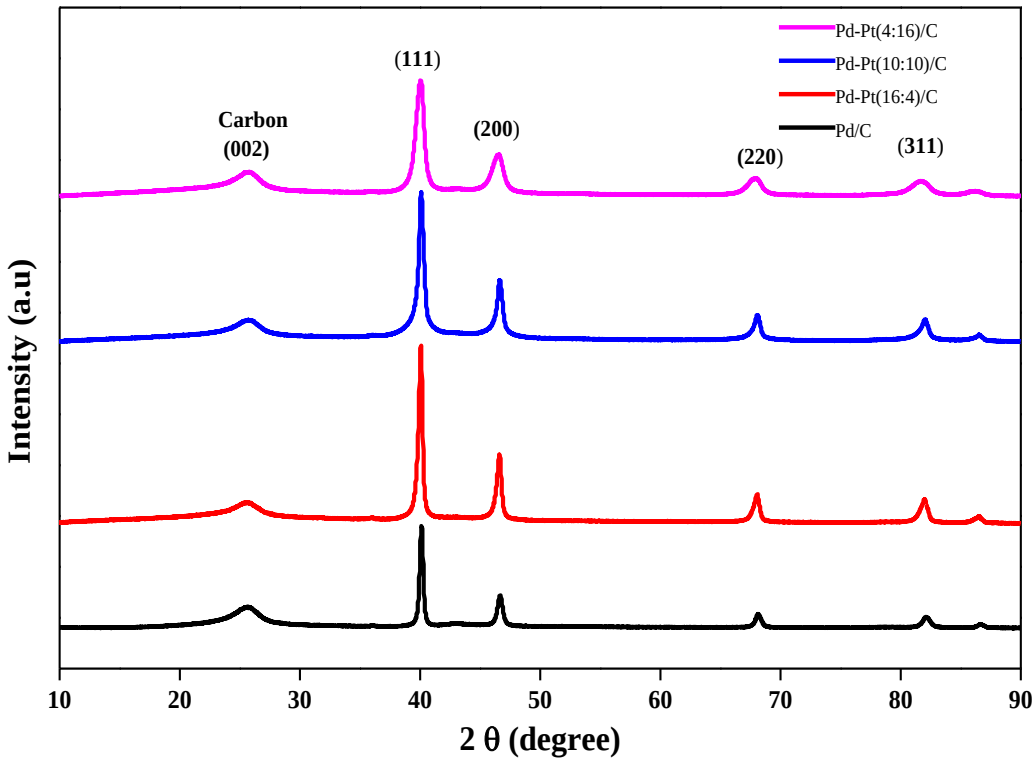

Figure 5.26 XRD profile for the Pd-Pt/C of different weight ratios and Pd/C electrocatalyst.

The degree of alloying was calculated using Vegard's law Equation (5.8) and using the relation lattice parameter of Pd and Pt given in Khan et al., (2015) shown in Equation (5.9). In Equation (5.9), a_{Pd} and a_{alloy} are the lattice parameter of pure Pd and Pd-Pt/C electrocatalyst, respectively. The Lattice parameter was calculated at (220) peak position. The value of atomic fraction of Pt (X_{Pt}) in the Pd-Pt/C was calculated by the lattice parameter and the $\left(\frac{Pt}{Pd}\right)_{nom}$ was calculated using the values of Pt and Pd atomic % obtained from EDX analysis i.e., Pt of 0.02, 0.051 and 0.082 % and Pd is 0.15, .094 and 0.082 % in for Pd-Pt (16:4)/C, Pd-Pt (16:4)/C and Pd-Pt (16:4)/C, respectively. The K value was calculated by assuming that the lattice parameter of Pd and Pt located in the line of lattice parameter of alloy. The calculated degree of alloying is shown in Table 5.4.

Table 5.4 Physical parameters derived from XRD data of the plane (111) for Pd/C and Pd-Pt/C bimetallic electrocatalyst.

Electrocatalyst type	2θ (deg)	Lattice Parameters (nm)	d-spacing (nm)	Crystallite size d_c (nm)	Degree of alloying (wt. %)
Pd/C	40.09	0.3891	0.2246	25.3	-
Pd-Pt(16:4)/C	40.08	0.3892	0.2247	24.0	47.9
Pd-Pt(10:10)/C	40.08	0.3893	0.2248	18.7	18.2
Pd-Pt(4:16)/C	40.04	0.3896	0.2249	11.1	10.0

$$a_{alloy} = a_{Pd} + KX_{Pt} \quad (5.8)$$

$$\text{Degree of alloying (\%)} = \frac{X_{Pt}}{(1-X_{Pt})\left(\frac{Pt}{Pd}\right)_{nom}} \quad (5.9)$$

The highest degree of alloying of 47.9 % was found for the Pd-Pt (16:4)/C. whereas, lower degree of alloying of 18.2 % and 10 % were observed for Pd-Pt (10:10)/C and Pd-Pt (4:16)/C electrocatalyst, respectively. Due to this fact, electrocatalyst Pd-Pt (16:4)/C

with largest crystallite size and high degree of alloying alloy probably would exhibit excellent electrocatalytic property for glycerol electrooxidation in the cyclic voltammetry (CV) studies (page no. 123) and single MFC which are discussed in the results and discussion section (page no. 128). The calculated crystallite sizes are a little larger than those obtained from TEM images which are discussed in the TEM analysis section (page no. 120). In electrocatalyst preparation by impregnation reduction method, metal complexes agglomerate into large particles either before or during the reduction process (Zhu et al., 2013; Nores-Pondal et al., 2009). In the XRD technique, the average crystallite size obtained by the scanning of complete sample which shows the macroscopic structure than TEM results.

5.2.1.2 SEM-EDX analysis

Figure 5.27a to Figure 5.27d show the SEM images of the prepared electrocatalyst Pd/C, Pd-Pt (16:4)/C, Pd-Pt (10:10)/C, and Pd-Pt (4:16)/C, respectively. The SEM analyses help to understand the surface morphology of the dispersered electrocatalyst. The surface morphology of electrocatalysts show spherical and uniform particles of nano range (Figure 5.27a to Figure 5.27d). Along with SEM analyses, the EDX analysis was also performed to check the surface concentration of metals and carbon support in the synthesized electrocatalysts. The EDX analysis shows the presence of all the elements i.e., Pd, Pt, and C for all the Pd-Pt/C electrocatalyst having different metal ratios. Table 5.5 shows the elemental compositions of prepared electrocatalyst, which are not exactly the same as that of nominal composition calculated them initially. Since the electrocatalytic surface is heterogeneous and thus, the EDX result of elemental composition varies from point to point (Panjiara and Pramanik 2020a).

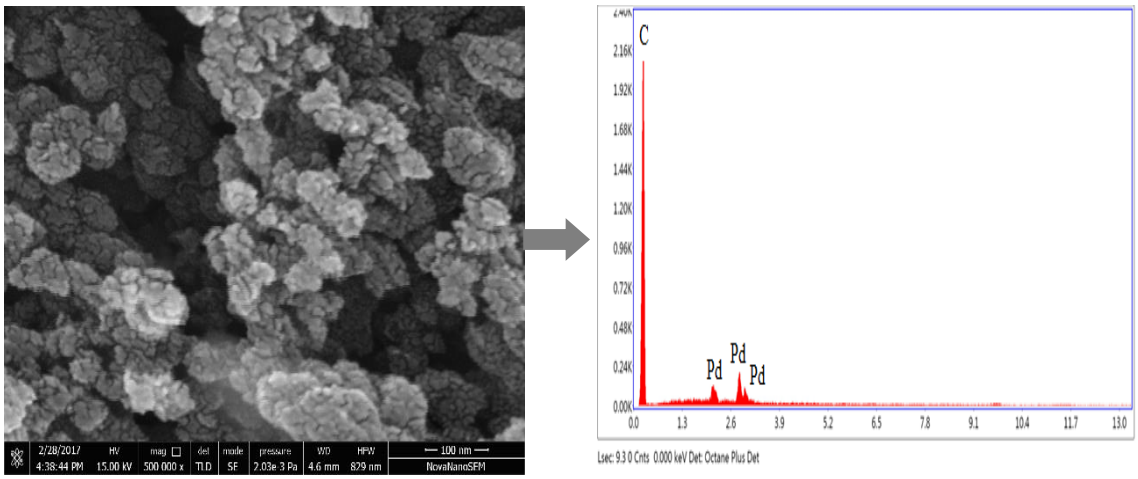

Figure 5.27a SEM/EDX image of synthesized Pd/C electrocatalyst.

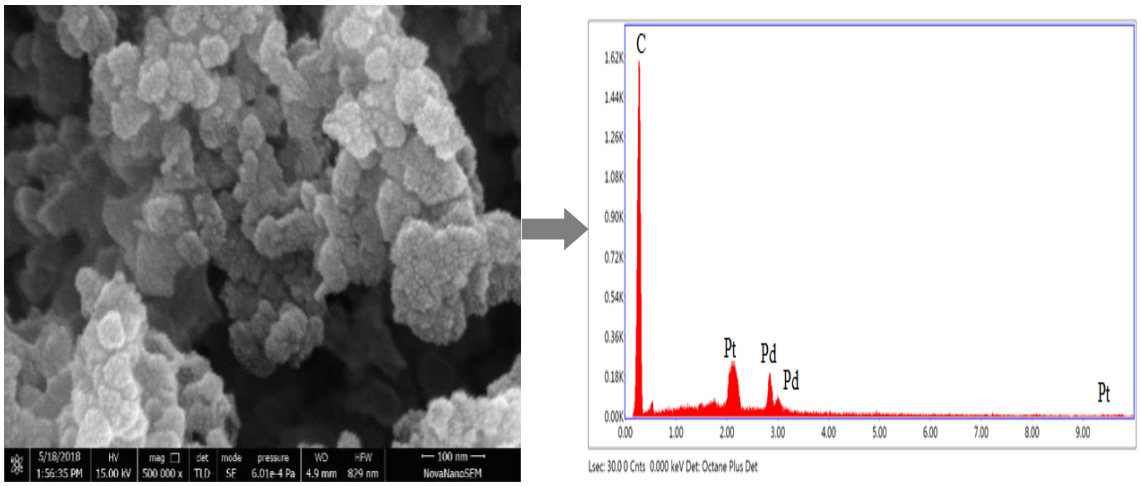

Figure 5.27b SEM/EDX image of synthesized Pd-Pt (16:4)/C electrocatalyst.

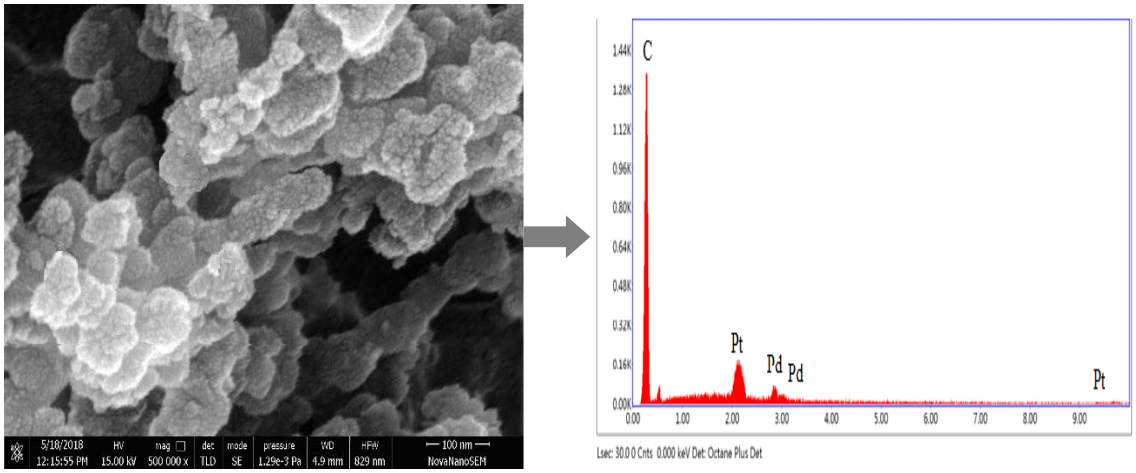

Figure 5.27c SEM/EDX image of synthesized Pd-Pt (10:10)/C electrocatalyst.

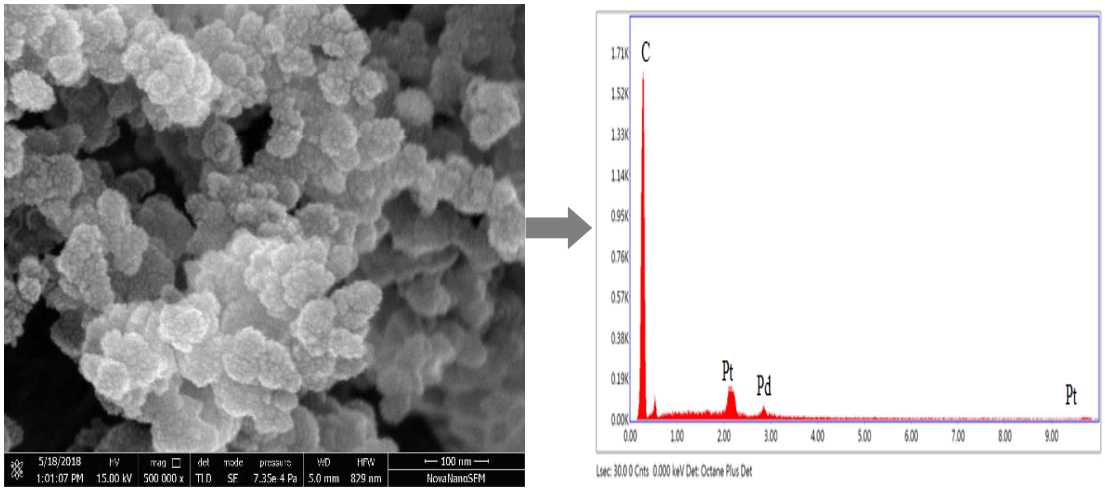

Figure 5.27d SEM/EDX image of synthesized Pd-Pt (4:16)/C electrocatalyst.

Table 5.5 Surface concentration of metal in synthesized electrocatalysts with different weight ratio.

Electrocatalyst type	EDX composition		Nominal composition	
	Pd (wt. %)	Pt (wt. %)	Pd (wt.%)	Pt (wt. %)
Pd/C	14.66	-	20	-
Pd-Pt (16:4)/C	13.43	3.37	16	4
Pd-Pt (10:10)/C	9.26	8.07	10	10
Pd-Pt (4:16)/C	3.86	10.71	4	16

5.2.1.3 TEM analysis

Figure 5.28a to Figure 5.28d show the TEM images of the Pd/C, Pd-Pt (16:4)/C, Pd-Pt (10:10)/C and Pd-Pt (4:16)/C electrocatalysts, respectively. The particle size distribution histogram was used to find the average particle size of all types of electrocatalyst. It is clearly seen in the TEM image that the electrocatalysts comprise of nano range size and homogeneously distributed on the support material. The electrocatalyst particles are spherical and slightly agglomerated due to the impregnation reduction method used in electrocatalyst preparation (Qian et al., 2008). The particle size was calculated by taking 100 particles from the TEM images with the help of Image J software. The average particle sizes of electrocatalysts are were 6.01 ± 0.28 nm, 5.05 ± 0.15 nm, 4.65 ± 013 nm

and 4.29 ± 0.12 nm for Pd/C, Pd-Pt(16:4)/C Pd-Pt(10:10) /C and Pd-Pt(4:16)/C, respectively. The TEM results also show a similar trend for the particle size as it was seen in the XRD analysis (Table 5.4) (page no. 117). The difference between crystallite sizes obtained from XRD analysis and particle sizes obtained from the TEM analysis were observed. It may be due to the special characteristics of XRD analysis where it reflects crystalline particles, not the actual morphology of electrocatalysts (Tayal et al., 2011). Moreover, larger size crystallites are selected in XRD patterns, while most small particles are counted in TEM images (Tayal et al., 2011).

Although, particle size obtained by TEM analysis for all bimetallic electrocatalysts are smaller than obtained by XRD analysis, the average particle size of Pd-Pt (16:4)/C was found to be little high among all bimetallic electrocatalyst in the TEM analysis also. As already discussed in XRD section (page no. 115), the larger particle size result in high degree of alloying i.e, 47.9 %, 18.2 % and 10 % for Pd-Pt (16:4)/C, Pd-Pt (16:4)/C and Pd-Pt (16:4)/C, respectively. Due to this fact, the largest particle size of alloy (47.9 %) electrocatalyst Pd-Pt (16:4)/C probably would exhibit excellent electrocatalytic property for glycerol electrooxidation in the cyclic voltammetry (CV) studies and single MFC.

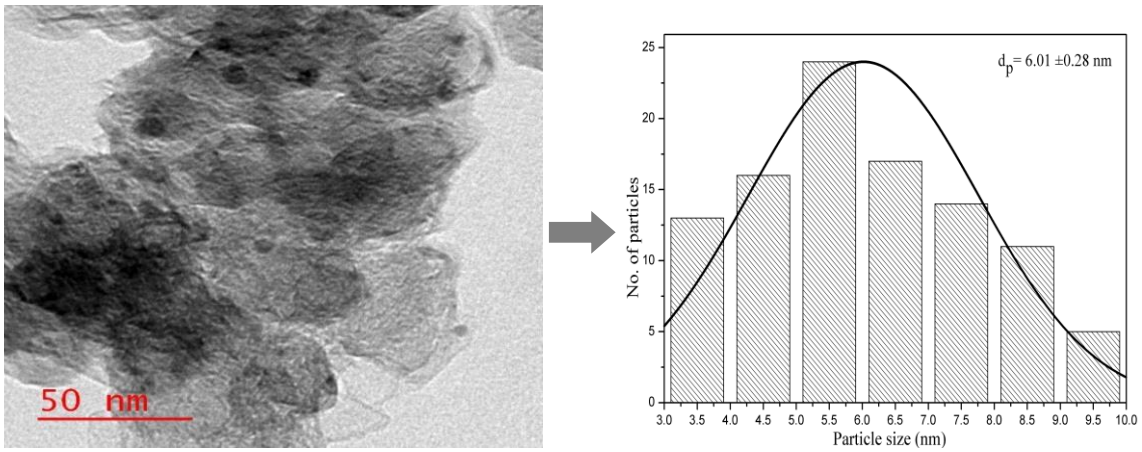

Figure 5.28a TEM image and histogram of particles distribution of synthesized Pd/C electrocatalyst.

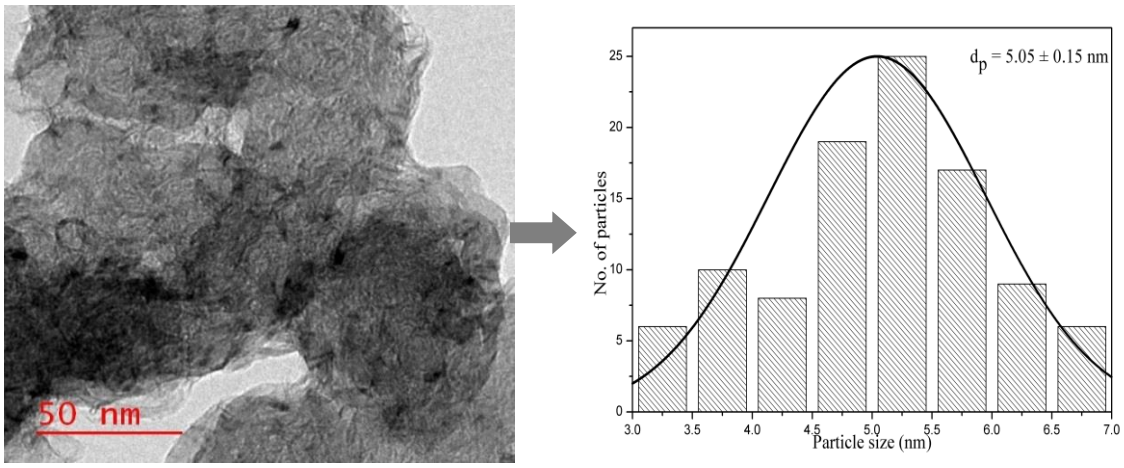

Figure 5.28b TEM image and histogram of particles distribution for Pd-Pt (16:4)/C electrocatalyst.

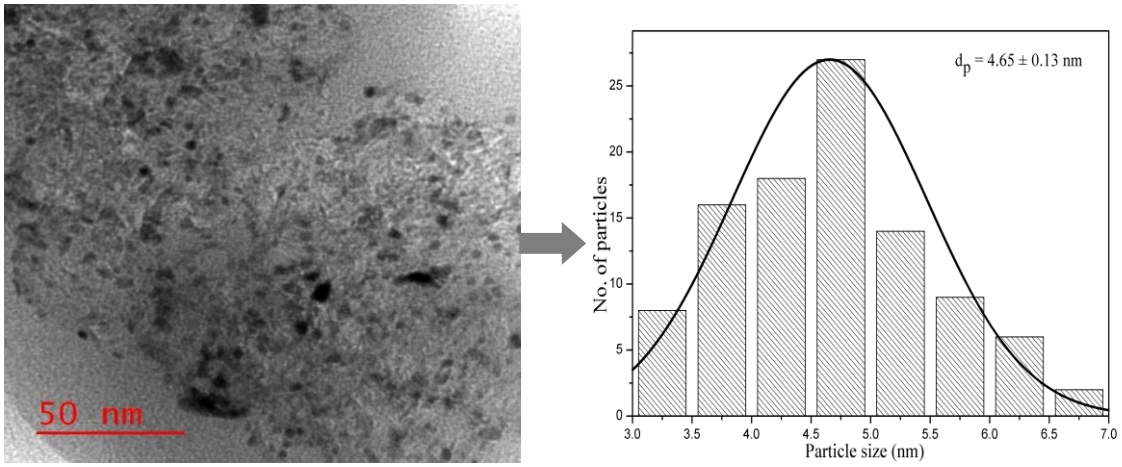

Figure 5.28c TEM image and histogram of particles distribution for Pd-Pt (10:10)/C electrocatalyst.

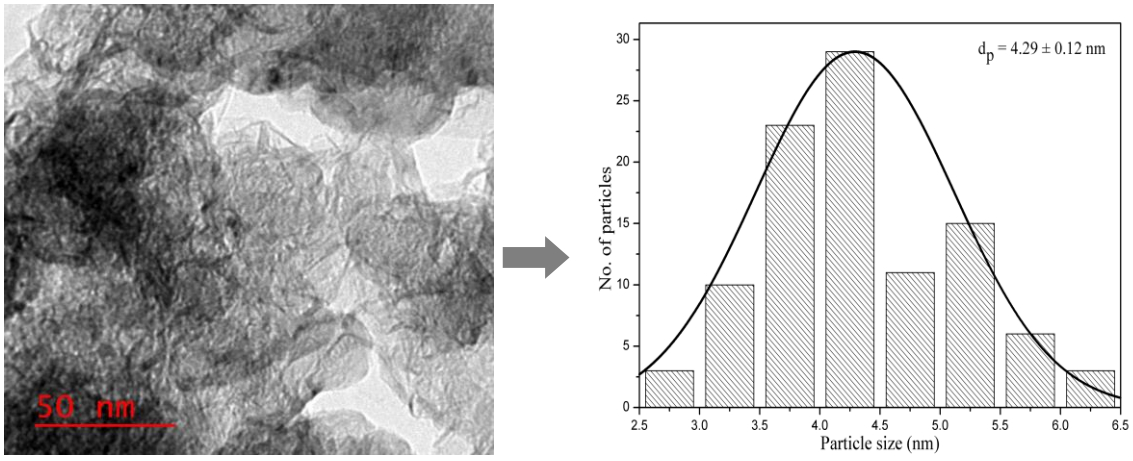

Figure 5.28d TEM image and histogram of particles distribution for Pd-Pt (4:16)/C electrocatalyst.

5.2.2 Electrochemical characterization of electrocatalyst

5.2.2.1 Cyclic voltammetry of anode electrocatalysts

Figure 5.29 represents the cyclic voltammograms for 1 M glycerol mixed with 1 M KOH using synthesized electrocatalyst Pd/C and Pd-Pt(16:4)/C, Pd-Pt(10:10)/C and Pd-Pt(4:16)/C, respectively. The applied potential was varied from -1.0 V to 1.0 V (Vs. Ag/AgCl). The scan rate was fixed at 50 mV/sec, as the observed electrochemical peaks were prominent at this scan rate. The CV characterstics for other scan rates are presented in the Appendix D (Figure D1 to Figure D4). The peak current density of 11.97 mA/cm^2 at a potential of -0.157 V (Vs Ag/AgCl) was obtained for Pd/C. The bimetallic Pd-Pt(10:10) /C showed the highest electrooxidation peak current density of 24.51 mA/cm^2 at a potential of -0.133 V (Vs Ag/AgCl). On the other hand Pd-Pt(16:4)/C and Pd-Pt(4:16)/C produced peak current density of 13.58 mA/cm^2 and 8.08 mA/cm^2 at the potential of -0.189 V (Vs Ag/AgCl) and -0.179 V (Vs Ag/AgCl), respectively. Although, the peak current density of Pd-Pt(10:10)/C was high, the electrooxidation potential shifted to the less negative side by 0.056 V and 0.046 V with respect to Pd-Pt(16:4)/C and Pd- Pt (4:16)/C. It implies that the activation overpotential is very high for the synthesized bimetallic Pd-Pt (10:10) /C and expected to give poor result in MFC device. Whereas, Pd-Pt (16:4) /C comes up with moderate peak current density (13.58 mA/cm^2) at very high negative potential (-0.189 V (Vs Ag/AgCl)). It indicates, Pd-Pt (16:4) /C to be very promising bimetallic electrocatalyst for MFC using glycerol as anode fuel. It is clearly seen from the Figure 5.29 that peak current density increases with the increase in Pt content upto Pd to Pt ratio of 10:10 and further increase in Pd to Pt ratio to 4:16, the peak current density decreases.

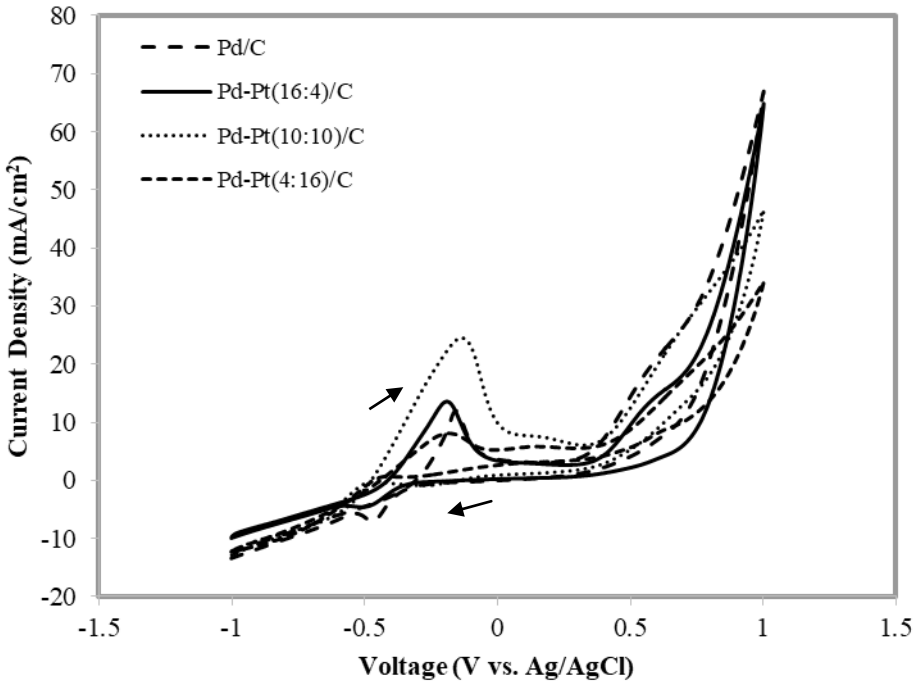

Figure 5.29 Cyclic voltammetry for 1 M glycerol in 1 M KOH at scan rate of 50 mV/sec using Pd/C and different ratios of Pd-Pt/C as anode electrocatalyst; Temperature: 25 ^{o}C.

As reported in the published literature, Pt helps to split the C-C bond of the glycerol molecules and Pd atoms reduce the adsoption of CO on Pt sites and thus, Pd-Pt/C electrocatalysts show better electrocatalytic property for glycerol electrooxidaion than pure Pd or Pt (Yildiz and Kadirgan 1994). However, formation of metal alloy and better degree of alloying are essential for the bimetallic electrocatalyst to exibit excellent electroocatalytic property (Choudhary and Pramanik 2019). It is clearly seen in the XRD analysis (Table 5.4), highest degree of alloying (47.9 wt. %) is observed for the Pd rich in the Pd-Pt (16:4)/C bimetallic electrocatalyst and thus, it resulting in electroxidation peak at very high negative potential (-0.189 V (Vs Ag/AgCl)). The peak current density is moderate due to low Pt amount in the synthesized electrocatalysts of Pd-Pt (16:4)/C. Whereas, peak current density is very high for Pd-Pt (10:10)/C and it may be due to increased amount of Pt metal in this electrocatalyst in comparison to that of Pd-Pt (16:4)/C. However, peak potential was observed at relatively low negative poptential (-

0.133 V) which might results in high overpotentials. It may be due to lower degree of alloying (18.2 wt. %). The electrocatalyst with highest amount of Pt i.e., Pd-Pt (4:16)/C produced very low peak current density as the active electerocatalyst sites were not formed due to poor alloying of 10 wt. % and poisoning of active Pt sites also take place by the formation of intermediate products due to low amount of Pd (Grace and Pandian 2006). Undoubtadely, the electronic properties of Pd is improved by the addition of small amount of Pt in Pd-Pt bimetallic electrocatalyst (Cho et al., 2007). It should be noted that lower over potential of synthesized electrocatalyst is also important for achieving high power density from the single MFC studeis (Panjiara and Pramanik 2020a).

From the results of CV experimets, it can be predicted that synthesized Pd-Pt (16:4)/C electrocatalysts would results in excellent cell performance and it may be due to the higher degree of alloying in comparison to other bimetallic electrocatalysts, as discussed ealier in the XRD and TEM analysis (Choudhary and Pramanik 2019). The single metal based Pd/C shows relatively low peak current density (11.97 mA/cm^2) at less negative potential (-0.157 V (Vs Ag/AgCl)). Thus, the performance of Pd/C would be poor in a single MFC test.

5.2.2.2 EIS study of anode electrocatalysts

Figure 5.30a illustrates the Nyquist plots of glycerol electrooxidation on the different synthesized electrodes in a solution containing 1 M glycerol mixed with 1 M KOH. The EIS was performed at a frequency range of 100 kHz to 10 mHz with amplitude of 10 mV at the potential of - 0.2 V (vs Ag/AgCl). The shape of the Nyquist plots of different electrocatalyst having different arcs diameter. The diameter of the arc represents the charge transfer resistance of the electrooxidation reaction (Rezaei et al., 2016). The larger arc diameter of Pd/C electrocatalsyt indicates higher charge transfer resistance compared to smaller arc diameter generated by the bimetallic electrocatalysts. Even among all the

bimetallic Pd-Pt/C electrocatalysts, the Pd-Pt (16:4)/C, generates smallest arc diameter compared to other bimetallic electrocatalysts. The shifting of intercept may be due to the varying electrode conductivity or electrode resistance of different types of electrocatalysts. This is the main reason for change in the cell resistance or individual electrodes resistance (López–Coronel et al., 2019). Also, the intercept at lower value idicates the lower electronic resistance compared with other electrocatalysts of the electrode (Maghsodi et al., 2011).

The equivalent circuit corresponds to the Nyquist plot is shown in Figure 5.30b was used to calculate the information of the Pd/C, Pd-Pt (16:4)/C, Pd-Pt (10:10)/C and Pd-Pt (4:16)/C electrocatalysts. In the equivalent circuit, the solution resistance/electrolyte resistance is represented by R_s, constant-phase element is the double layer capacitance at the interface of electrolye and electrocatalyst represented by CPE, the charge-transfer resistance is represented by R_{ct} and Warburg diffusion resistance of ions in the solution is represented by W_s. The R_{ct} is the mesurement of the semicircle arc diameter which is associated to the obstruction of passing of electron across the electrode area to adsorbed the species, similary from the adsorbed species to the electrode surface. The results shows that the smaller R_{ct} indicates a faster reaction rate of glycerol electrooxidation reaction. The conductivity is calculated using the formula $\sigma = \frac{L}{RA}$, where, σ is the conductivity, L is thickness of the working electrode i.e., 0.016 cm, A is the area of the working electrode i.e. 0.5 cm^2 and R is the charge transfer resistance. The conductivity for Pd/C,Pd-Pt (16:4)/C, Pd-Pt (10:10)/C and Pd-Pt (4:16)/C are 1.54×10^{-5} $\Omega^{-1}cm^{-1}$, 1.38×10^{-4} $\Omega^{-1}cm^{-1}$, 8.26×10^{-5} $\Omega^{-1}cm^{-1}$ and 2.91×10^{-5} $\Omega^{-1}cm^{-1}$, respectively. The bode phase angle at high frequency (56899 Hz) obtained from Z view software for Pd/C,Pd-Pt (16:4)/C, Pd-Pt (10:10)/C and Pd-Pt (4:16)/C are -12.88^o, -30.34^o, -23.14^o and -10.40^o, respectively. The bode magnitude for Pd/C,Pd-Pt (16:4)/C, Pd-Pt (10:10)/C and Pd-Pt

(4:16)/C are 21.04, 5.17, 8.49 and 22.30, respectively. The chi square fit, CPE, Rs,and R_{ct} values are shown in Table 5.6. Thus, in the present EIS study, the results indiciate that Pd-Pt (16:4)/C has lowest charge transfer resistance (115.2 Ω) than other electrocatalyst. It is clear from the EIS analysis that the Pd-Pt (16:4)/C would obviously results in excellent electrocatalytic activity for glycerol electrooxidation.

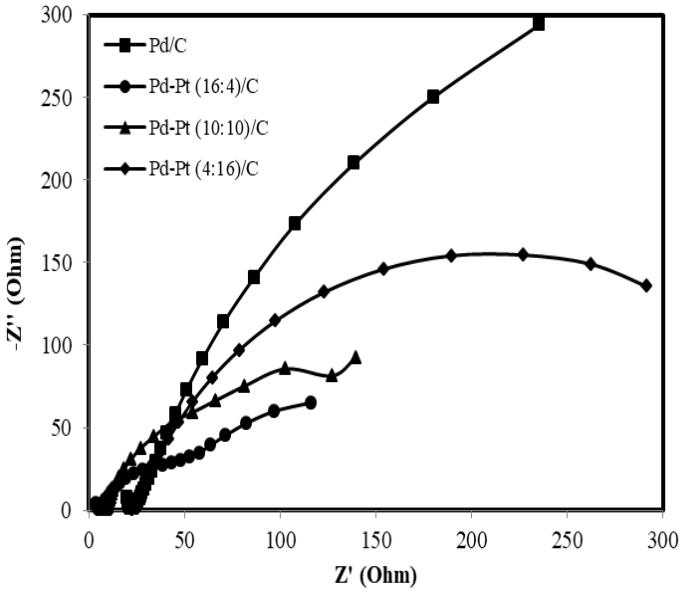

Figure 5.30a Nyquist plots of synthesized electrocatalysts recorded at - 0.2 V in 1 M glycerol mixed with 1 M KOH solution;Temperature: 25 ^{o}C.

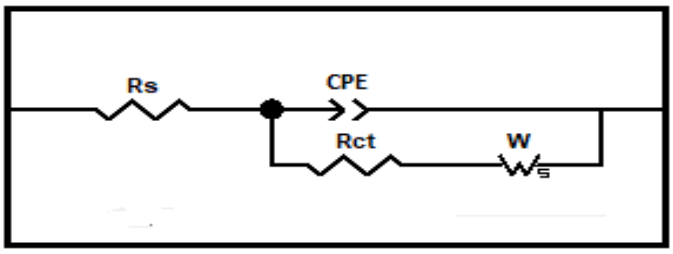

Figure 5.30b Equivalent circuit diagram corresponds to Nyquist plot.

Table 5.6 Equivalent circuit related term for Pd/C and Pd-Pt/C electrocatalysts.

Electrocatalyst type	**Chi square fit**	**R_s (ohm)**	**R_{ct} (ohm)**	**CPE (mF)**
Pd/C	0.713	22.28	2067	2
Pd-Pt (16:4)/C	0.130	5.26	115.2	2.5
Pd-Pt (10:10)/C	0.232	8.61	193.1	5.1
Pd-Pt (4:16)/C	0.049	22.54	549	4.6

5.2.3 Performance of Pd-Pt/C anode electrocatalyst in MFC

5.2.3.1 Y-shaped air breathing MFC

5.2.3.1.1 Effect of anode electrocatalyst type

Figure 5.31 shows the performance characteristics of the Y-shaped air breathing microfluidic fuel cell operated with synthesized Pd-Pt/C of different ratios and Pd/C anode electrocatalysts, respectively. The cathode electrocatalysts was commercial Pt/C_{HSA}. Both the electrodes were constructed with the electrocatalysts loading of 2 mg/cm^2. The anode fuel glycerol of 0.5 M mixed with 0.5 M KOH was fed at anode, whereas atmospheric oxygen was used as oxidant at cathode along with 0.5 M KOH. The optimum flow rates of 1 ml/min were kept for anode and cathode stream throughout the experiments in Y-shaped air breathing MFC.

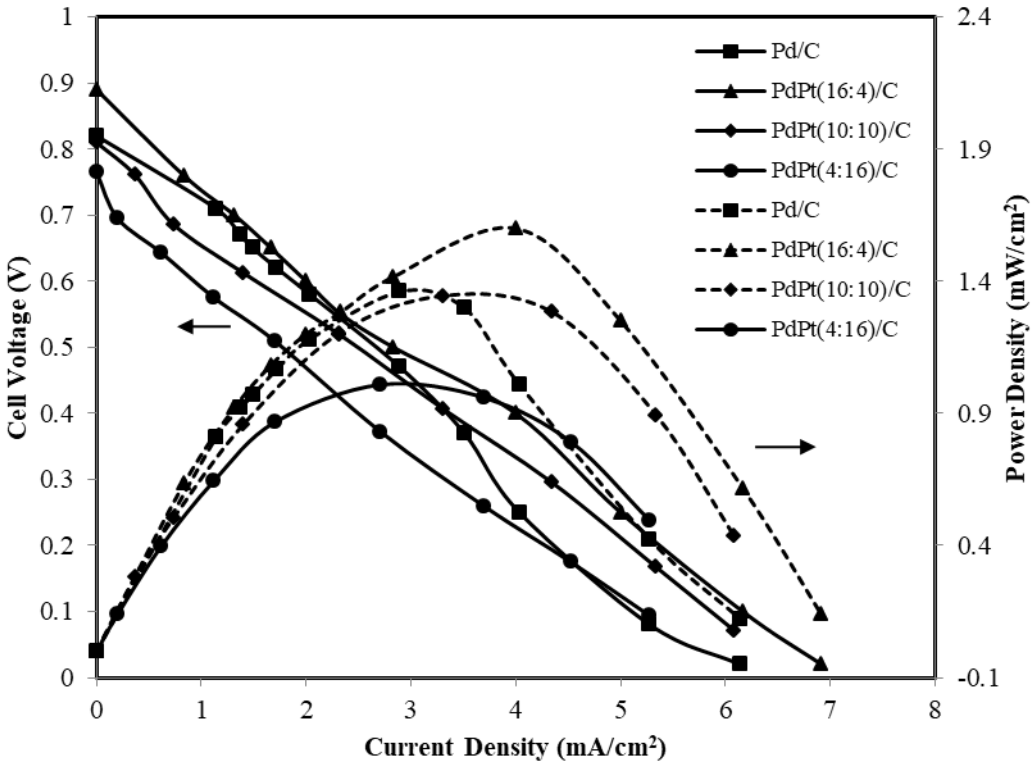

Figure 5.31 Polarization and power density curves of MFC for different types of anode electrocatalyst and fixed cathode electrocatalyst Pt/C_{HSA} with 2 mg/cm^2 loading at both side, using 0.5 M glycerol and 0.5 M KOH at anode side and 0.5 M KOH at cathode side with ambient air as oxidant at a temperature of 35 ^oC. Solid line – polarization curves; Dotted line – power density curves.

The highest OCV of 0.88 V and power density of 1.6 mW/cm^2 at a current density of 4 mA/cm^2 were obtained for synthesized bimetallic electrocatalyst Pd-Pt (16:4)/C. Whereas, OCV of 0.82 V and maximum power density of 1.36 mW/cm^2 at a current density of 2.89 mA/cm^2 were obtained for single metal Pd/C. The OCV of 0.81 V and maximum power density 1.35 mW/cm^2 at a current density of 3.3 m/cm^2 were for Pd-Pt (10:10)/C electrocatalyst. The Pd-Pt (4:16)/C produced lowest OCV of 0.76 V and power density 1 mW/cm^2 at a current density of 2.7 m/cm^2, respectively. The reason for highest performance of Pd-Pt (16:4)/C may be due to higher degree of alloying and low overpotential as already discussed in XRD (page no.115) and CV observation (page no. 123), respectively.

5.2.3.1.2 Effect of anode electrocatalyst loading

The synthesized Pd-Pt (16:4)/C proved itself as the best electrocatalyst among all tested electrocatalysts in the single cell study in Y-shaped air breathing MFC. Thus, the anode loading was varied using synthesized best electrocatalyst Pd-Pt (16:4)/C to get the highest cell performance at optimum loading. The anode fuel glycerol of 0.5 M mixed with 0.5 M KOH was fed at anode, whereas atmospheric oxygen was used as oxidant at cathode mixed with 0.5 M KOH. Figure 5.32 shows the performance characteristics of Y-shaped air breathing MFC for different loading at anode varying from 1 mg/cm^2 to 2.5 mg/cm^2. The electrocatalyst loading of 2 mg/cm^2 Pt/C_{HSA} at cathode was kept fixed for each set of experiments. It is seen for the Figure 5.32 that the cell performance increases with the increase in loading from 1 mg/cm^2 to 2 mg/cm^2. Further increase in loading beyond 2 mg/cm^2, the cell performance decreases. The maximum power density of 1.6 mW/cm^2 at a current density of 4 mA/cm^2 was obtained for 2 mg/cm^2 electrocatalyst loading. At the lowest loading of 1 mg/cm^2 and 1.5 mg/cm^2, the maximum power density was 1.26

mW/cm^2 at a current density of 3.64 mA/cm^2 and 1.28 mW/cm^2 at a current density of 3.75 mA/cm^2, respectively. The recorded power density for the loading of 2.5 mg/cm^2 was quite low i.e., 1.3 mW/cm^2 at a current density of 2.69 mA/cm^2. It shows that even very high loading resulting in low power density. The active sites of electrocatalyst increases with increase in electrocatalyst loading. Thus, more fuel molecules and OH^- ions interact with the electrocatalyst surface resulting in more electrooxidation reaction which gives more current density and power density.

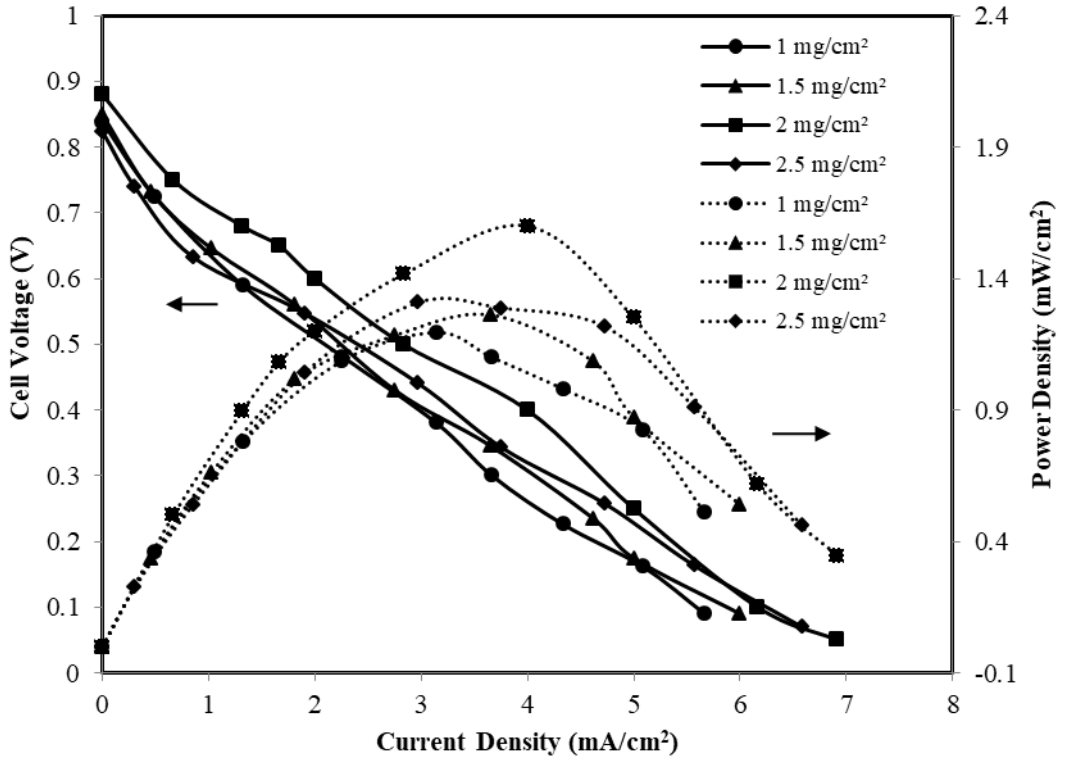

Figure 5.32 Polarization and power density curves of MFC for different anode electrocatalyst loading of Pd-Pt (16:4)/C and cathode electrocatalyst loading 2 mg/cm^2 of Pt/C_{HSA}, using 0.5 M glycerol and 0.5 M KOH at anode side and 0.5 M KOH with ambient air as oxidant at cathode side at a temperature of 35 ^oC. Solid line – polarization curves; Dotted line – power density curves.

However, increase in loading beyond the optimum loading (2 mg/cm^2) the electrocatalyst particles starts agglomerating at the electrode surface and make it more compact. It creates hindrance for the diffusion of fuel molecules and OH^- ions at the electrode surface which reduces the cell performance.

5.2.3.1.3 Effect of cathode electrocatalyst loading

After optimizing the anode electrocatalyst loading at anode, the cathode side electrocatalyst (Pt/C_{HSA}) loading was also optimized to obtain highest performance from the Y-shaped air breathing MFC. The anode fuel glycerol of 0.5 M mixed with 0.5 M KOH was fed at anode whereas atmospheric oxygen was used as oxidant cathode mixed with 0.5 M KOH. Figure 5.33 shows the performance characteristics of air breathing MFC for different cathode electrocatalyst loading ranging from 1 mg/cm^2 to 2.5 mg/cm^2 keeping anode electrocatalyst fixed at the optimum loading of 2 mg/cm^2 of Pd-Pt (16:4)/C. In is seen from the Figure 5.33 that the cell performance increases with the increase in electrocatalyst loading upto 2 mg/cm^2 of Pt/C_{HSA} and further increase in loading beyond 2 mg/cm^2, the cell performance decreases.

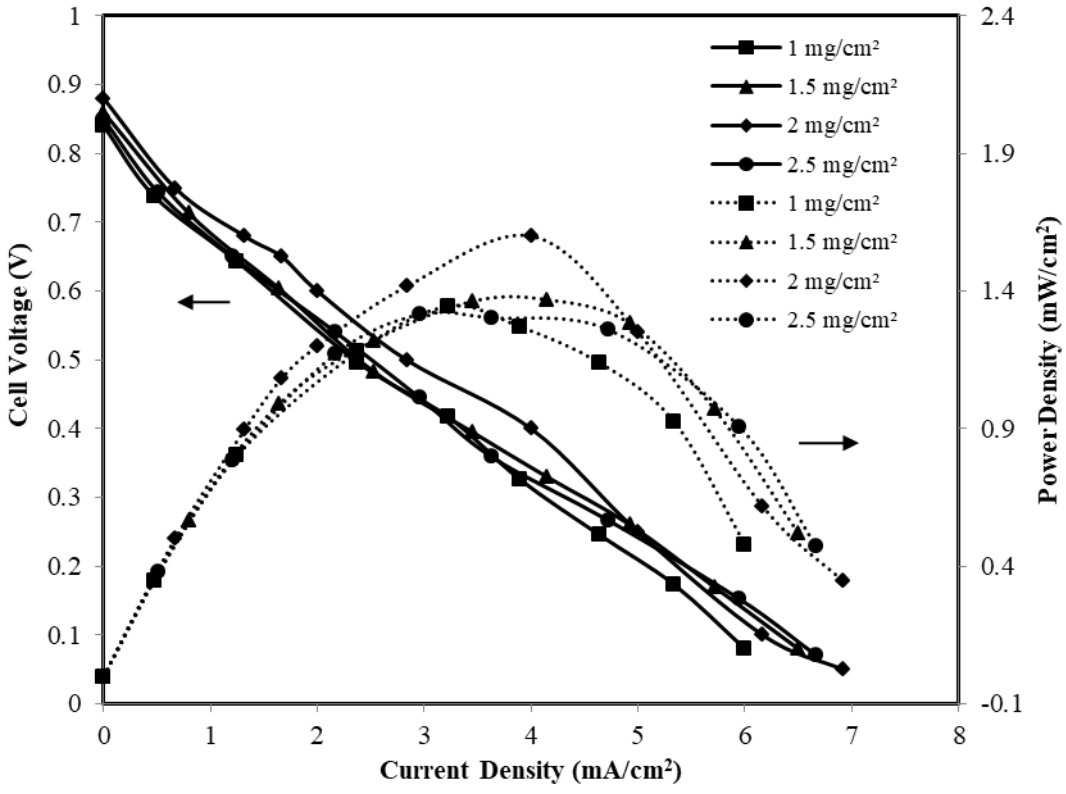

Figure 5.33 Polarization and power density curves of MFC for different cathode electrocatalyst loading of Pt/C_{HSA} and cathode electrocatalyst loading of 2 mg/cm^2 Pd-Pt/C, using 0.5 M glycerol and 0.5 M KOH at anode side and 0.5 M KOH with ambient air as oxidant at cathode side at a temperature of 35 ^oC. Solid line – polarization curves; Dotted line – power density curves.

The highest power density of 1.6 mW/cm^2 at a current density of 4 mA/cm^2 was obtained for 2 mg/cm^2. Whereas, Pt/C_{HSA} of 2.5 mg/cm^2 loading produced maximum power density of 1.31 mW/cm^2 at a current density of 2.95 mA/cm^2. At low electrocatalyst loading of 1 mg/cm^2 and 1.5 mg/cm^2, MFC produced maximum power density of 1.34 mW/cm^2 at a current density of 3.22 mA/cm^2 and 1.36 mW/cm^2 at a current density of 4.14 mA/cm^2, respectively. The highest power density (1.6 mW/cm^2) at the loading of 2 mg/cm^2 was due to optimal compromise between the available surface and particle available without any agglomeration as it has already been discussed in the previous section "5.2.3.1.2 Effect of anode electrocatalyst loading" (page no. 129).

5.2.3.1.4 Effect of anode KOH electrolyte concentration

The effect of anode electrolyte concentration on the performance of Y-shaped air breathing MFC is shown in Figure 5.34. The anode and cathode were fabricated using optimum loading of 2 mg/cm^2 of synthesized Pd-Pt (16:4)/C and commercial Pt/C_{HSA} electrocatalyst both. The electrolyte (KOH) concentration was varied from 0.3 M to 1.5 M, while the glycerol concentration was kept fixed at 0.5 M. The electrolyte provides ionic mobility of the OH^- ions and reduces the ohmic loss and thus, increase in electrolyte concentration, the mobility of anions increases for the KOH concentration upto 0.5 M. Further increase in electrolyte concentration beyond 0.5 M KOH, the concentration of glycerol molecules get replaced by OH^- ions at the electrode surface thus, cell performance fall down (Gupta and Pramanik 2019). As per anode reaction Equation (1.1) (page no. 9), the presence of glycerol and OH^- ions both are required. A delicate balance between glycerol and OH^- ions will ensure the highest cell performance of MFC and the balance is achieved at the anode KOH concentration of 0.5 M. The optimum concentration of KOH electrolyte was recorded 0.5 M at which the maximum power density 1.6 mW/cm^2 at a current density of 4 mA/cm^2 was generated by the cell.

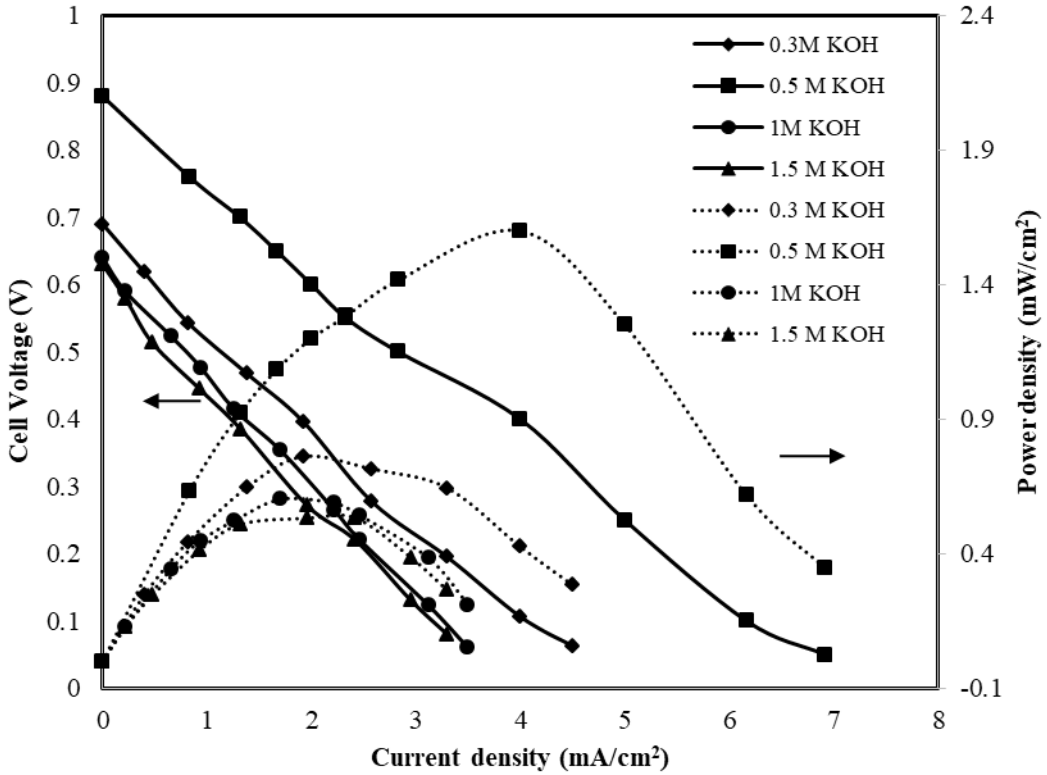

Figure 5.34 Polarization and power density curves of MFC for different anode electrolyte concentration using 0.5 M glycerol at anode side and 0.5 M KOH with ambient air as oxidant at cathode side; Anode: Pd-Pt (16:4)/C of 2 mg/cm^2 and cathode: Pt/C_{HSA} of 2 mg/cm^2; MFC temperature: 35 ^oC. Solid line – polarization curves; Dotted line – power density curves.

At low concentration of 0.3 M KOH, the maximum power density of 0.76 mW/cm^2 at a current density of 1.9 mA/cm^2 was obtained. Moreover, at higher concentration of 1 M and 1.5 M KOH beyond the optimum concentration, the power densities were 0.6 mW/cm^2 and 0.53 mW/cm^2 at a current density of 1.7 mA/cm^2 and 1.9 mA/cm^2, respectively.

5.2.3.1.5 Effect of cathode KOH electrolyte concentration

The cathode side KOH electrolyte concentration was optimized after the anode KOH concentration was optimized to achieve highest power density from Y-shaped air breathing MFC as shown in Figure 5.35. The KOH electrolyte concentration of 0.3 M, 0.5 M, 1 M and 1.5 M KOH were used at cathode side for each set of experiments keeping the anode electrolyte at optimum value of 0.5 M KOH.

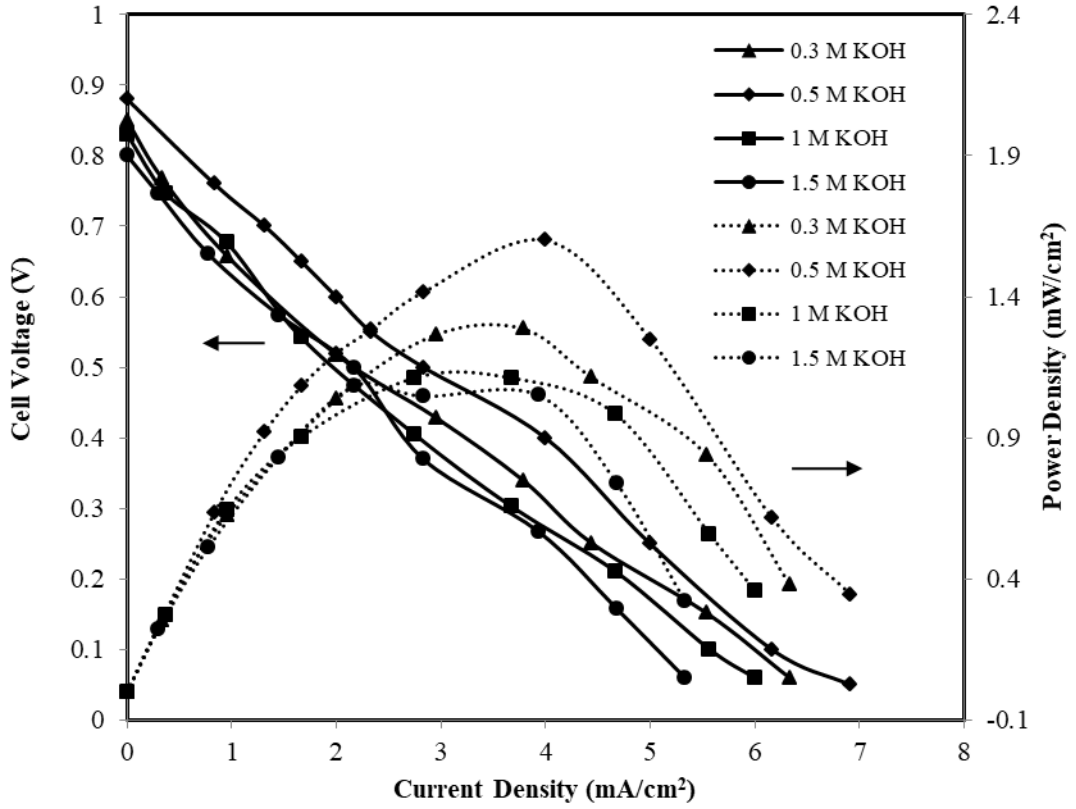

Figure 5.35 Polarization and power density curves of MFC for different cathode KOH electrolyte concentration with ambient air as oxidant at cathode and 0.5 M glycerol mixed with 0.5 M KOH at anode side Anode: Pd-Pt (16:4)/C of 2 mg/cm^2 and cathode: Pt/C_{HSA} of 2 mg/cm^2; MFC temperature: 35 ^oC; Solid line – polarization curves; Dotted line – power density curves.

The glycerol of 0.5 M of was fed as anode of MFC. The oxidant at cathode was atmospheric oxygen. The Figure 5.35 shows that the polarization and power density curves shifted to upward direction when KOH concentration at cathode was increased

from 0.3 M to 0.5 M and further increase in KOH concentration beyond 0.5 M, the curves shifted to downward direction. The highest OCV of 0.88 V and power density of 1.6 mW/cm^2 at a current density of 4 mA/cm^2 were obtained at 0.5 M KOH at cathode. While, at low concentration of 0.3 M KOH, the maximum power density of 1.26 mW/cm^2 at a current density of 3.78 mA/cm^2 was obtained. The KOH concentration of 1 M and 1.5 M produced quite low power density of 1.12 mW/cm^2 and 1.05 mW/cm^2 at a current density of 3.63 mA/cm^2 and 3.93 mA/cm^2, respectively.

5.2.3.1.6 Effect of glycerol concentration

The effect of glycerol concentration on the performance characteristics i.e., polarization and power density curves of Y-shaped air breathing MFC is presented in Figure 5.36. The glycerol concentration was varied from 0.3 M to 1.5 M keeping the anode and cathode electrolyte concentration both fixed at optimum value of 0.5 M KOH. It is seen in the Figure 5.36, the cell performance increases with the increase in glycerol concentration upto 0.5 M and further increase in glycerol concentration beyond 0.5 M, the cell performance decreases. This decreasing trend in the cell performance was recorded upto 1.5 M of glycerol concentration. It may be due to the increase in glycerol concentration, electrolyte KOH concentration gets decreased at the electrocatalysts surface which is unfavourable for the anode electrooxidation reaction.

As per the reaction anode scheme (Equation 1.1), a delicate balance is required between glycerol and OH^- ions at the anode electrocatalysts sites (page no. 9), and this has already been discussed in the section "5.2.3.1.4 Effect of anode KOH concentration" (page no.132).

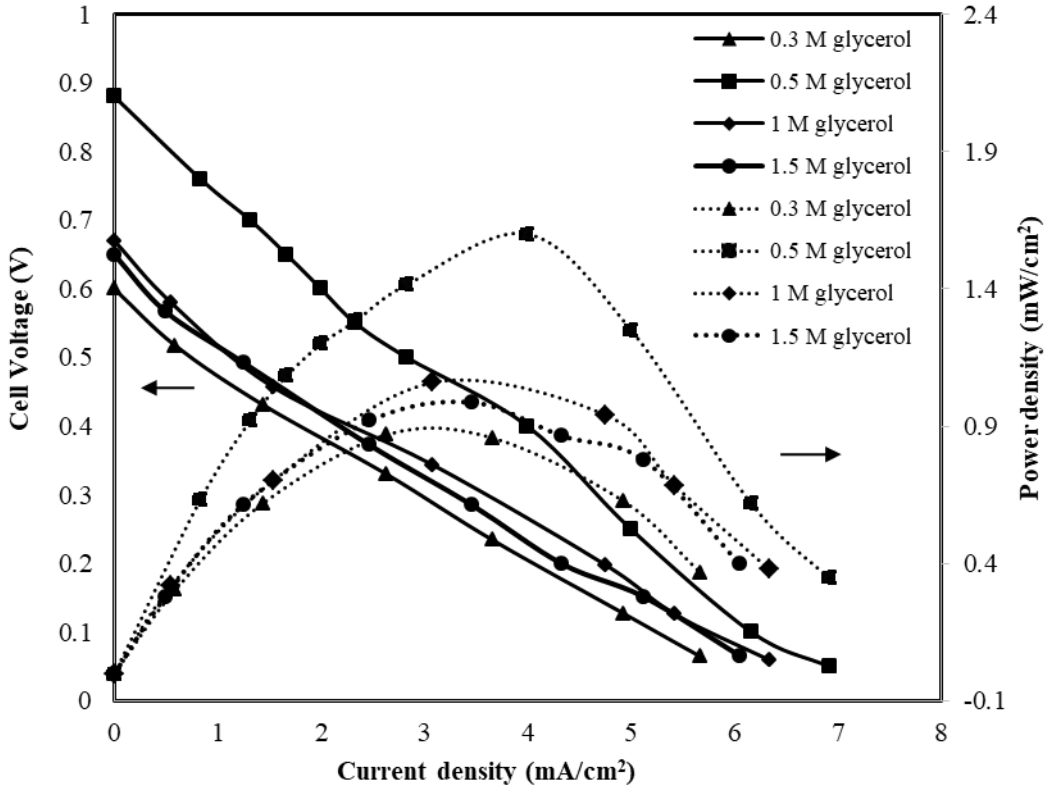

Figure 5.36 Polarization and power density curves of MFC for different fuel concentration with optimum electrolyte concentration of 0.5 M KOH at anode side and at cathode side 0.5 M KOH with ambient air as oxidant Anode: Pd-Pt (16:4)/C of 2 mg/cm^2 and cathode: Pt/C_{HSA} of 2 mg/cm^2; MFC temperature: 35 ^oC.; Solid line – polarization curves; Dotted line – power density curves.

The OCV of 0.88 V and maximum power density 1.6 mW/cm^2 were obtained for 0.5 M glycerol concentration mixed with optimum KOH concentration of 0.5 M. The cell performance was very low at 0.3 M glycerol concentration, where OCV of 0.6 V and maximum power density 0.86 mW/cm^2 at a current density of 2.64 mA/cm^2 were obtained, due to less presence of OH^- ions relative to glycerol molecules at the surface of electrode. On the other side, the relative concentration OH^- ions at the surface of electrocatalysts get decreased at very high concentration i.e., 1 M and 1. 5 M of glycerol which results lower cell performance in terms of power density. The maximum power density of 1.06 mW/cm^2 and 0.98 mW/cm^2 at a current density of 3.08 mA/cm^2 and 3.46 mA/cm^2, were obtained for the glycerol concentration of 1 M and 1.5 M, respectively.

5.2.3.1.7 Effect of cell temperature

Figure 5.37 shows the polarization and power density curves of Y-shaped air breathing MFC for the varying temperature from 35 °C to 95 °C using 0.5 M glycerol (optimum) mixed with 0.5 M KOH (optimum) at anode and 0.5 M KOH (optimum) at cathode. The oxidant at cathode was atmospheric oxygen. The maximum cell temperature of 95 ^{o}C was maintained keeping in mind the boiling point of water (100 ^{o}C) and avoid two phase flow which would hinder the flow dynamics in the microchannel (Wang et al., 2019). It is seen for the Figure 5.37**,** the cell performance increases with increase in temperature upto 75 ^{o}C. Further increase in temperature beyond 75 ^{o}C, the cell performance decreases rapidly.

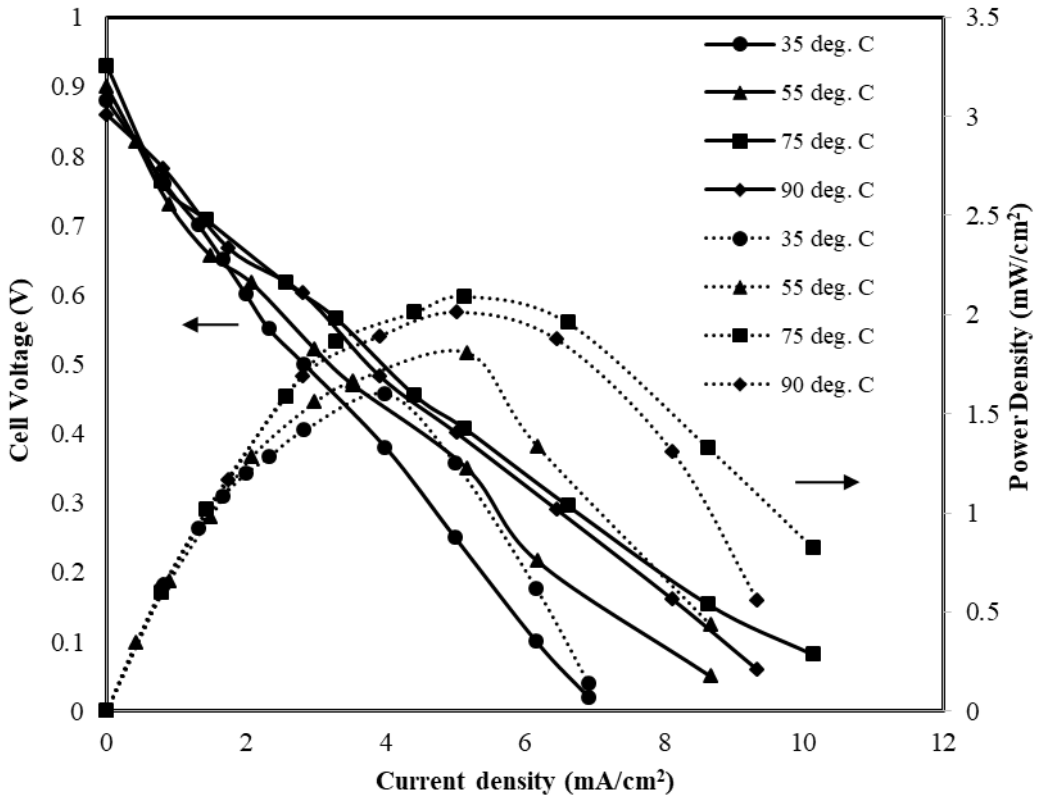

Figure 5.37 Polarization and power density curves of MFC for different cell temperature with optimum fuel and electrolyte concentration of 0.5 M KOH at anode side and at cathode side 0.5 M KOH with ambient air as oxidant Anode: Pd-Pt (16:4)/C of 2 mg/cm^2 and cathode: Pt/C_{HSA} of 2 mg/cm^2; MFC temperature: 35 ^{o}C.; Solid line – polarization curves; Dotted line – power density curves.

It may be due to increase in KOH solution conductivity with the increase in temperature for increased mobility of the ions in the solution (Gilliam et al., 2007). It also reduces the ohmic resistance. The maximum power density of 2.11 mW/cm^2 at a current density of 5.14 mA/cm^2 was obtained at the temperature of 75 ^{o}C. While, at lower temperature of 35 ^{o}C and 55 ^{o}C, the power density were 1.6 mW/cm^2 at a current density of 4 mA/cm^2 and 1.8 mW/cm^2 at a current density of 5.16 mA/cm^2, respectively.

Whereas, very high cell temperature of 95 ^{o}C, produce the maximum power density of 2 mW/cm^2 at a current density of 5.01 mA/cm^2 which is lower than the maximum power density obtained at the temperature 75 ^{o}C (2.09 mW/cm^2). The power density increased by 30.6 % for the rise in cell temperature from 35 ^{o}C to 75 ^{o}C.

Though, the conductivity of KOH solution has a higher value at an optimum KOH concentration (0.5 M) and it start to decreases for higher concentration due to increase in solution viscosity. The another reason may be due to an increase in water vapour partial pressure, which accelerates the vaporization process of solution, even though the boiling point of water increases by the presence of KOH (Nascimento et al., 2014). The increase in temperature also improves the electrooxidation rate of glycerol molecules at the electrode surface resulting in high current density due to better reaction kinetics (Zhang et al., 2012).

5.2.3.2 T-shaped air breathing MFC

5.2.3.2.1 Effect of anode electrocatalyst type

Figure 5.38 shows the performance characteristics of the T-shaped air breathing MFC with synthesized Pd-Pt (16:4)/C, Pd-Pt (10:10)/C, Pd-Pt (4:16)/C and Pd/C electrocatalysts respectively. The cathode electrocatalyst was commercial Pt/C_{HSA}. Both the electrodes were constructed with the electrocatalysts loading of 1 mg/cm^2. The anode fuel glycerol of 1 M mixed with 1 M KOH was fed at anode, whereas atmospheric

oxygen was used at cathode. The anode and cathode streams were fixed at the optimum flow rates of 1.2 ml/min and 1 ml/min, respectively. The maximum OCV of 0.67 V and maximum power density of 2.27 mW/cm^2 were obtained for the electrocatalyst Pd-Pt (16:4)/C. Whereas, OCV 0.53 V and maximum power density of 1.46 mW/cm^2 at a current density of 6.56 mA/cm^2 and OCV 0.42 V and maximum power density 0.80 mW/cm^2 at the current density of 4.24 mA/cm^2 were obtained for Pd-Pt (10:10)/C and Pd/C electrocatalyst, respectively. The Pd-Pt (4:10)/C produces lowest OCV of 0.33 V and maximum power density of 0.57 mW/cm^2 at the current density of 3.8 mA/cm^2. The reason for best performance of Pd-Pt (16:4)/C may be due to higher degree of alloying (47.9 %) and low overpotential as already discussed in the XRD (page no. 115) and CV observation (page no. 123), respectively.

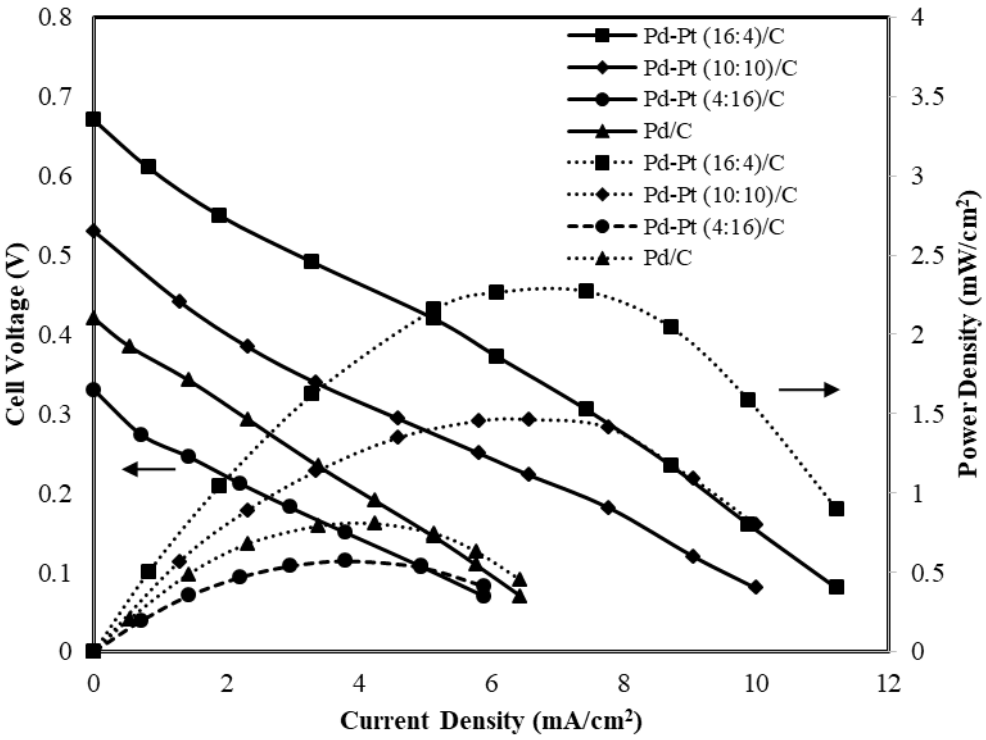

Figure 5.38 Polarization and power density curves of MFC for the different types of anode electrocatalyst using anode fed of 1 M glycerol mixed with 1 M KOH and cathode electrolyte of 0.5 M KOH; MFC temperature: 35 ^oC ; Dotted line – power density curves; Solid lines – polarization curves.

5.2.3.2.2 Effect of anode electrocatalyst loading

The single cell study using various type of anode electrocatalyst shows that Pd-Pt (16:4)/C performs better among all Pd based tested electrocatalysts. Thus, the anode loading was varied in the T-shaped air breathing MFC using synthesized Pd-Pt (16:4)/C electrocatalyst to get highest cell performance at the optimum loading. The anode fuel glycerol of 0.5 M mixed with 0.5 M KOH was fed at anode, whereas atmospheric oxygen was used as oxidant at cathode. The anode and cathode flow rates were maintained at optimum values i.e., 1.2 ml/min and 1 ml/min, respectively. Figure 5.39 shows the performance characteristics of air breathing MFC using varying anode electrocatalyst loading in the range of 0.5 mg/cm^2 to 2 mg/cm^2 of Pd-Pt (16:4)/C. The electrocatalyst loading of 1 mg/cm^2 Pt/C_{HSA} was kept fixed for each set of experiments.

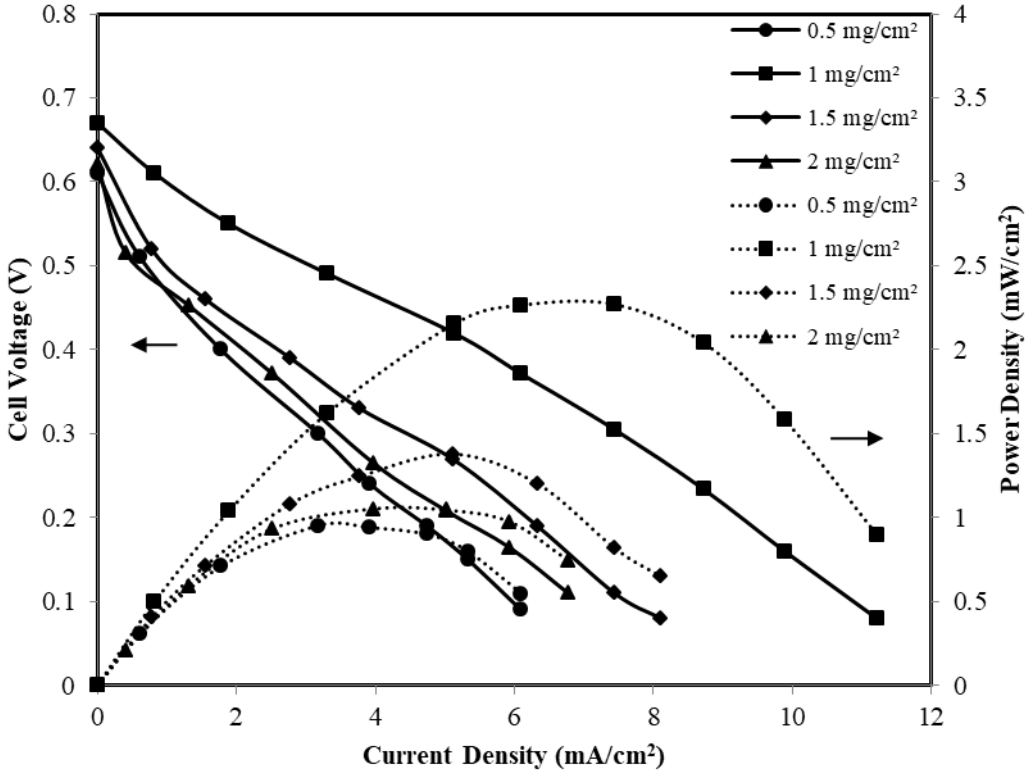

Figure 5.39 Polarization and power density curves of MFC for different loading of anode electrocatalyst and fixed cathode loading of 1 mg/cm^2 Pt/C_{HSA} using anode fed of 1 M glycerol mixed with 1 M KOH and cathode electrolyte of 0.5 M KOH; MFC temperature: 35 ^oC; Dotted line – power density curves; Solid lines – polarization curves.

It is seen from Figure 5.39 that the cell performance increases with the increase in the electrocatalyst loading from 0.5 mg/cm^2 to 1 mg/cm^2. Further increase in loading beyond 1 mg/cm^2, the cell performance decreases. The maximum power density of 2.27 mW/cm^2 at a current density of 7.44 mA/cm^2 was obtained at the anode electrocatalyst loading of 1 mg/cm^2. At lowest electrocatalyst loading of 0.5 mg/cm^2 produced lowest power density of 0.95 mW/cm^2 at a current density of 3.17 mA/cm^2. Whereas, 1.5 mg/cm^2 and 2 mg/cm^2 loading produced power density of 1.38 mW/cm^2 and 1.04 mW/cm^2 at a current density of 5.11 mA/cm^2 and 5.2 mA/cm^2, respectively. It shows that even high loading resulting in very low power density.

The active site of electrocatalyst increases with the increase in electrocatalysts loading. Thus, more glycerol molecules and OH^- ions interact with the increase in electrocatalyst surface resulting in more electrooxidation reaction which gives more current density and power density. However, increase in loading beyond the optimum loading, the electrocatalyst particles starts to agglomerate at the electrode surface and make it more compact. It creates hindrance for the diffusion of glycerol molecules and OH^- ions at the electrode surface which reduces the cell performance (Kim et al., 2005). This has already been discussed earlier (page no. 129-130).

5.2.3.2.3 Effect of cathode electrocatalyst loading

After optimizing the anode electrocatalyst loading at anode, the cathode side electrocatalyst loading was also optimized to obtain highest performance from the T-shaped air breathing MFC. The anode fuel glycerol of 1 M mixed with 1 M KOH was fed at anode, whereas atmospheric oxygen with 0.5 M was used as oxidant. Figure 5.40 shows the performance characteristics of air breathing MFC for different cathode electrocatalyst loading ranging from 0.5 mg/cm^2 to 2.5 mg/cm^2 keeping anode electrocatalyst fixed at the optimum loading of 1 mg/cm^2 of Pd-Pt (16:4)/C.

It is seen from the Figure 5.40 that the cell performance increases with the increase in the electrocatalyst loading upto 1 mg/cm^2 of Pt/C_{HSA} and further increase in loading beyond 1 mg/cm^2, the cell performance decreases. The highest power density of 2.27 mW/cm^2 at a current density of 7.44 mA/cm^2 was obtained for 1 mg/cm^2. Whereas, Pt/C_{HSA} of 1.5 mg/cm^2 and 2 mg/cm^2 loading produced power density of 2 mW/cm^2 at a current density of 6.49 mA/cm^2 and 1.29 mW/cm^2 at a current density of 4.77 mA/cm^2. At low electrocatalyst loading of 0.5 mg/cm^2, the MFC produced maximum power density of 0.97 mW/cm^2 at a current density of 5.11 mA/cm^2. The highest power density (2.27 mW/cm^2) at the loading 1 mg/cm^2 was due to optimal compromise between the available surface and particle available without any agglomeration as already been discussed in the previous section "5.2.3.2.2 Effect of anode electrocatalyst loading" (page no. 140).

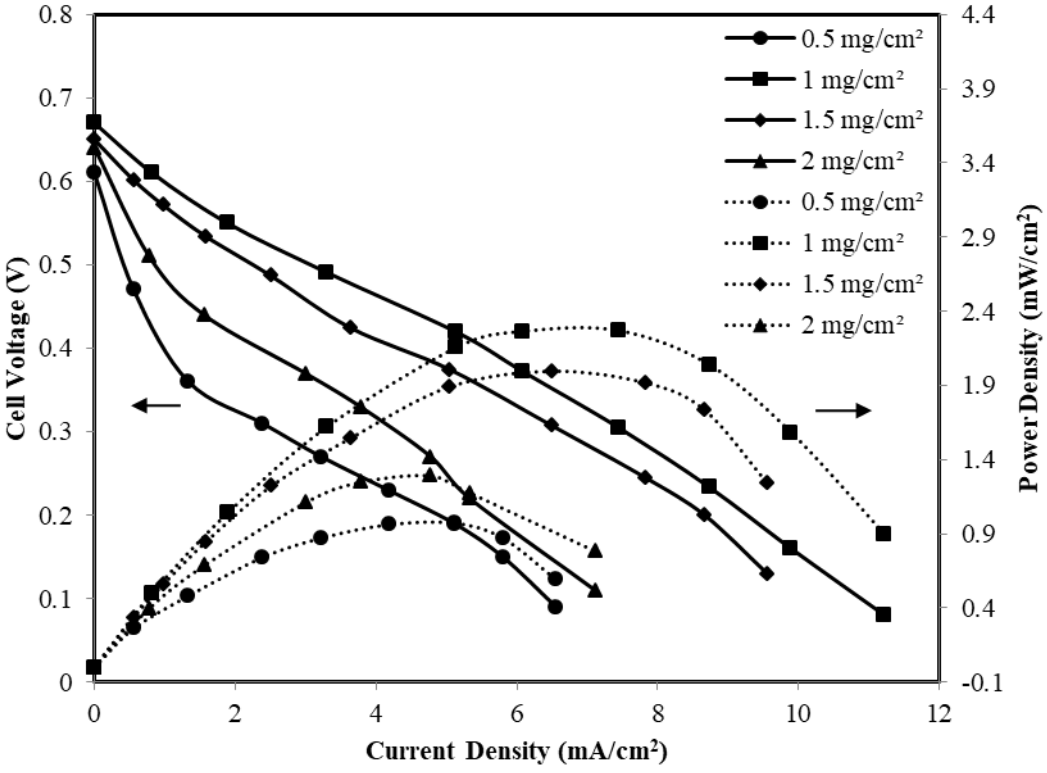

Figure 5.40 Polarization and power density curves of MFC for different loading of cathode electrocatalyst and fixed anode loading of 1 mg/cm^2 Pd-Pt (16:4)/C using anode fed of 1 M glycerol mixed with 1 M KOH and cathode electrolyte of 0.5 M KOH; MFC temperature: 35 ^oC ; Dotted line – power density curves; Solid lines – polarization curves.

5.2.3.2.4 Effect of glycerol concentration

The effect of glycerol concentration on the performance characteristics i.e., polarization and power density curves of T-shaped air breathing MFC is presented in Figure 5.41. The glycerol concentration was varied from 0.5 M to 2 M keeping the anode and cathode electrolyte concentration fixed at 1 M and 0.5 M KOH, respectively. It is seen in the Figure 5.41, the cell performance increases with the increase in glycerol concentration upto 1 M and further increase in glycerol concentration beyond 1 M, the cell performance decreases. This decreasing trend in the cell performance was recorded upto 2 M of glycerol concentration. It may be due to the increase in glycerol concentration, electrolyte KOH concentration gets decreased at the electrocatalysts surface which is unfavourable for the anode electrooxidation reaction. As per the reaction anode scheme (Equation 1.1), a delicate balance is required between glycerol and OH^- ions at the anode electrocatalysts sites (page no. 9). The maximum OCV of 0.67 V and highest power density 2.27 mW/cm^2 were obtained for 1 M glycerol concentration mixed with KOH concentration of 1 M. The cell performance was low at 0.5 M glycerol concentration, where OCV of 0.61 V and maximum power density 1.48 mW/cm^2 at a current density of 6.4 mA/cm^2 were obtained, due to less presence of OH^- ions relative to glycerol molecules at the surface of electrode. On the other side, the relative concentration OH^- ions at the surface of electrocatalysts get decreased at very high concentration i.e., 1.5 M and 2 M of glycerol which results in lower cell performance. The maximum power density of 1.41 mW/cm^2 and 0.64 mW/cm^2 at a current density of 5.2 mA/cm^2 and 2.7 mA/cm^2 were obtained for the glycerol concentration of 1.5 M and 2 M, respectively.

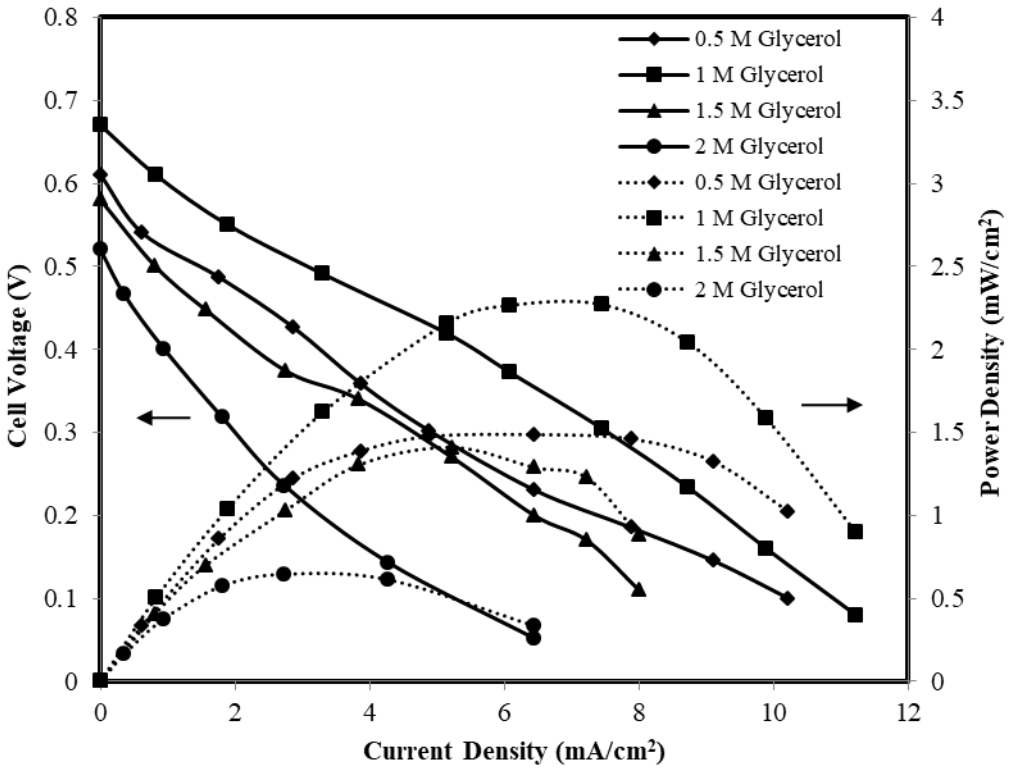

Figure 5.41 Polarization and power density curves of MFC for anode fed glycerol of different concentration mixed with 1 M KOH and cathode electrolyte of 0.5 M KOH; Anode: Pd-Pt (16:4)/C of 1 mg/cm^2 and cathode: Pt/C_{HSA} of 1 mg/cm^2; MFC temperature: 35 ^oC ; Dotted line – power density curves; Solid lines – polarization curves.

5.2.3.2.5 Effect of anode KOH concentration

The effect of anode electrolyte concentration on the performance of T-shaped air breathing MFC is shown in Figure 5.42. The anode and cathode were fabricated using optimum loading of 1 mg/cm^2 of synthesized Pd-Pt (16:4)/C and commercial Pt/C_{HSA} electrocatalyst both. The electrolyte KOH concentration was varied from 0.5 M to 2 M, while the glycerol concentration was kept at optimum value of 0.5 M. The electrolyte provides ionic mobility of the OH^- ions and reduces the ohmic loss and thus, increase in electrolyte concentration increases the movements of anions for the KOH concentration upto 1.5 M. Further increase in electrolyte concentration beyond 1.5 M KOH, the concentration of glycerol molecules get replaced by OH^- ions at the electrode surface and thus, cell performance fall down (Gupta and Pramanik 2019).

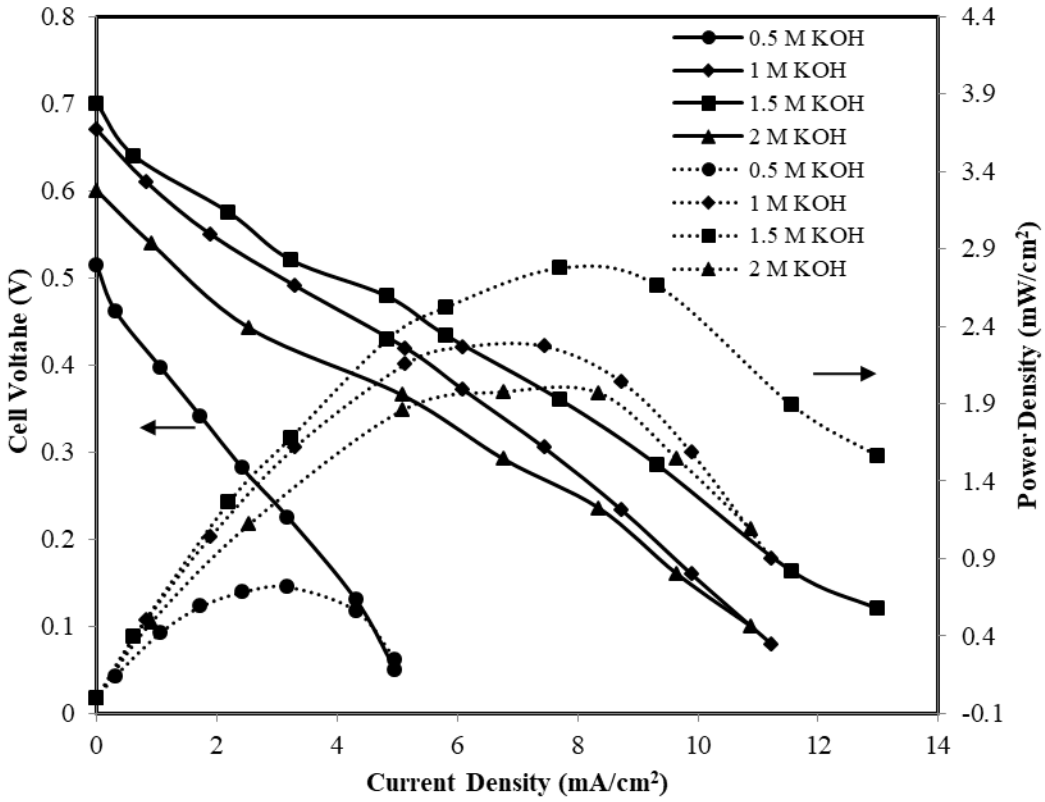

Figure 5.42 Polarization and power density curves of MFC for different KOH concentration mixed with 1 M glycerol at anode and fixed cathode electrolyte of 0.5 M KOH; Anode: Pd-Pt (16:4)/C of 1 mg/cm^2 and cathode: Pt/C_{HSA} of 1 mg/cm^2; MFC temperature: 35 ^oC; Dotted line – power density curves; Solid lines – polarization curves.

As already mentioned, the presence of glycerol and OH^- ions both are required for anode reaction (Equation (1.1)). A delicate balance between glycerol and OH^- ions will ensure the highest cell performance of MFC which is achieved at the anode KOH concentration of 1.5 M. The optimum concentration of KOH electrolyte was recorded 1.5 M at which the maximum power density 2.77 mW/cm^2 at a current density of 7.71 mA/cm^2 was generated by the cell. At low concentration of 0.5 M KOH and 1 M, the maximum power density of 0.71 mW/cm^2 and 2.77 mW/cm^2 were obtained at a current density of 3.17 mA/cm^2 and 7.4 mA/cm^2, respectively. Moreover, at higher concentration of 2 M KOH beyond the optimum concentration (1.5 M), the recorded power density was 1.97 mW/cm^2 a current density of 8.35 mA/cm^2.

5.2.3.2.6 Effect of cathode KOH concentration

The cathode side electrolyte KOH concentration was optimized after optimizing the anode KOH concentration to achieve highest power density from T-shaped air breathing MFC as shown in Figure 5.43. The KOH electrolyte concentration of 0.25 M, 0.5 M, 0.75 M and 1 M KOH were used at the cathode side for each set of experiments keeping the anode electrolyte at optimum value of 1.5 M KOH. The optimum concentration of glycerol of 1 M was fed as at anode side of MFC. The oxidant at cathode was atmospheric oxygen. The Figure 5.43 shows that the polarization and power density curves shifted to upward direction when KOH concentration at cathode was increased from 0.25 M to 0.5 M.

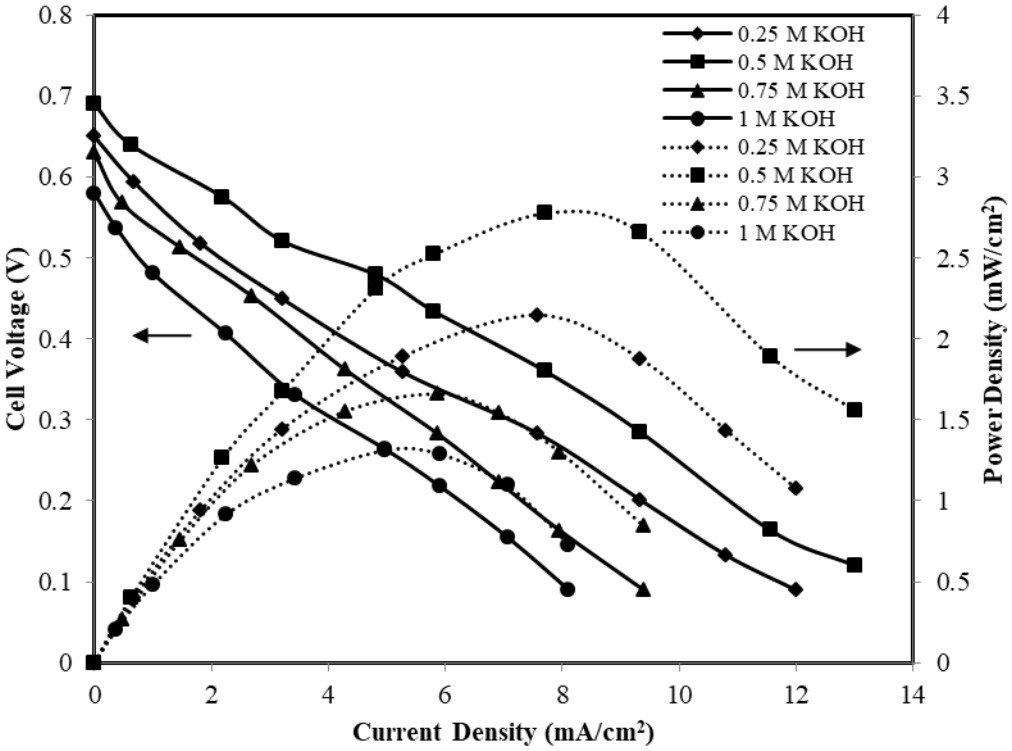

Figure 5.43 Polarization and power density curves of MFC for different cathode KOH electrolyte concentration and 1 M glycerol mixed with1.5 M KOH at anode side. Anode: Pd-Pt (16:4)/C of 1 mg/cm^2 and cathode: Pt/C_{HSA} of 1 mg/cm^2; MFC temperature: 35 ^oC; Dotted line – power density curves; Solid lines – polarization curves.

Further increase in KOH concentration beyond 0.5 M, both the curve shifted downward due to replacement of water molecules by OH^- ions and thereby reducing water molecules at the active sites of cathode. As shown in Equation (1.2) (page no. 9), the water molecules are essential for the completion of cathodic reaction. Thus, the performance of MFC hindered due to slowness of the cathode kinetics. The highest OCV of 0.69 V and power density of 2.77 mW/cm^2 at a current density of 7.71 mA/cm^2 were obtained at KOH concentration of 0.5 M. While, at low concentration of 0.25 M KOH, the maximum power density of 2.14 mW/cm^2 at a current density of 7.57 mA/cm^2 was obtained. The KOH concentration of 0.75 M and 1 M produced low power density of 1.66 mW/cm^2 and 1.31 mW/cm^2 at a current density of 5.85 mA/cm^2 and 4.97 mA/cm^2, respectively.

5.2.3.2.7 Effect of cell temperature

Figure 5.44 shows the polarization and power density curves of T-shaped air breathing MFC for the varying temperature ranging from 35 °C to 95 °C using 1 M glycerol (optimum) mixed with 1.5 M KOH (optimum) at anode and 0.5 M KOH (optimum) at cathode. The oxidant at cathode was atmospheric oxygen. The highest cell temperature of 95 ^oC was maintained keeping in mind the boiling point of water (100 ^oC) and avoid two phase flow which would hinder the flow dynamics in the microchannel (Wang et al., 2019). It is seen for the Figure 5.44**,** the cell performance increases with increase in temperature upto 75 ^oC. Further increase in temperature beyond 75 ^oC, the cell performance decreases rapidly. It may be due to increase in KOH solution conductivity with the increase in temperature for increased mobility of the ions in the solution (Gilliam et al., 2007). It also reduces the ohmic resistance. The OCV 0.78 V and maximum power density of 4.03 mW/cm^2 at a current density of 10.47 mA/cm^2 were obtained at the temperature of 75 ^oC. While, at lower temperature of 35 ^oC and 55 ^oC, power density of

2.27 mW/cm^2 and 3.03 mW/cm^2 were obtained at a current density of 7.71 mA/cm^2 and 9.95 mA/cm^2, respectively.

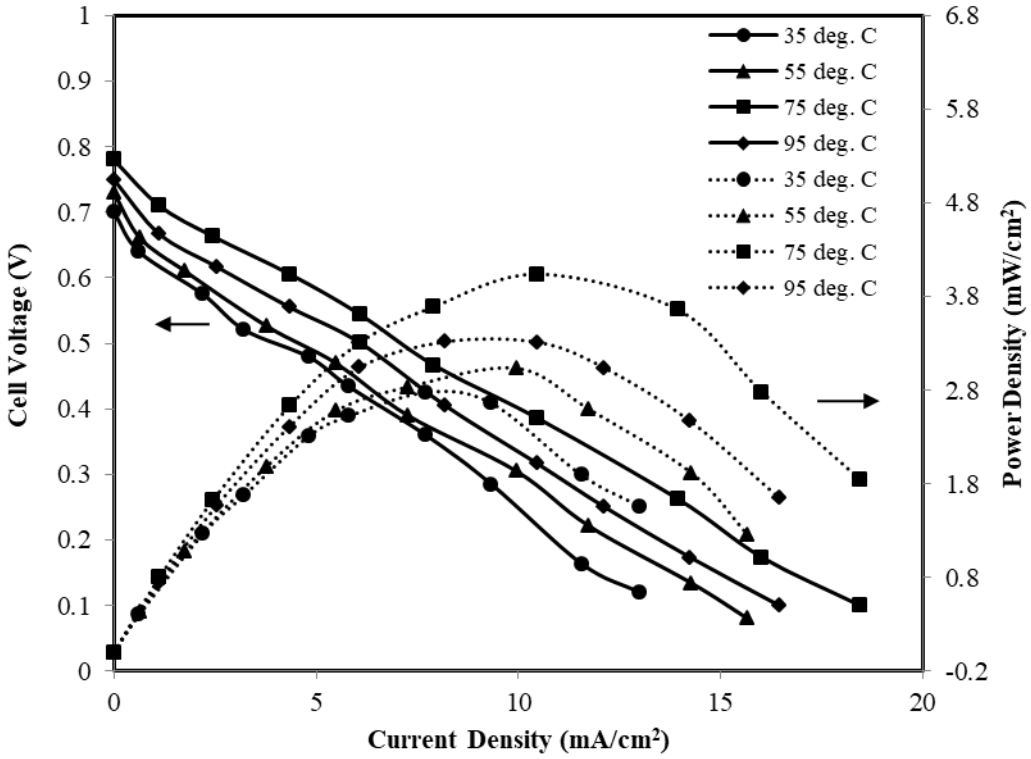

Figure 5.44 Polarization and power density curves of MFC at different temperatures and anode fed of 1 M glycerol mixed with 1.5 M KOH, and cathode electrolyte of 0.5 M KOH; Anode: Pd-Pt (16:4)/C of 1 mg/cm^2 and cathode: Pt/C_{HSA} of 1 mg/cm^2, Dotted line – power density curves; Solid lines – polarization curves.

Whereas, very high cell temperature of 95 ^oC, produce the maximum power density of 3.31 mW/cm^2 at a current density of 10.4 mA/cm^2 which is lower than the maximum power density obtained 75 ^oC (4.03 mW/cm^2). The power density increased by 45.4 % for the rise in cell temperature from 35 ^oC to 75 ^oC. The reason for such trend of cell performance with temperatures has already been discussed earlier (page no. 137).

5.2.3.2.8 Bleaching and air as mixed oxidant for air breathing MFC

Figure 5.45 shows the polarization and power density characteristics of varying concentrations of calcium hypochlorite/$Ca(OCl)_2$ in presence of air mixed oxidant at the room temperature of 35 ^oC. The purpose of using mixed oxidant was to study the effect of

calcium hypochlorite along with atmospheric oxygen as oxidant in T-shaped MFC. The calcium hypochlorite of varying concentrations was mixed with optimum electrolyte concentration of 0.5 M KOH before the solutions fed to the cathode side of the MFC. It has already been discussed in T-shaped MFC (page no. 111), Momoh, (2011) proposed that calcium hypochlorite reacts with water to form hypochorous acid and calcium hydroxide. The formed calcium hydroxide settle down in the beaker and rest of the liquid was used as oxidant for the MFC experiment. In alkaline medium, hypochlorous acid is converted into hypochlorite ions as shown in Equation (5.5) (page no. 111). The reaction from the conversion of calcium hypochlorite to hypochlorite ion is given in Equation (5.6), and the overall cathode side reaction is given by Equation (5.7) (Martins et al., 2018).

The combined effect of mixed oxidant air and hypochlorite ion as shown in cathode reduction in Equation (1.2) (page no. 9) and Equation (5.7) (page no. 111) which enhanced the MFC performance significantly. The CV study of the cathode in the half cell using mixed oxidant calcium hypochlorite and oxygen also showed better performance in comparison to only oxygen as oxidant (page no. 82). The cathode peak shifted towards more positive potential (-0.27 V) for the mixed oxidant condition. It is seen from the Figure 5.45 that MFC performace increases with the increase in $Ca(OCl)_2$ concentration upto 1.5 M and futher increase in oxidant concentration 2 M, the cell performance decreases. It may be due to the less avialability of water molecules at the active catalysts sites at higher oxidant concentration and thus, the cell performace reduces in terms of OCV and power density. The mixed oxidant/$Ca(OCl)_2$ concentration of 1.5 M and air produced very high OCV of 0.81 V with highest power density of 4.5 mW/cm^2 at a current density of 13.61 mA/cm^2.

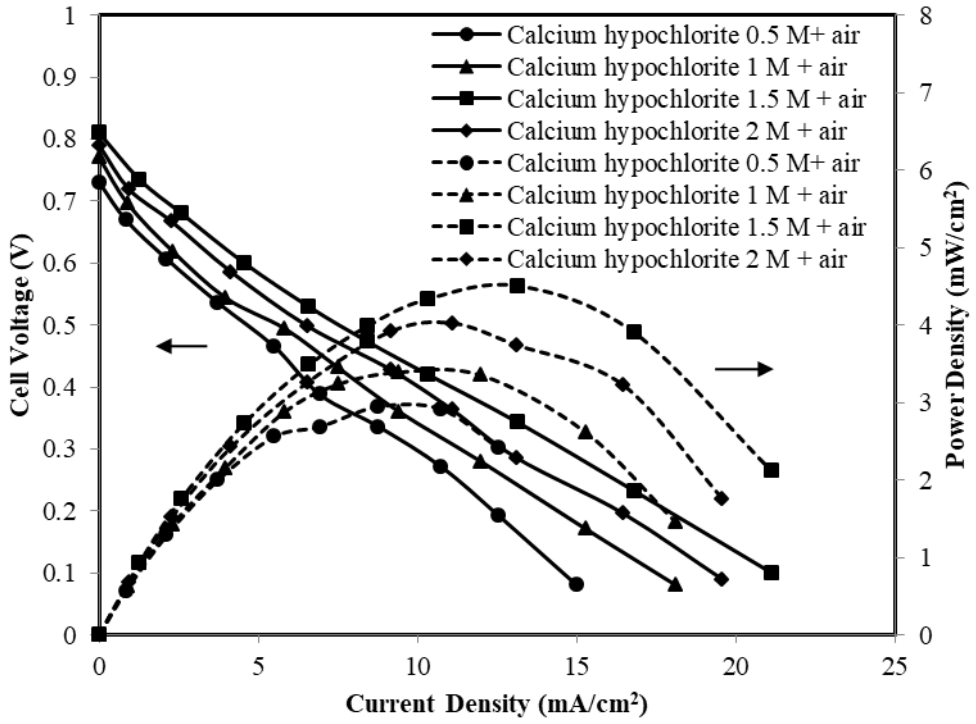

Figure 5.45 Polarization and power density curves from air breathing MFC for varying concentrations of calcium hypochlorite and atmospheric air as mixed oxidant as catholyte and optimum 1 M glycerol mixed with 1.5 M KOH electrolyte as anolyte. The anode electrocatalyst was 1 mg/cm^2 of Pd-Pt (16:4)/C and cathode electrocatalyst was 1 mg/cm^2 of Pt/C_{HSA}. MFC temperature: 35 ^oC; Solid line – polarization curves; Dotted line – power density curves.

Whereas, OCV of 0.73 V was found at oxidant concentration of 0.5 M with a maximum power density of 2.94 mW/cm^2 at the current density of 8.77 mA/cm^2. At mixed oxidant/$Ca(OCl)_2$ concentration of 1 M in presence of air produced OCV of 0.77 V with maximum power density of 3.38 mW/cm^2 at a current density of 9.39 mA/cm^2. Very high concentration of oxidant/$Ca(OCl)_2$ of 2 M in presence of air produced OCV of 0.79 V and maximum power density (4.02 mW/cm^2) was also low in comparison to mixed oxidant condition $Ca(OCl)_2$ of 1.5 M in presence of air (4.5 mW/cm^2). It should be noted that the performance of MFC was found highest for the mixed oxidant condition using 1.5 M of $Ca(OCl)_2$ in presence of air. At this condition a delicate balance is establish between water molecules, OCl^- ions and oxygen which are essential to complete the ctahode reations at the active sites of the Pt/C_{HSA} electrocatalysts.

5.2.4 Comparison of performance of synthesized best electrocatalysts in Y-shaped and T-shaped MFC

Table 5.7 shows the performance comparison of best bimetallic electrocatalysts Pd-Pt (16:4)/C in both Y-shaped and T-shaped MFC for glycerol fuel at room temperature of 35 ^{o}C and optimized MFC conditions, respectively. The optimum conditions for the Pd-Pt (16:4)/C electrocatalyst were anode electrocatalyst loading of 2 mg/cm^2 Pd-Pt (16:4)/C and cathode electrocatalyst loading of 2 mg/cm^2 Pt/C_{HSA}, cell temperature of 75 ^{o}C, anode fuel of 0.5 M glycerol mixed with 0.5 M KOH and cathode oxidant atmospheric/oxygen mixed with 0.5 M KOH in Y-shaped air breathing MFC. Whereas, the optimum conditions obtained T-shaped air breathing MFC for the same electrocatalyst Pd-Pt (16:4)/C were anode electrocatalyst loading of 1mg/cm^2 and cathode electrode loading 1 mg/cm^2 of Pt/C_{HSA}, anode fuel 1 M glycerol mixed with 1.5 M KOH and cathode oxidant atmospheric air/oxygen mixed with 0.5 M KOH. It is clearly seen from the Table 5.7 that the highest power density of 4.03 mW/cm^2 is obtained from the T-shaped air breathing MFC at optimum cell condition.

Table 5.7 Comparison of Pd-Pt (16:4)/C anode electrocatalyst in Y-shaped and T-shaped air breathing MFC at optimum MFC conditions and at room temperature.

Temperature (^{o}C)	**Y-shaped air breathing MFC**		**T-shaped air breathing MFC**	
	Maximum Power Density (mW/cm^2)	**Current Density at max. power density (mA/cm^2)**	**Maximum Power Density (mW/cm^2)**	**Current Density at max. power density (mA/cm^2)**
35 (Room temp.)	1.6	4	2.77	7.71
75 (Optimum temp.)	2.11	5.14	4.03	10.47

Whereas, maximum power density of 2.11 mW/cm^2 was obtained from the Y-shaped air breathing MFC operating at the optimum cell condition as mentioned above. The observed power density for the Y-shaped MFC (2.11 mW/cm^2) is lower than the T-shaped MFC (4.03 mW/cm^2) while comparing at their corresponding optimum cell conditions.

Similarly, Y-shaped and T-shaped MFC produced maximum power density of 1.6 mW/cm^2 and 2.77 mW/cm^2, respectively at room temperature of 35 ^{o}C. It should be noted that T-shaped air breathing MFC showed better performance than the Y-shaped air breathing MFC at room temperature and optimized process conditions both. Table 5.8 shows the performance comparison of best bimetallic electrocatalyst Pd-Ni (10:10)/C in Y-shaped and T-shaped air breathing MFC for glycerol electrooxidation at room temperature 35 ^{o}C and optimized MFC conditions, respectively.

Table 5.8 Comparison of Pd-Ni (10:10)/C anode electrocatalyst in Y-shaped and T-shaped air breathing MFC at optimum MFC conditions and at room temperature.

Temperature (^{o}C)	**Y-shaped air breathing MFC**		**T-shaped air breathing MFC**	
	Maximum Power Density (mW/cm^2)	**Current Density at max. power density (mA/cm^2)**	**Maximum Power Density (mW/cm^2)**	**Current Density at max. power density (mA/cm^2)**
35 (Room temp.)	1.16	2.92	1.27	5.77
75 (Optimum temp.)	1.6	4.41	2.14	8.96

The optimum conditions obtained for the Pd-Ni (10:10)/C in Y-shaped air breathing MFC were anode electrocatalyst loading of 1.5 mg/cm^2, cathode electrocatalyst loading of 1.5 mg/cm^2 Pt/C_{HSA}, cell temperature of 75 ^oC, anode fuel glycerol of 0.5 M mixed with 0.5 M KOH electrolyte and oxidant atmospheric air/oxygen mixed with 0.5 M KOH at cathode. Whereas, the optimum conditions for the same electrocatalyst Pd-Ni (10:10)/C in T-shaped MFC were anode loading of 1 mg/cm^2, cathode loading of 1 mg/cm^2 Pt/C_{HSA}, anode fuel glycerol of 1 M mixed with 1 M KOH and oxidant atmospheric air/oxygen mixed with 1 M KOH.

Similar trend in cell performance is also observed for Pd-Ni (10:10)/C electrocatalyst (Table 5.8), as it was seen in the case of Pd-Pt (16:4)/C when comparing performance of two different cell architecture and design (Table 5.7). The cell performance obtained in terms of power density is always higher for Pd-Ni (10:10)/C electrocatalyst in T-shaped MFC than that of Y-shaped MFC design at room temperature and optimized cell conditions both. It is seen from the Table 5.8 that the maximum power density of 2.14 mW/cm^2 and 1.6 mW/cm^2 were obtained at the optimum temperature of 75 ^oC from T-shaped and Y-shaped MFC, respectively. Whereas, maximum power density of 1.27 mW/cm^2 and 1.16 mW/cm^2 were obtained at the room temperature of 35 ^oC from T-shaped and Y-shaped MFC, respectively.

It should be noted that the best performance was exhibited by Pd-Pt (16:4)/C electrocatalyst among all synthesized single metal and bimetallic electrocatalyst i.e., Pd/C, Pd-Pt/C and Pd-Ni/C as discussed under the section “5.1 Performance evaluation of Pd-Ni/C anode electrocatalyst: Part I” (page no. 84-114) and section “5.2 Performance evaluation of Pd-Pt/C anode electrocatalyst: Part II” (page no. 115-150). The best performance of Pd-Pt (16:4)/C electrocatalyst for glycerol fuel was noted, irrespective of cell design types i.e., Y-shaped and T-shaped MFC.

The reasons for best performance of Pd-Pt (16:4)/C electrocatalyst among all synthesized electrocatalyst have already been discussed like higher degree of alloying (page no. 115), more negative anodic peak potential resulting in low activation loss (page no.123) and least charge transfer resistance of the electrocatalyst (page no. 125). The T-shaped air breathing MFC gives better performance than the from Y-shaped MFC at room temperature and optimized MFC condition due to the top and bottom electrode position in T-shape which enables more fuel contact with the electrode and least boundary layer thickness. In view of the best performance of the synthesized Pd-Pt (16:4)/C anode electrocatalyst, it was selected for optimization study using RSM in T-shaped air breathing MFC.

5.2.5 Process parameter optimization using RSM

5.2.5.1 ANOVA analysis and model development

The power density (Y) as a response for the glycerol electrooxidation reaction performed in the T-shaped air breathing MFC is presented in Table 5.9. The actual values of power densities from each experiment and predicted values of power densities from the model are also presented in Table 5.9.

Table 5.9 BBD arrangements and response for glycerol electrooxidation regarding power density.

Run	A-glycerol conc. (M)	B-anode electrolyte conc. (M)	C-anode electrocatalyst loading (mg/cm^2)	D-cathode electrolyte conc. (M)	Experimental power density (mW/cm^2)	Predicted power density (mW/cm^2)
1	1	1	1	0.75	1.9	1.99
2	1	1	1.5	0.5	1.38	1.29
3	1	1.5	1.5	0.75	2.2	2.02
4	1	2	0.5	0.5	1.1	1.08
5	1	2	1	0.25	2.44	2.29
6	1	1.5	0.5	0.25	2.2	2.27
7	1	1.5	1	0.5	2.65	2.71
8	1	1.5	1	0.5	2.6	2.71
9	1.5	1.5	0.5	0.5	0.96	0.85
10	1	2	1	0.75	2.43	2.39
11	1	1.5	1	0.5	2.77	2.71
12	1.5	2	1	0.5	2.1	2.08
13	1.5	1.5	1	0.75	2.32	2.34
14	1	1.5	0.5	0.75	1.1	1.08
15	0.5	1.5	1	0.25	1.95	2.10
16	1	1.5	1.5	0.25	1.4	1.44
17	0.5	1	1	0.5	1.48	1.47
18	1	1.5	1	0.5	2.77	2.71
19	1	1	1	0.25	2.1	2.08
20	1	1	0.5	0.5	0.95	0.93
21	0.5	1.5	1	0.75	1.8	1.68
22	1	1.5	1	0.5	2.77	2.71
23	0.5	1.5	0.5	0.5	1	1.08
24	1.5	1	1	0.5	1.4	1.44
25	1.5	1.5	1	0.25	1.64	1.92
26	0.5	2	1	0.5	1.65	1.50
27	1.5	1.5	1.5	0.5	1.7	1.56
28	1	2	1.5	0.5	1.3	1.48
29	0.5	1.5	1.5	0.5	0.8	0.85

The experimental data of current density vs. cell voltage and current density vs. power density of all 29 experiments under various cell conditions as mentioned in Table 5.9 is given in the Appendix E (Table E1). A second order polynomial regression given by Equation (4.2) was modelled to find the power density (Y) in the T-shaped MFC for the glycerol electrooxidation. The maximum power density of 2.77 mW/cm^2 is achieved when the MFC was operating with glycerol concentration of 1 M, anode electrolyte concentration 1.5 M, cathode electrolyte concentration of 0.5 M and anode electrocatalyst loading of 1 mg/cm^2. However, the lowest performance in terms of power density 0.8 mW/cm^2 was observed at glycerol concentration of 0.5 M, anode electrolyte concentration of 1.5 M, cathode electrolyte concentration of 0.5 M and anode electrocatalyst loading of 1.5 mg/cm^2. The model summary statistics of four types models viz. linear, two factor interaction (2FI), quadratic and cubic are shown in Table 5.10which focuses on maximizing the adjusted and predicted R^2. Out of four models, the quadratic model shows the maximum adjusted and predicted R^2 values (Myers et al., 2016). The predicted residual error sum of squares (PRESS) statistic specifies how fine the model fits the data. The PRESS value, which is smaller in comparison to other chosen model should be taken into consideration.

Table 5.10 Model summary statistics**.**

Source	Std. dev (σ)	R- squared	Adjusted R-squared	Predicted R-squared	PRESS values
Linear	0.65	0.0538	-0.0986	-0.2924	13.87
2FI	0.70	0.1876	-0.2637	-0.8637	20.01
Quadratic	0.17	0.9634	0.9268	0.7995	2.15
Cubic	0.14	0.9897	0.9519	-0.1330	12.16

Table 5.11 shows the statistical analysis for the power density of the glycerol electrooxidation reaction obtained from the analysis of variance (ANOVA) using the quadratic model. The source is just the name of the column, the sum of squared is the

deviation from the mean, whereas Df is the degree of freedom for the model and it denotes the model terms plus the intercepts minus one. The mean square (MS) is the ratio of the sum of squares to the Df, and it estimates the model variance. The F-value for each term is the test for relating the variance connected with that term with the residual variance.

Table 5.11 ANOVA for Response Surface Quadratic Model.

Source	**Sum of squares (SS)**	**Df**	**Mean square (MS)**	**F value**	**p-value prof>F**	**Remarks**
Model	10.34	14	0.74	26.32	< 0.0001	significant
A-glycerol concentration	0.17	1	0.17	6.16	0.0264	…..
B-anode electrolyte concentration	0.27	1	0.27	9.73	0.0075	…..
C-anode electrocatalyst loading	0.18	1	0.18	6.42	0.0239	…..
D-cathode electrolyte concentration	0.00003	1	0.00003	0.0011	0.97	…...
AB	0.070	1	0.070	2.5	0.1360	…..
AC	0.22	1	0.22	7.87	0.0140	……
AD	0.17	1	0.17	6.14	0.0266	……
BC	0.013	1	0.013	0.47	0.5036	…..
BD	0.009	1	0.009	0.32	0.5797	……
CD	0.90	1	0.90	32.16	< 0.0001	…..
A^2	2.69	1	2.69	95.70	< 0.0001	……
B^2	1.40	1	1.40	49.92	< 0.0001	…..
C^2	6.26	1	6.26	222.98	< 0.0001	……
D^2	0.022`	1	0.022`	0.79	0.3889	……
Residual	0.39	14	0.028	…..	……	……
Lack of Fit	0.37	10	0.037	5.54	0.0568	Not significant
Pure Error	0.026	4	0.0066	……	…..	……
Cor Total	10.73	28	…..	…..	…..	……

It is the ratio of mean Square for the term and the mean square for the residual. The p-value found for this model is < 0.0001 and F-value greater than 1 (26.32). The significant process parameters can be studied from the p-values, i.e., glycerol concentration (A), anode electrolyte/KOH concentration (B), cathode electrolyte/KOH concentration (C) and anode electrocatalyst loading (D) and had the p- values of 0.0265, 0.0075, and 0.0239 however, and the p-value of 0.97 for cathode electrolyte/KOH concentration is non-significant term according to the model. The second-order model equation, which relates dependent and independent parameters, was obtained in terms of actual factors in Equation (5.10) below:

$$\text{Power density (Y)} = -4.74358 + 2.82300 \times A + 5.38867 \times B + 5.60800 \times C - 5.08733 \times D + 0.53000 \times A \times B + 0.94000 \times A \times C + 1.66000 \times A \times D - 0.23000 \times B \times C + 0.38000 \times B \times D + 3.80000 \times C \times D - 2.574 \times A^2 - 1.85900 \times B^2 - 3.92900 C^2 - 0.9360 \times D^2 \quad (5.10)$$

Where A is glycerol concentration, B is anode electrolyte/KOH concentration, C is anode electrocatalyst loading and D is cathode electrolyte/KOH concentration. Power density (Y) is the predicted values calculated by taking the actual data of the parameters.

The coefficient with positive values in Equation (5.10) indicates that these terms affect in favours of the response. However, the terms with negative coefficients show incompatibility with the response. The model equation with positive coefficient terms as A, B, C, AB, AC, AD, BD and CD have positive effect on power density. However, negative coefficient terms as D, A^2, B^2, C^2, D^2 and BC have negative effects on the power density. The value of Predicted R-Squared is 0.7995 which is in suitable agreement with the Adjusted R-Squared of 0.9268 (Yahya et al., 2017). The value of adequate precision measures the signal to noise ratio, a ratio greater than 4 is considerable, and the present ratio of 15.464 shows a suitable signal (Panjiara and Pramanik 2020b).

The Figure 5.46 shows relation among the predicted data from the model and actual data of power density obtained from the experiments graph, where point of the actual power density of the experiment is close to the predicted values of power density. This graph with linear direction indicates that the power density obtained from experiments had an orderly distribution and thus, that this model can satisfactorily predict the response (Kahveci et al., 2014).

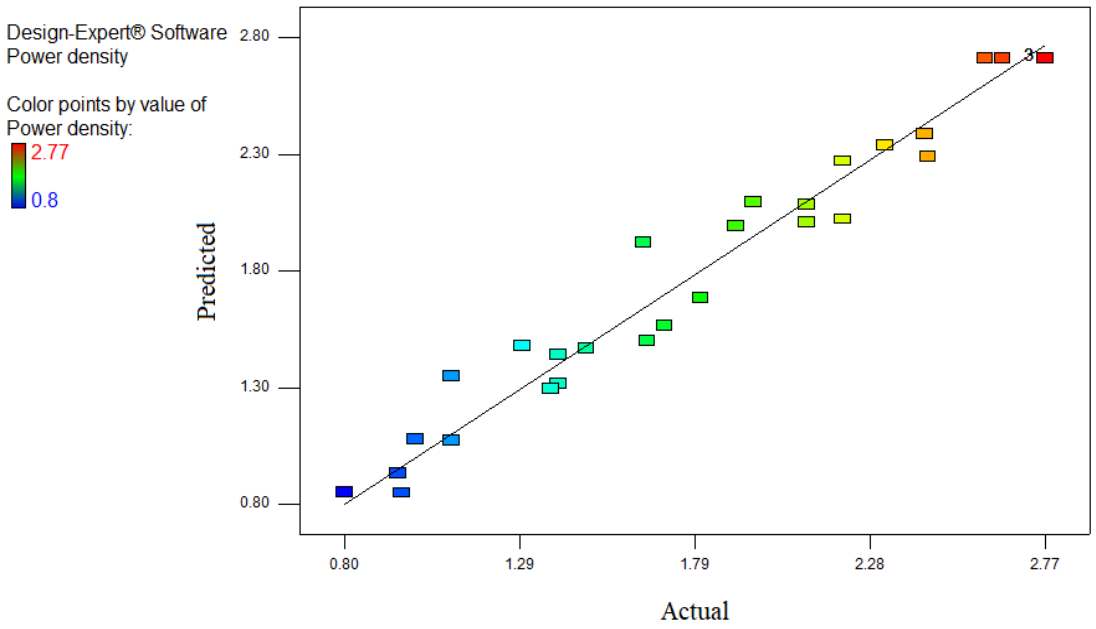

Figure 5.46 Actual versus model predicted power density comparison**.**

The R^2 coefficient value is 0.9634 for this model shows that the model is well fitted to the experimental data. The difference between the values of predicted R^2 and adjusted R^2 for this model is less than 0.3 (Table 5.10), which suggests that the non-significant terms do not affect the quadratic model. The predicted vs. residual graph is shown in the Figure 5.47.

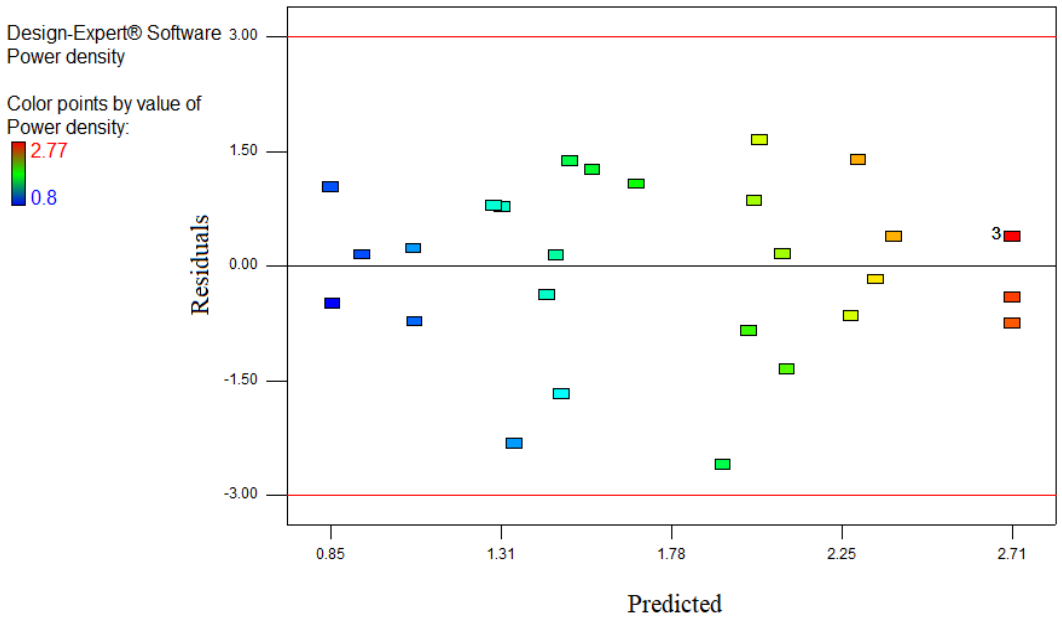

Figure 5.47 Predicted vs. Residual value of power density obtains from air breathing T-shaped MFC.

The graph obtained from the difference between experimental and predicted values, which is called residual values. It shows the accurateness of prediction. The values on the Y-axis from the positive side describes that the predicted value was too low. While the higher predicted values are shown on the negative side of the Y-axis (Figure 5.47). The values near the X-axis represent that the experiment values are close to the predicted values.

5.2.5.2 Polarization and power density curves

Figure 5.48a shows the polarization and power density curves for the T-shaped air breathing microfluidic fuel cell using anode electrocatalyst Pd-Pt (16:4)/C and operated at optimum condition obtained by RSM analysis. The polarization and power density curves were drawn to find the maximum power density at a given load. Here, the polarization curve on the optimum condition predicted by the model was shown to compare the actual to the predicted values of power density.

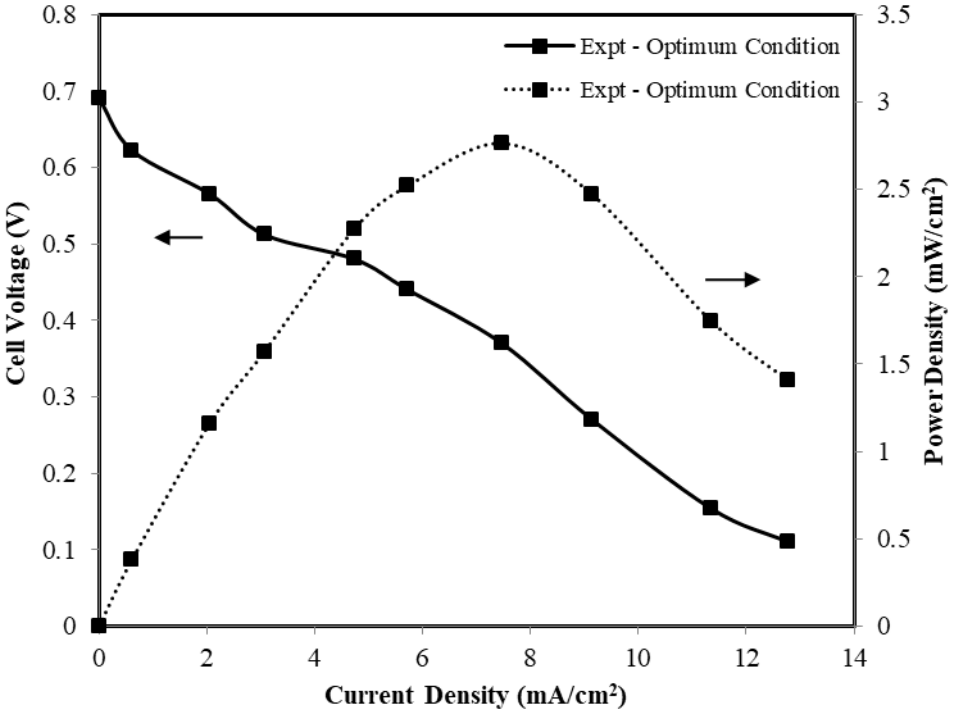

Figure 5.48a Polarization and power density curves for optimum condition of 1.07 M glycerol fuel mixed with 1.62 M KOH as electrolyte, anode electrocatalyst loading of 1.12 mg/cm^2 and cathode electrolyte of 0.69 M KOH, Solid line – polarization curves; Dotted line – power density curves.

The optimum conditions obtained by RSM analyses were glycerol concentration (A) of 1.07 M, anode electrolyte concentration (B) of 1.62 M, anode electrocatalyst loading (C) of 1.12 mg/cm^2 and cathode electrolyte concentration (D) of 0.69 M KOH. The flow rate of anode and cathode streams were maintained at 1.2 ml/min and 1 ml/min, respectively. The temperature for single cell experiment was maintained at room temperature of 35 ºC. All the experiments were repeated three times to confirm consistent polarization behaviour of MFC. The polarization curves of three repeated experiments under optimum condition are shown in the Appendix E (Figure E1). Table 5.12 shows the actual/experimental value of power density obtained at the optimum condition and comparison of the same with the predicted value**.**

Table 5.12 Comparison of predicted and actual power density at the optimum condition obtained from the model.

Conditions and criteria	**Glycerol concentration (M)**	**Anode electrolyte concentration (M)**	**Electrocatalyst loading (mg/cm^2)**	**Cathode electrolyte concentration (M)**	**Power density (mW/cm^2)**
Criteria	In range	In range	In range	In range	maximum
Predicted	1.07	1.62	1.12	0.69	2.79
Actual/ Experimental	1.07	1.62	1.12	0.69	2.76

The maximum OCV of 0.69 V and power density 2.76 mW/cm^2 at a current density of 7.46 mA/cm^2 were produced from the MFC experiment at the optimum condition obtained by RSM analysis. Whereas, model predicted power density was 2.79 mW/cm^2 at the same optimum condition. It is clearly seen from the Appendix Table E2 that the standard deviation of the three repeated experiments is in the range of 1.6 % only.

The deviation of model predicted response i.e., maximum power density (Y) from experimental power density at optimum condition is only 1.08 %. Thus, the developed quadratic model is consistent and reasonably predicted the response. The model equation for the response power density (Y) in Equation (5.10) was verified with experimental data by taking all the factors to the unit values randomly i.e., glycerol concentration (A) of 1 M, anode electrolyte concentration (B) of 1 M KOH, cathode electrolyte concentration (C) of 1 M KOH and anode electrocatalyst loading (D) of 1 mg/cm^2, respectively. The experimental power density and predicted power density at the given random conditions of MFC is presented in the Table 5.13. The power density calculated from Equation (5.10) using all the factors to 1 gives 1.77 mW/cm^2. Whereas, the experimental value of obtained power density at the same MFC conditions was 1.73 mW/cm^2 with a deviation

of only 2.25 % from the predicted value (Figure 5.48b). This result shows that the model equation can be used to predict the power density using T-shaped MFC.

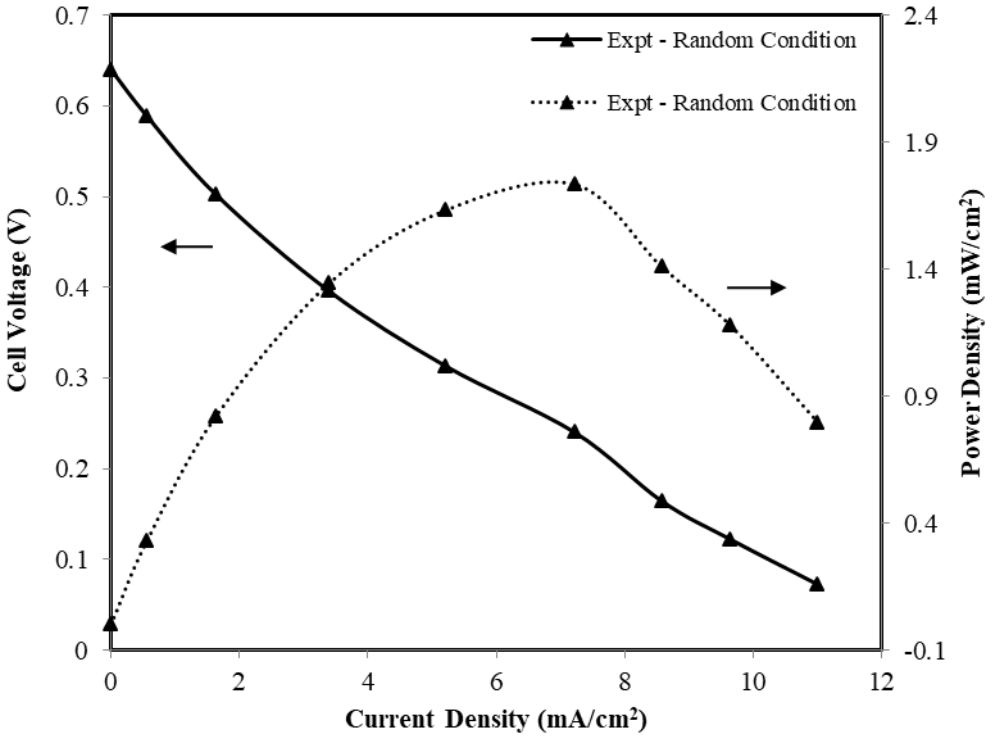

Figure 5.48b Polarization and power density curves of MFC for random condtion of 1 M glycerol fuel mixed with 1 M KOH as electrolyte, anode electrocatalyst loading of 1 mg/cm^2 and cathode electrolyte of 1 M KOH; Solid line – polarization curves; Dotted line – power density curves.

Table 5.13 Comparison of predicted and actual/experimental power density at the random condition of MFC**.**

Conditions and criteria	**Glycerol concentration (M)**	**Anode electrolyte concentration (M)**	**Electrocatalyst loading (mg/cm^2)**	**Cathode electrolyte concentration (M)**	**Power density (mW/cm^2)**
Criteria	In range	In range	In range	In range	maximum
Predicted	1	1	1	1	1.77
Actual/ Experimental	1	1	1	1	1.73

5.2.5.3 Process parameter optimization and its effect on response

Figure 5.49a to Figure 5.49f shows the 3D surface plot of the response/power density as a function of two independent variables keeping the third variable fixed. All 3D plots represent an infinite number of groupings of the two test variables keeping the other two fixed. The polynomial regression Equation (4.2) (page no. 68) was used to generate 3D plots between the response and the process parameters. The different colour codes of the 3D plots symbolize the values of the power density, as shown by the surface. Figure 5.49a shows the effect of glycerol concentration (A) and anode electrolyte concentration (B) on the power density (Y). The Pt/C_{HSA} cathode electrocatalyst of fixed loading 1 mg/cm^2 was used for all experiments. The atmospheric air was used as an oxidant at the cathode side and the operating temperature was maintained 35 ^oC for all set of experiments. The glycerol concentration was varied from 0.5 M to 1.5 M and the anode electrolyte concentration/KOH was varied from 1 M to 2 M, keeping other variables fixed at their optimum values i.e., 1.12 mg/cm^2 anode electrocatalyst loading and cathode electrolyte concentration/KOH of 0.69 M. It is seen from the 3D plot that the power density (Y) increases when the concentration of glycerol was varied from 0.5 M to 1.07 M, and beyond the glycerol concentration 1.07 M, the power density goes down. Initially, at low glycerol concentration, the active sites of electrocatalyst are occupied by glycerol molecules and the OH^- ions which are essential for anode reaction as shown Equation (1.1) (page no. 9). Further increase in glycerol concentration from 1.07 M to 1.5 M , the OH^- ions is replaced by the glycerol molecules at the surface of the electrocatalyst which resulting in decrease of MFC performance. The electrolyte plays an important role for the electrooxidation of fuel as shown in Equation (1.1) and (1.2) (page no. 9).

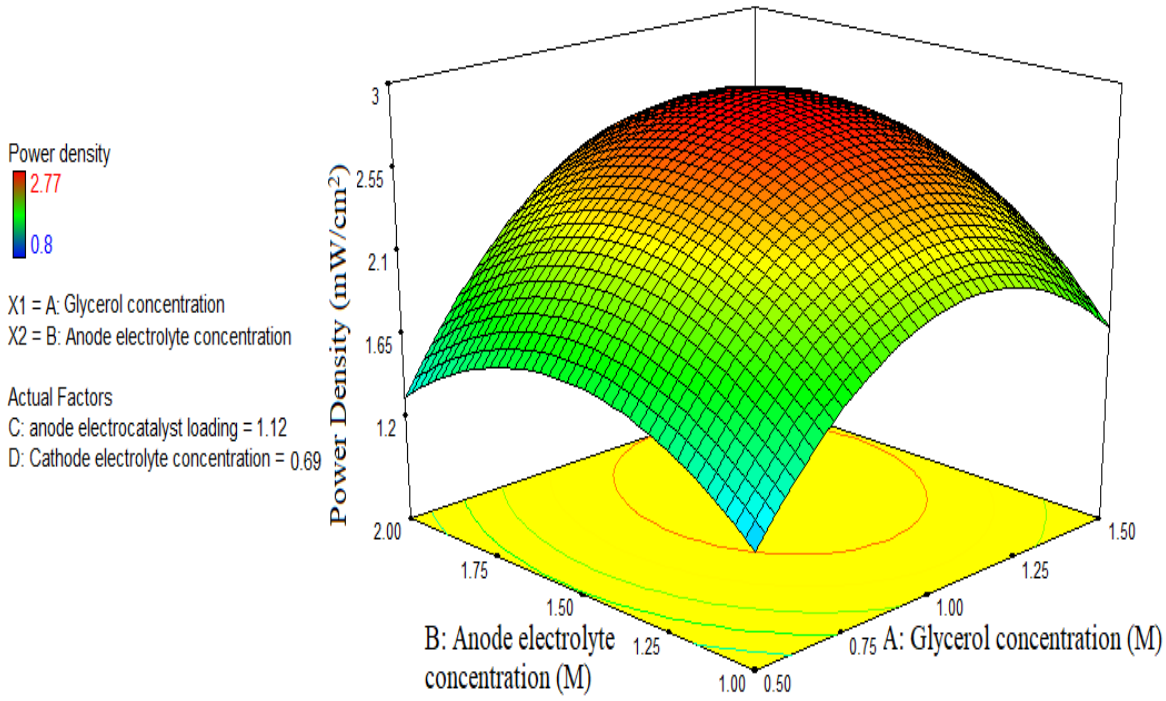

Figure 5.49a Response surface 3D plot showing the effect of glycerol concentration (A) and anode electrolyte concentration (B).

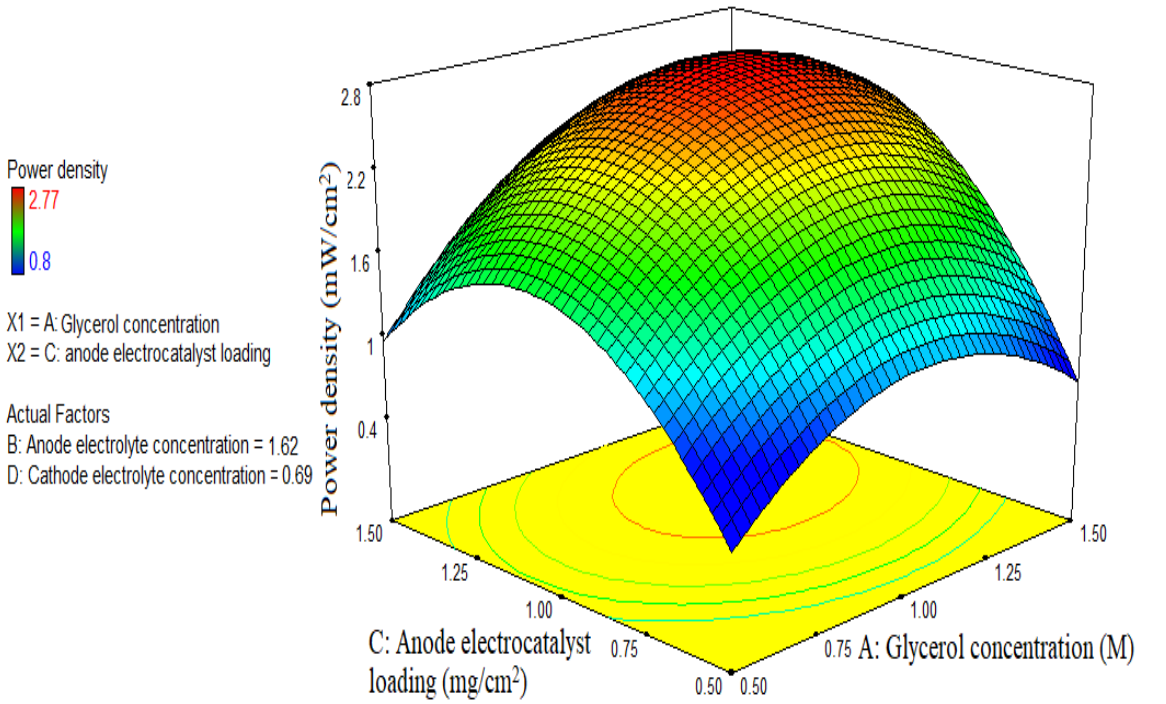

Figure 5.49b Response surface 3D plot showing the effect of glycerol concentration (A) and anode electrocatalyst loading (C).

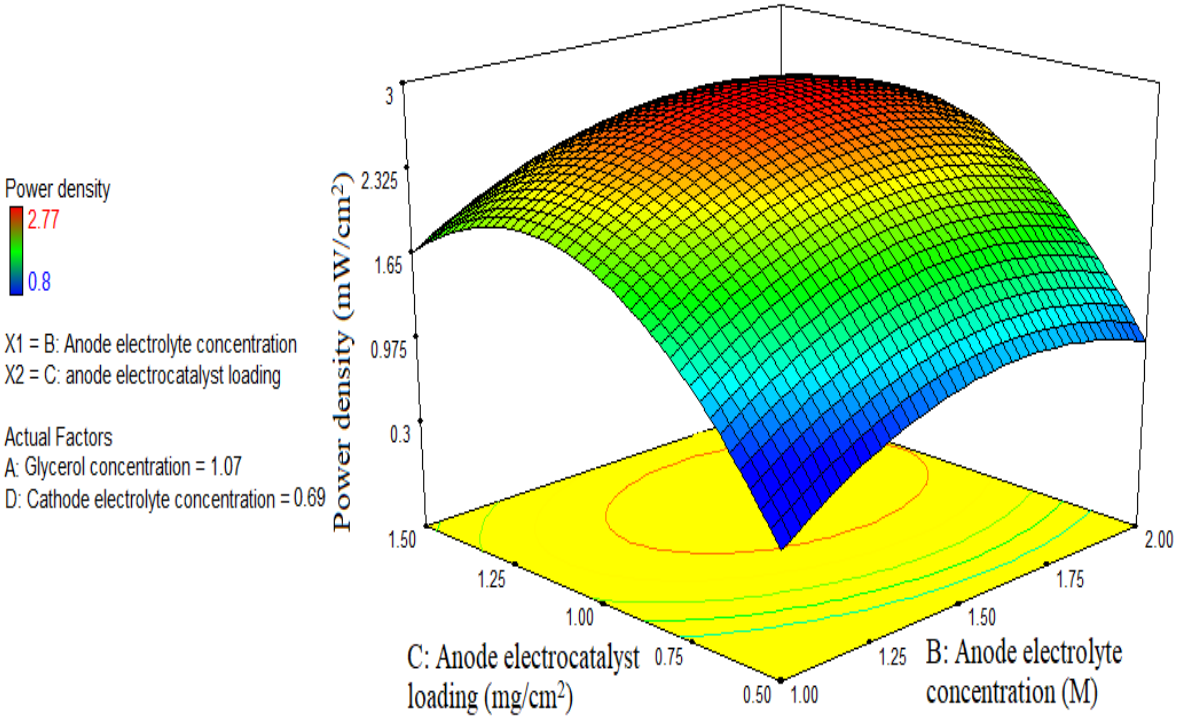

Figure 5.49c Response surface 3D plot showing the effect of anode electrolyte concentration (B) and anode electrocatalyst loading (C)

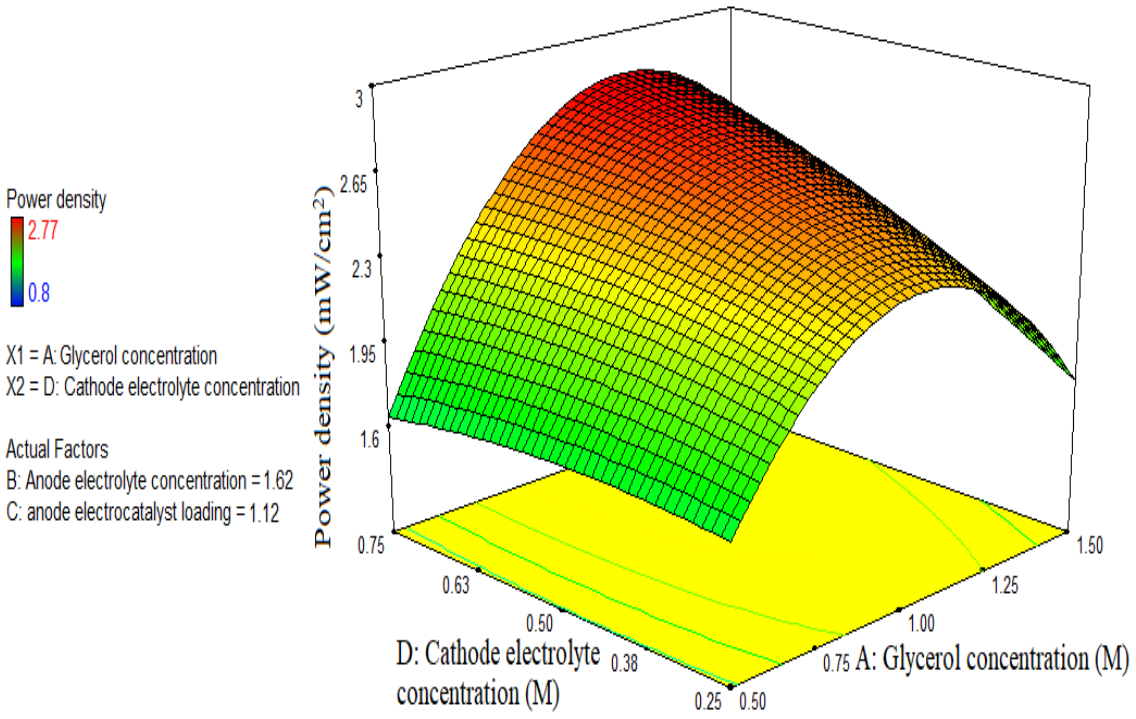

Figure 5.49d Response surface 3D plot showing the effect of glycerol concentration (A) and cathode electrolyte concentration (D).

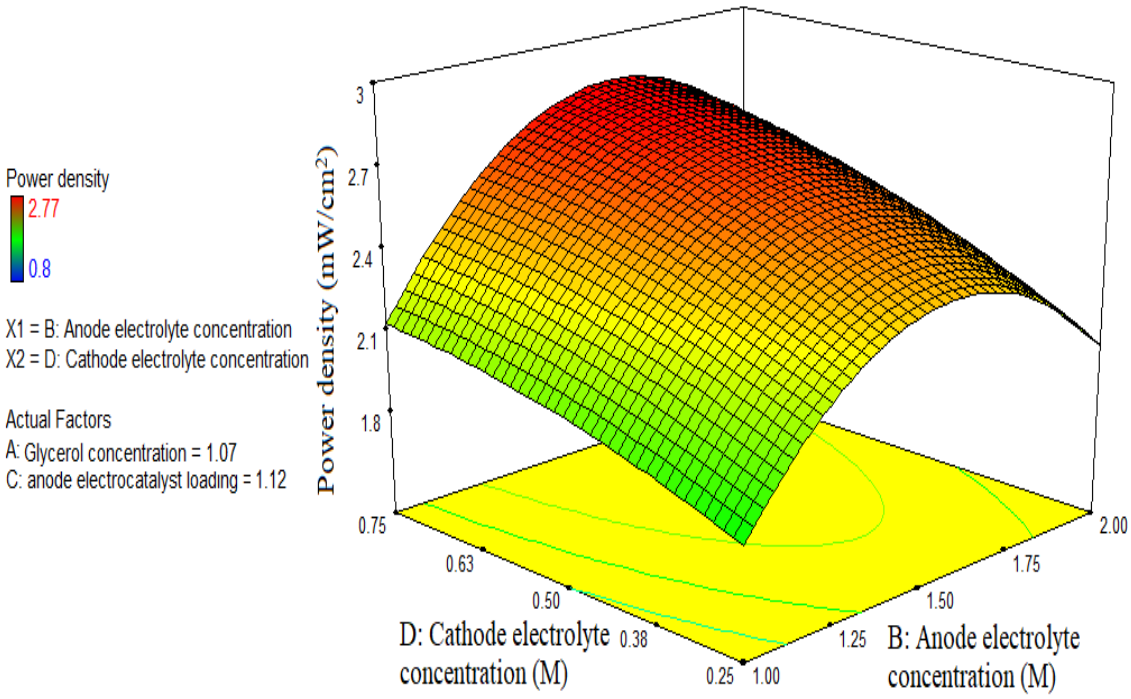

Figure 5.49e Response surface 3D plot showing the effect of anode electrolyte concentration (B) and cathode electrolyte concentration (D).

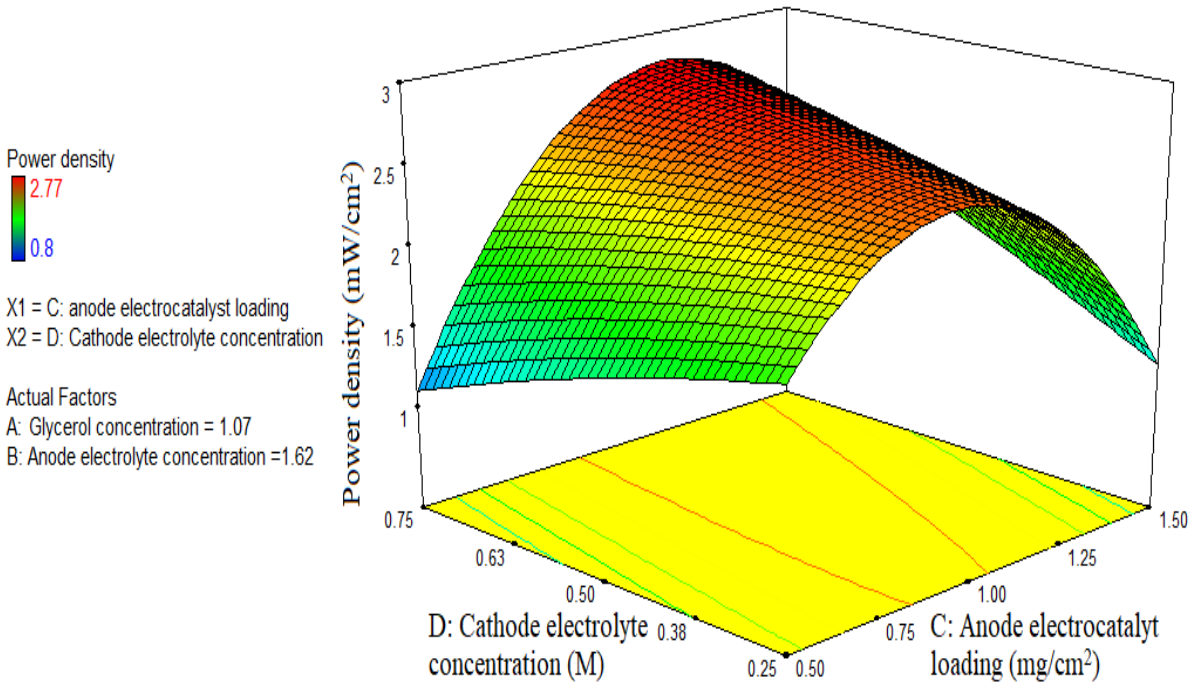

Figure 5.49f Response surface 3D plot showing the effect of anode electrocatalyst loading (C) and cathode electrolyte concentration (D).

As seen in the case of glycerol concentration, similar effect was also observed for anode electrolyte concentration. This has already been discussed in the section 5.2.3.2.4 “Effect of glycerol concentration” (page no. 143). Figure 5.49a shows that the power density increases with the increase in anode KOH concentration upto 1.62 M and further increase in electrolyte concentration beyond 1.62 M, the power density decreases due to the replacement of glycerol molecules by the OH^- ions at the higher concentration and the remaining OH^- ions may begin to behave as poison species by blocking the active sites of the electrocatalyst (Pramanik and Rathoure 2017). The effect of glycerol concentration (A) and anode electrocatalyst loading (C) on cell performance in terms of power density for a fixed/optimum concentration of anode electrolyte (1.62 M) and cathode electrolyte concentration (0.69 M) is shown in Figure 5.49b. The effect of glycerol concentration on cell performance was similar as discussed earlier (Figure 5.49a). The power density increases with the increase in electrocatalyst loading up to 1.12 mg/cm^2, due to the increase in the active sites of the electrocatalyst which helps in more ineraction of fuel and electrocatalyst resulting in better performance of MFC. However, further increase in electrocatalyst loading beyond 1.12 mg/cm^2 causes the reduction of active sites due to the depostion of electrocatalyst in the small area of the electrode. Thus, the fuel molecules have less access of active electrocatalyst sites for the electrooxidation reaction (Gupta and Pramanik 2019). This has already been discussed in the section “5.2.3.2.2 Effect of anode electrocatalyst loading” (page no. 140). Similarly, the effect of the anode electrolyte concentration and anode electrocatalyst loading on cell performance for a fixed/optimum concentration glycerol (1.07 M) and cathode electrolyte (KOH) concentration (0.69 M) is shown in Figure 5.49c. The maximum power density of 2.79 mW/cm^2 was obtained for the anode KOH concentration of 1.62 M and anode electrocatalyst loading of 1.12 mg/cm^2.

The trend of 3D plot for the varying concentration of anode KOH and anode electrocatalyst loading is similar as discussed in Figure 5.49a and Figure 5.49b, respectively.

Figure 5.49d shows the effect of glycerol concentration (A) and cathode electrolyte/KOH concentration (D) on cell performance for a fixed/optimum concentration of anode electrolyte/KOH concentration (1.62 M) and anode electrocatalyst loading (1.12 mg/cm^2). The effect of glycerol concentration on cell perfomance was similar as discussed earlier. In the cathode reaction, oxygen from the air diffuses through the air breathing cathode where the oxygen reduction reaction takes place. The cell performance increases when the cathode electrolyte/KOH concentration was increased from 0.25 M to 0.69 M and further increase in cathode KOH concentration beyond 0.69 M, power density decreases. It may be due the presence of more OH^- ions on the electrocatalyst surface at higher KOH concentration replace the water molecules which are necessary to complete the cathode reactions (Equation (1.2)) (page no. 9).

Figure 5.49e shows the effect of anode electrolyte/KOH concentration and cathode electrolyte/KOH concentration on the cell performance for a fixed/optimum glycerol concentration (1.07 M) and anode electrocatalyst loading (1.12 mg/cm^2). The effect of anode and cathode electrolyte/KOH concentration on cell performance was similar as discussed earlier.

Similarly, the effect of anode electrocatalyst loading and cathode electrolyte concentration on the cell performance for a fixed/optimum concentration of glycerol (1.07 M) and anode electrolyte concentration (1.62 M) is shown in Figure 5.49f**.** The trend of 3D response plot for anode electrocatalyst loading and cathode electrolyte/KOH concentration were similar as discussed earlier (Figure 5.49a to Figure 5.49d). The

maximum power density of 2.76 mW/cm^2 was obtained for anode loading of 1.12 mg/cm^2 and cathode KOH concentration of 0.69 M. All the 3D plots are very helpful for finding the optimum conditions and to check the effect of process parameters in the given range. The effect of independent operating parameters on power density is shown in the perturbation graph Figure 5.50. All the independent variables are in coded form. It is seen from the Figure 5.50, the effect of glycerol concentration (A) and anode electrocatalyst loading (C) on power density (Y) is higher than that of other variables. The cathode electrolyte/KOH concentration (D) shows the least effect on power density. Experimental results also showed similar trend.

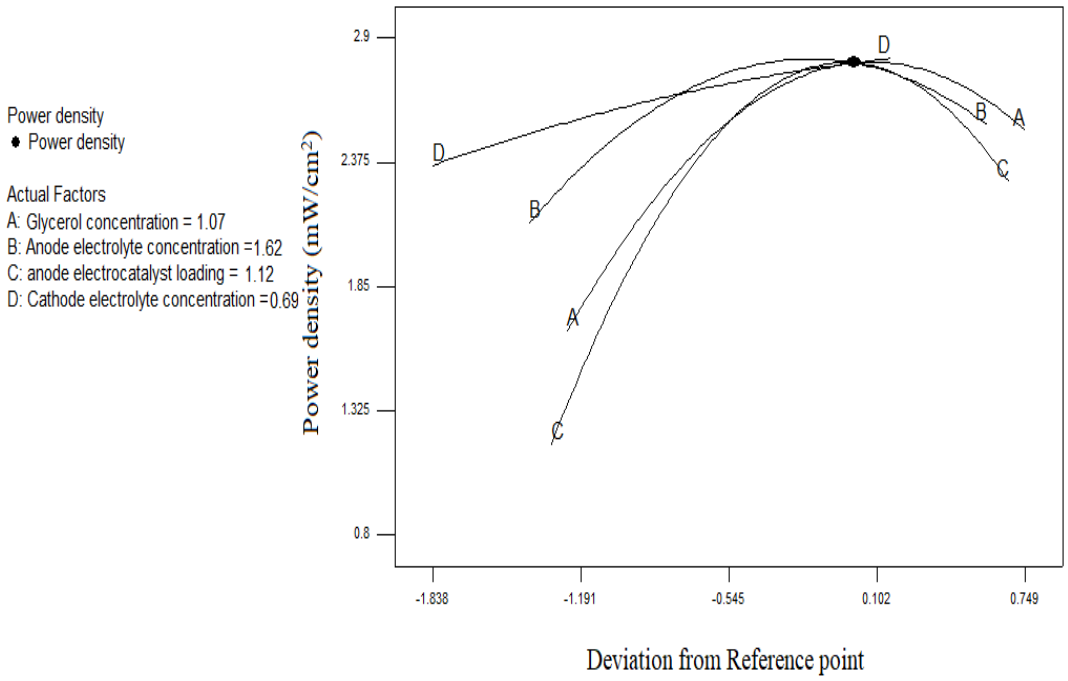

Figure 5.50 Perturbation plot displaying the effect independent variables on power density.

5.3 Evaluation of dimensionless numbers

5.3.1 Y-shaped air breathing MFC device

In the MFC operation, intermixing of fuel and oxidant and the stability of the liquid-liquid interface are the key factors in controlling cell performance. The intermixing of fuel and oxidant and the stability of the liquid-liquid interface in a microchannel depends upon the Reynolds Number (Re), Peclet number (Pe) and Schmidt number (Sc), respectively. The flow rate at anode and cathode were maintained at 0.3 ml/min, 0.5 ml/min, 1 ml/min and 1.5 ml/min to obatined optimum flow rate for maximizing the MFC performance. The dimensionless numbers were calculated at the optimum conditions of the MFC at room temperature. All these three dimensionless numbers are within the permissible range for the Y-shaped air breathing MFC as discussed below.

The Reynolds number $\mathrm{Re} = \frac{D_h V \rho}{\mu}$ is the ratio of inertia force to viscous force(Kjeang et al., 2009). Where Dh is hydraulic diameter, V is the average velocity of the flow, ρ is the density of liquid and μ is the viscosity of the liquid. Normally, Re describes the nature of flow of liquid (Re<2100 for laminar flow and Re>2100 turbulent flow). In microfluidic devices the Re is maintained less than 1 and upto 100 (Banerjee et al., 2019). The calculated Reylonds number (Re) at different flow rates is shown in Table 5.14. The laminar flow with low Reynolds number implies parallel flow of fluids without convective mixing. The values of different physical properties and parameters which are used to calculate the dimensionless numbers are presented below:

Hydraulic diameter D_h is 1.515×10^{-3} m. The calculated average velocity of inlet streams were 0.005 m/s, 0.0083 m/s, 0.0166 m/s and 0.025 m/s for the flow rate of 0.3 ml/min, 0.5 ml/min, 1 ml/min and 1.5 ml/min, respectively. The calculated densities of the 0.5 M glycerol mixed with 0.5 M KOH and 0.5 M KOH electrolyte using specific gravity bottle

at 35 ^{o}C were 1023 kg/m^3 and 1015 kg/m^3, respectively. The measured viscosities of the 0.5 M glycerol mixed with 0.5 M KOH and 0.5 M KOH electrolyte using LVDV-II Pro Brookfield digital viscometer at 35 ^{o}C were 8.7×10^{-4} Pa s and 7.5× 10^{-4} Pa s, respectively. The diffusion coefficient of glycerol in water of 9.4× 10^{-10} m^2/sec was taken from Perry's Chemical Engineers Hand Book (Perry and Green 1999).Whereas, the diffusion coefficient of oxygen in water is 2×10^{-10} m^2/sec (Jayashree et al., 2005).

Table 5.14 Reynolds numbers for different flow rates in Y-shaped MFC.

Flow rate (ml/min)	0.3	0.5	1	1.5
Re (anode stream)	8.9	14.7	29	44.7
Re (cathode stream)	10.4	17.2	34	51.9

The Schmidt number $Sc = \frac{\mu}{\rho D}$ is the ratio of molecular diffusivity to momentum diffusivity (Choban et al., 2004), where μ is viscosity, ρ is the density of liquid and D is diffusivity of the species in the solvent. The Sc >1 indicates viscous force effect is more than concentration effect confirming the concentration boundary layer to a linear velocity profile (Choban et al., 2004). In the present study, calculated Schmidt number (Sc) are 904 and 3694 which is in good agreement to maintain laminar flow in the MFC for anode and cathdoe streams, respectively.

Similarly, the degree of mixing during laminar flow depends upon the value of Peclet number $Pe = \frac{V D_h}{D}$, which is defined as the ratio of convection transport to diffusive transport (Choban et al., 2004). Where V is the average velocity in the channel, D_h is the hydraulic diameter of the channel and D is the diffusion coefficient of glycerol in water. The hydraulic diameter D_h of the microchannel is calculated using the formula, $D_h = \frac{4A}{P}$

, where A is the cross section area of the flow channel and P is the wetted perimeter of the channel cross section. The calculated Pe for different flow rates are presented in Table 5.13. Very high Pe more than 10^4 ensures there is no intermixing of two streams within the flow channel as shown in Table 5.15 (Choban et al., 2004).

Table 5.15 Peclet numbers for different flow rates in Y-shaped MFC.

Flow rate (ml/min)	0.3	0.5	1	1.5
Pe (anode stream)	8058	13377	26754	40292
Pe (cathode stream)	37875	62872	125745	189375

5.3.2 T-shaped air breathing MFC device

In T-shaped MFC, the important dimensionless numbers such as Reynolds Number (Re), Peclet Number (Pe) and Schmidt Number (Sc) were calculated and compared these dimensionless numbers with literature reported standard data which confirms the laminar flow within the T-shaped micro channel. The flow rates of anode and cathode streams were maintained at 0.5 ml/min, 0.8 ml/min, 1 ml/min, 1.2 ml/min and 1.6 ml/min to find out the optimum flow rate for maximizing the cell performance. The dimensionless numbers were calculated at the optimum conditions of the MFC at room temperature. The calculated dimensionless numbers estimate the intermixing of fuel and oxidant and stability of the liquid-liquid interface. The calculated values of all three dimensionless numbers were found within the permissible range.

The Reynolds number is used to find out the nature of fluid flow in the channel (Kjeang et al., 2009). The symbols used in the formula are described as follows:

Hydraulic diameter D_h of the microchannel in the T-shaped MFC is 0.782×10^{-3} m, where $D_h = \frac{4A}{P}$; A is the cross section area of the microchannel and P is the wetted parameter of the microchannel. The average velocity V were calculated from inlet flow

rates of both the streams i.e., 0.0061 m/s, 0.0098 m/s, 0.01229 m/s 0.0147 m/s and 0.0197 m/s, respectively. The viscosities μ of the anode stream 1 M glycerol mixed with 1 M KOH and cathode stream 0.5 M KOH electrolyte measured using LVDV-II Pro Brookfield digital viscometer were 14×10^{-4} Pa s and 7.3×10^{-4} Pa s, respectively. The calculated densities ρ using specific gravity bottle for anode stream 1 M glycerol mixed with 1 M KOH and cathode 0.5 M KOH electrolyte at the temperature of 35 ^{o}C were 1070 kg/m^3 and 1016 kg/m^3, respectively. The diffusion coefficient of glycerol in water of 9.4×10^{-10} m^2/sec was taken from Perry's Chemical Engineers Hand Book (Perry and Green 1999).Whereas, the diffusion coefficient of oxygen in water is 2×10^{-10} m^2/sec (Jayashree et al., 2005). The Re is the ratio of inertia force to viscous force and the value of Re in the microfluidic devices is less than 1 and upto 100 as per reported literature (Banerjee et al., 2019). In the present study, the Re values are found within the permissible range as mentioned in the Table 5.16 below.

Table 5.16 Reynolds numbers for different flow rates in T-shaped MFC.

Flow rate ((ml/min)	0.5	0.8	1	1.2	1.6
Re (anode stream)	3.6	5.8	7.3	8.7	11.6
Re (cathode stream)	6.6	10.64	13.6	15.9	21.4

As already mentioned, the Schmidt number (Sc) is the ratio of molecular diffusivity to momentum diffusivity. Where μ is the viscosity, ρ is the density and D is the diffusivity of the species of interest in the solvent i.e., glycerol in water which is 9.4×10^{-10} m^2/sec taken from the Perry's Chemical Engineers Hand Book (Perry and Green 1999). As per literaure, value of Sc > 1 suggest that the effect of viscous force is greater than concentration effect (Banerjee et al., 2019). The calculated value of Sc are 1391 and 3592 for anode and cathode streams, respectively.

Similarly, the degree of mixing during laminar flow depends on the Peclet number (Pe), which is defined as the ratio of convection transport to diffusive transport (Choban et al., 2004). The symbols in the formula is already discussed in the above explained dimensionless numbers. The high value of Peclet number ensures that there is no intermixing of two streams within the flow channel. The Peclet numbers calculated for different flow rates presented in Table 5.17 below:

Table 5.17 Peclet numbers for different flow rates in T-shaped MFC.

Flow rate (ml/min)	0.5	0.8	1	1.2	1.6
Pe (anode stream)	5074	8152	10224	12229	16388
Pe (cathode stream)	23851	38318	48054	57477	77027

The high Peclet number reduces the concentration boundary layer and enriches the concentration gradient. The value of Pe more than 10^4 shows thinner diffusion zones between the two streams and avoids the mixed potential at cathode due to fuel crossover in the MFC device (Chang et al., 2006).

5.4 Comparison of present study with published work

The present study is compared with glycerol based microfluidic fuel cell with published work operated at room temperature. Table 5.18 shows the studies on glycerol based microfluidic fuel cell by several investigators. In the present work, Y-shaped and T-shaped MFC was fabricated and studied using glycerol as fuel and KOH as electrolyte. Atmospheric air was as oxidant. Synthesized anode electrocatalyst Pd-Ni/C and Pd-Pt/C electrocatalyst in different ratios were used to fabricate the anode electrodes. The flow of fuel and electrolyte stream was over the electrode surface. The anode stream was glycerol mixed with KOH in different concentrations whereas; KOH of different concentrations

was used as cathode stream. The electrode areas were 0.6 cm^2 and 0.9 cm^2 for Y-shaped and T-shaped MFC, respectively. The maximum power density of 1.27 mW/cm2 at a current density of 5.77 mA/cm^2 and 2.77 mW/cm^2 at a current density of 7.71 mA/cm^2 were obtained using Pd-Ni (10:10)/C and Pd-Pt (16:4)/C electrocatalyst, respectively in T-shaped MFC at room temperature.

Several investigators are worked on glycerol based microfluidic fuel cell. Dector et al., (2013a) used Y-shaped microfluidic fuel cell with flow over electrode fluid delivery system. The length of the MFC channel was 45 mm and 1 mm depth with an active electrode area of 0.45 cm^2. The synthesized Pd/C and Pd/MWCNT as anode electrocatalyst and commercial Pt/C as cathode electrocatalyst was used for electrooxidation of glycerol. The electrocatalyst ink was deposited on the wall of the channel by spray technique. Very low power densities of 0.70 $mW/cm^2$and 0.51 mW/cm^2 were obtained using Pd/MWCNT and Pd/C electrocatalysts, respectively. Maya-Cornejo et al., (2015) used CuPd/C as anode electrocatalyst for electrooxidation of several fuels such as methanol, ethanol, glycerol and ethylene glycol in an air breathing nano fluidic fuel cell. The anodic and cathodic electrocatalyst were prepared by spray technique using 2.2 mg of CuPd/C and 2.9 mg Pt/C. The cell performance was obtained in flow through electrode in a high surface area carbon nanoform substrate. The cathode performance was also enhanced using dissolved oxygen and atmospheric oxygen. The maximum power density using glycerol as fuel was 20.43 mW/cm^2. In another work, Maya-Cornejo et al., (2016) synthesized CuPt/C and CuPd/C anode electrocatalyst for electrooxidation of crude and analytical glycerol in air breathing nanofluidic fuel cell. The electrocatalyst CuPd/C and Pt/C of 1 mg was impregnated in carbon nanofoam (Marketech International, Inc) as substrate for each anode and cathode, respectively. The dimension of the electrode in the cell was 20 mm long, 3 mm width and 0.1 mm height with active area of 0.02 cm^2.

The maximum power density using CuPd/C were 17.6 mW/cm^2 and 17.4 mW/cm^2 for crude and analytical glycerol, respectively. Similarly, CuPt/C produced maximum power density of 21.8 mW/cm^2 and 23 mW/cm^2 for crude and analytical glycerol at 25 ^{o}C, respectively. The power density was higher for CuPt/C that of CuPd/C. Martins et al., (2018a) studied on mixed media with flow through porous electrode in MFC using glycerol, ethylene glycol and methanol as fuel. Pt/C electrocatalyst was used for both anode and cathode. The KOH of 1 M was used as anode electrolyte and H_2SO_4 of 1 M as cathode electrolyte. The maximum power density of 39.5 mW/cm^2, 30.3 mW/cm^2 and 30 mW/cm^2 were obtained for the glycerol of 0.05 M, ethylene glycol of 1.5 M of and methanol of 3 M, respectively. Similarly, in another study Martins et al., (2018b) used bleach (sodium hypochlorite) as oxidant which increased the cell performance. The maximum power density of 71.2 mW/cm^2 was obtained in alkaline medium and 315 mW/cm^2 was observed in mixed media configuration with KOH mixed with glycerol and H_2SO_4 mixed with bleach. It is clear from the comparison that the maximum power density obtained from present study was higher from Dector et al., (2013a). However, the studies with flow of fuel and oxidant through the porous electrodes give higher power density due to increase in contact area of fuels with the active sites of electrocatalysts.

Table 5.18 Performance comparison of present MFC study with published work.

Fuel and electrolyte used	**Oxidant**	**Device Type/ electrode details/cell temperature**	**Maximum power density (mW/cm^2)**	**References**
051 M glycerol, 0.5 M KOH	Atmospheric air	MFC; Anode: Pd-Pt(16:4)/C (2 mg/cm^2) Cathode: Pt/C_{HSA} (2 mg/cm^2) Electrode area: 0.6 cm^2; Room temperature	2.77	Present study
0.1 M glycerol, 0.3 M KOH	Sat. dissolved oxygen	MFC; Anode: Pd/MWCNT (1.6mg/cm^2) Cathode: Pt/C (0.54 mg/cm^2) Electrode area: 0.45 cm^2; Room temperature	0.70	Dector et al., (2013a)
		MFC; Anode: Pd/C (1.3 mg/cm^2) Cathode: Pt/C (0.54 mg/cm^2) Electrode area: 0.45 cm^2; Room temperature	0.51	
0.1 M glycerol, 0.3 M KOH	Air + sat. dis. oxygen	AB-MNFC; Anode: Cu@Pt /C;2.2 mg/cm^2 Cathode: Pt/C ;2.9 mg $/cm^2$ Electrode area: 0.02 cm^2; Temperature: 25 ^oC	20.43	Maya-Cornejo et al., (2015)
Glycerol 5 vol%, 0.3 M KOH	Air + sat. dis. oxygen	AB-MNFC; Anode: Cu@Pd/C;1 mg/cm^2 Cathode: Pt/C ;1 mg $/cm^2$ Electrode area: 0.02 cm^2; Temperature: 25 ^oC	17.41	Maya-Cornejo et al., (2016)
		AB-MNFC; Anode: Cu@Pt/C;1 mg/cm^2 Cathode: Pt/C ;1 mg $/cm^2$ Electrode area: 0.02 cm^2; Temperature: 25 ^oC	23.16	
0.05 M glycerol, 1 M KOH	KOH, H_2SO_4 (mixed media), sat. dis oxygen	MFC; Anode: Pt/C : 70 mg Cathode: Pt/C: 70 mg Electrode area 0.015 cm^2 Room temperature	39.5	Martins et al., (2018a)
1 M glycerol, 1 M KOH	KOH, H_2SO_4 (mixed media), Sodium hypochlorite	MFC; Anode: Pt/C : 70 mg Cathode: Pt/C: 70 mg Electrode area 0.015 cm^2 Room temperature	315	Martins et al., (2018b)

5.5 Efficiency of the air breathing microfluidic fuel cell

The air breathing microfluidic fuel cell efficiency is calculated in various aspects of the cell and the overall efficency of the cell is calculated by the multiplying all specific efficiencies (Carrette et al., 2001). The efficiency of air breathing microfluidic fuel cell is calculated using the Equation (5.11) given below:

$$\eta_{MFC} = \eta_r^{cell} \times \eta_V \times \eta_F \times \eta_U \times \eta_H \quad (5.11)$$

The symbol for total efficiency of microfluidic fuel cell is denoted by η_{MFC}, for thermodynamics efficiency is η_r^{cell}, for electrochemical efficiency is η_V, Faradaic efficiency is η_F, fuel utilization efficiency is η_U and heating value efficiency is η_H.

The thermodynamic efficiency (η_r^{cell}) is found from Gibbs free energy change (ΔG) and enthalpy change (ΔH) and the of the reactions taking place for glycerol fuel through electrooxidation and combusion, respectively. The thermodynamics efficiency for glycerol fuel was calculated at room temperature of 35 ^oC with the help of the literture data (Ragsdale and Ashfield 2008). The electrochemical efficiency (η_V) is calculated by finding the ratio of operating cell potential to theoretical cell potential. The Faradaic efficiency (η_F) is calculated from the ratio of experimental current to theoretical maximum current. The fuel utilization efficiency (η_U) is considered to be 0.95 (Larminie and Dicks 2003). However, the heating value efficiency (η_H) is neglected in the current study because the glycerol fuel is in pure form. It is defined as the ratio of heating value of the fuel that is converted electrochemically to heating value of all the fuels component present in the fuel (Carrette et al., 2001). Thus, the final form of the Equation (5.12) is obtained without using the heating value effciency (η_H) in Equation 5.11. From the Table 5.19 it is clearly seen that the total effciency using Pd-Pt (16:4)/C is higher than Pd-Ni(10:10)/C compared in both type of cell.

$$\eta_{FC} = \eta_r^{cell} \times \eta_V \times \eta_F \times \eta_U \quad (5.12)$$

Table 5.19 Efficiency of Y-shaped and T-shaped MFC using best Pd-Pt/C and Pd-Ni/C anode electrocatalysts at room temperature (35 ^{o}C) and atmospheric pressure (1 atm).

Electrocatalyst type	Type of MFC	η_r^{cell}	η_V	η_F	η_U	η_{FC}
Pd-Pt (16:4)/C	Y-Shaped	0.99	0.66	0.71	0.95	0.44
	T-Shaped	0.99	0.57	0.71	0.95	0.38
Pd-Ni (10:10)/C	Y-Shaped	0.99	0.58	0.71	0.95	0.39
	T-Shaped	0.99	0.34	0.71	0.95	0.22

5.6 Stability test of Y-shaped and T-shaped air breathing MFC

The stability test of MFC is very important for getting electrical power without any interruption from the developed microfluidic fuel cell. In the present study, best electrocatalyst Pd-Pt (16:4)/C used as anode electrocatalyst in Y-shaped and T-shaped MFC and tested at a constant load for 12 h only due to safety issue. The short cuircuit voltage were recored at the equal interavl of 1 hr upto 12 hrs as shows in Figure 5.51**.** The cell parameters were maintained at the optimum conditions obtained from the experimental studies for both type of MFC.The cathode was made of commercial electrocatalyst Pt/C_{HSA}. The maximum power density decreased slightly from 2.77 mW/cm^2 to 2.36 mW/cm^2 for T-shaped MFC and 1.6 mW/cm^2 to 1.12 mW/cm^2 for Y-shaped MFC, respectively after 12 h of air breathing MFC operation. The cell performance reduced slightly with time and it may be due to the poisoning of electrocatalyst sites by the formation of carbonate layer and adsorption of intermediate products in alkaline medium (Zhiani et al., 2013).

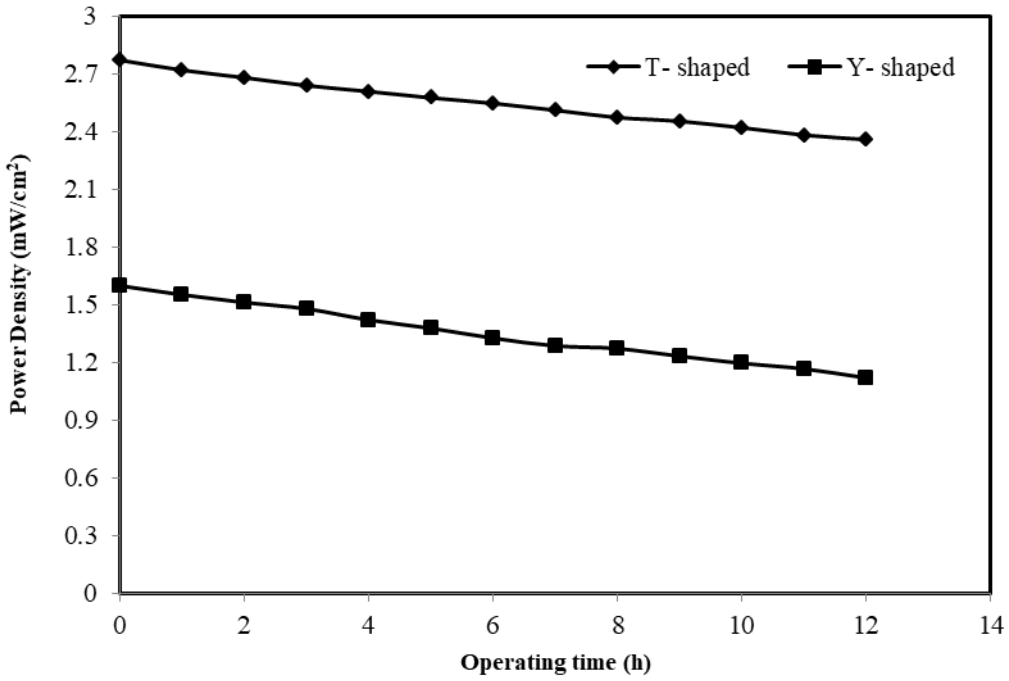

Figure 5.51 Stability test of the Y-shaped and T-shaped air breathing MFC using the optium conditions of operation at constant load at a temperature of 35 ^{o}C.